Power Allocation and Cell Association in Cellular Networks

by

Danh Huu Ho
B.Sc., University of Can Tho, 2008
M.Sc., University of Westminster, 2013

A Dissertation Submitted in Partial Fulfillment of the
Requirements for the Degree of

DOCTOR OF PHILOSOPHY

in the Department of Electrical and Computer Engineering

Power Allocation and Cell Association in Cellular Networks

by

Danh Huu Ho
B.Sc., University of Can Tho, 2008
M.Sc., University of Westminster, 2013

Supervisory Committee

Dr. T. Aaron Gulliver, Supervisor
(Department of Electrical and Computer Engineering)

Dr. Xiaodai Dong, Departmental Member
(Department of Electrical and Computer Engineering)

Dr. Kui Wu, Outside Member
(Department of Computer Science)

Supervisory Committee

Dr. T. Aaron Gulliver, Supervisor
(Department of Electrical and Computer Engineering)

Dr. Xiaodai Dong, Departmental Member
(Department of Electrical and Computer Engineering)

Dr. Kui Wu, Outside Member
(Department of Computer Science)

ABSTRACT

In this dissertation, power allocation approaches considering path loss, shadowing, and Rayleigh and Nakagami-m fading are proposed. The goal is to improve power consumption, and energy and throughput efficiency based on user target signal to interference plus noise ratio (SINR) requirements and an outage probability threshold. First, using the moment generating function (MGF), the exact outage probability over Rayleigh and Nakagami-m fading channels is derived. Then upper and lower bounds on the outage probability are derived using the Weierstrass, Bernoulli and exponential inequalities. Second, the problem of minimizing the user power subject to outage probability and user target SINR constraints is considered. The corresponding power allocation problems are solved using Perron-Frobenius theory and geometric programming (GP). A GP problem can be transformed into a nonlinear convex optimization problem using variable substitution and then solved globally and efficiently by interior point methods. Then, power allocation problems for throughput maximization and energy efficiency are proposed. As these problems are in a convex fractional programming form, parametric transformation is used to convert the original problems into subtractive optimization problems which can be solved iteratively. Simulation results are presented which show that the proposed approaches are better than existing schemes in terms of power consumption, throughput, energy efficiency and outage probability.

Prioritized cell association and power allocation (CAPA) to solve the load balancing issue in heterogeneous networks (HetNets) is also considered in this dissertation. A Hetnet is a group of macrocell base stations (MBSs) underlaid by a diverse set of small cell base stations (SBSs) such as microcells, picocells and femtocells. These networks are considered to be a good solution to enhance network capacity, improve network coverage, and reduce power consumption. However, HetNets are limited by the disparity of power levels in the different tiers. Conventional cell association approaches cause MBS overloading, SBS underutilization, excessive user interference and wasted resources. Satisfying priority user (PU) requirements while maximizing the number of normal users (NUs) has not been considered in existing power allocation algorithms. Two stage CAPA optimization is proposed to address the prioritized cell association and power allocation problem. The first stage is employed by PUs and NUs and the second stage is employed by BSs. First, the product of the channel access likelihood (CAL) and channel gain to interference plus noise ratio (GINR) is

considered for PU cell association while network utility is considered for NU cell association. Here, CAL is defined as the reciprocal of the BS load. In CAL and GINR cell association, PUs are associated with the BSs that provide the maximum product of CAL and GINR. This implies that PUs connect to BSs with a low number of users and good channel conditions. NUs are connected to BSs so that the network utility is maximized, and this is achieved using an iterative algorithm. Second, prioritized power allocation is used to reduce power consumption and satisfy as many NUs with their target SINRs as possible while ensuring that PU requirements are satisfied. Performance results are presented which show that the proposed schemes provide fair and efficient solutions which reduce power consumption and have faster convergence than conventional CAPA schemes.

Contents

List of Acronyms

MG	Moment Generating Function
GP	Geometric Programming
PU	Priority User
NU	Normal User
5G	Fifth Generation
BS	Base Station
MBS	Macrocell Base Station
SBS	Small cell Base Station
CAL	Channel Access Likelihood
ICT	Information and Communication Technology
MWC	Mobile and Wireless Communications
CRE	Cell Range Expansion
ABS	Almost Blank Subframe
QoS	Quality of Service
CPA	Centralized Power Allocation
DPA	Distributed Power Allocation
CSI	Channel State Information
SIC	Successive Interference Cancellation
CVX	ConVex Optimization
TPC	Target SINR tracking Power Control
OPC	Opportunistic Power Control
PDF	Probability Density Function
D2D	Device to Device
PUF	Power Update Function
SINR	Signal to Interference plus Noise Ratio
CAPA	Cell Association and Power Allocation
GINR	Channel Gain to Interference plus Noise Ratio
MIMO	Multiple Input Multiple Output
RSRP	Reference Signal Received Power
RSRQ	Reference Signal Received Quality
ISPC	Iterative SINR tracking Power Control
DUPC	Distributed Uplink Power Control

List of Acronyms

RAPC	Rate Adaptive and opportunistic Power Control
IDPC	Iterative Distributed Power Control
TOPC	Target SINR and Opportunistic based Power Control
FSPC	Fixed Step Power Control
TTPA	Distributed Target SINR Tracking Power Allocation
DOPA	Distributed algorithm for Opportunistic Power Allocation
PARF	Power Allocation with temporary Removal and Feasibility check
COPA	Constrained Opportunistic Power Allocation
VOPA	Variable SINR Opportunistic Power Allocation
DTPA	Dynamic Target SINR Tracking Power Allocation
VTPA	Variable Target SINR Tracking Power Allocation
UDCN	Ultra Dense Cellular Network
NOMA	Non-Orthogonal Multiple Access
MTPA	Multiple Target SINR tracking Power Allocation
AWGN	Additive White Gaussian Noise
HetNet	Heterogeneous Network

List of Figures

List of Tables

ACKNOWLEDGEMENTS

I am very grateful to Dr. Gulliver for his patient instruction and invaluable suggestions during this research. Dr. Gulliver has enlightened me on cellular networks and in particular the approaches and algorithms to solve power allocation and cell association problems in cellular networks. He shares his precious experience and inspires me to make greater progress on my research. Furthermore, I would like to express my appreciation to Dr. Xiaodai Dong, Dr. Kui Wu, and Dr. Ha Nguyen for their great insight and professional advice on my research. I also thank Dr. Wu-Sheng Lu for his sincere solicitude and significant encouragement towards finishing this work.

I would also like to express my gratitude and appreciation to my dear parents, my younger brother, Khang Ho, and my friends for instilling in me the love for learning and knowledge, and for their continuous support and encouragement not only for my studies but for my whole life. Finally, I would like to thank my cousins for their inspiration and love.

DEDICATION

To my beloved parents, my younger brother, and my great supervisor, Dr. Gulliver, for their endless love, encouragement, and support.

Life never ends if you keep going with effort and determination.

Chapter 1

Introduction

Information and communication technology (ICT) contributes 2% to 4% of global carbon dioxide emissions, and 37% of ICT emissions are due to mobile and wireless communications (MWC) [1]. Even with technological advances in MWC infrastructure, a 6% yearly growth rate in carbon dioxide emissions is expected in 2019 and 2020 [2]. This rate is expected to increase with the evolution of the internet of things (IoT) and fifth generation (5G) wireless networks. The number of connected mobile users is estimated to reach 50 billion by 2020, and mobile data traffic is expected to grow to approximately 50 exabytes (1 exabyte $= 10^8$ bytes) per month by 2021 which is five times the 2017 level [3]. If no countermeasures are taken, the energy to provide such massive data rates will become unmanageable.

While restricting global MWC usage is unrealistic, optimizing the power consumption, throughput, and energy efficiency of MWC systems is a promising approach. The goal is to improve the amount of information reliably transmitted per joule of consumed power. Energy efficiency is of paramount importance for operators to reduce electricity costs and for users to prolong battery life. This should influence the design of new network architectures and power allocation strategies. Thus, power allocation approaches for throughput and energy efficiency have received significant attention in the literature [4–6]. Other solutions include improving the macrocell base station (MBS) architecture, employing multi radio access technology, massive multiple input multiple output (MIMO) technology, millimeter wave technology, heterogeneous networks (HetNets) and direct D2D communications [7]. Among these solutions, HetNets are a promising area for research.

1.1 Heterogeneous Networks (HetNets)

A HetNet is a group of macrocell base stations (MBSs) underlaid by a diverse set of small cell base stations (SBSs) [8]. MBSs typically transmit at high power levels (5-100 W) while SBSs transmit at substantially lower power levels (100 mW-2 W). SBSs are often used to offload traffic from MBSs. There are three types of SBSs, microcells, picocells and femtocells [9]. Microcells have a coverage area smaller than MBSs, typically less than 500 m. Microcells can be deployed temporarily in anticipation of high traffic, or installed permanently in cellular networks. MBSs and microcells are deployed outdoors in a planned manner. Picocells are similar to microcells but with lower transmit power, and a coverage area less than 100 m. Picocells are typically equipped with omnidirectional antennas and deployed indoors or outdoors in a planned manner. Femtocells are typically deployed indoors in an unplanned manner with omnidirectional antennas and a coverage area less than 30 m. Unlike picocells and microcells, femtocells are designed to support only a few users. Due to their lower transmit power and smaller size, SBS deployment is more flexible than MBS deployment.

In HetNets, the reuse distance (the distance between two same frequency BSs), and the communication distance (the distance between a user and BS) can be reduced [10], which improves the system capacity and energy efficiency. However, HetNets are limited by the disparity of power levels in the different tiers. Conventional cell association approaches such as maximum signal strength based cell association, cell range expansion (CRE) and CRE with almost blank subframe (ABS) can cause MBS overloading, SBS underutilization, excessive user interference and wasted resources [11]. BS overloading implies that the number of users at a BS is more than the BS capacity, and BS underutilization means the available resources at the BS are not fully utilized. Thus, there is a crucial need to efficiently assign users to BSs and to effectively control user transmit power to maintain communication links with minimal interference. Further, users perceive different signal strengths and experience different channel conditions from MBSs and SBSs. These problems can be addressed with an efficient cell association and power allocation (CAPA) scheme. In particular, cell association is used to establish network utility efficient connections between users and BSs according to the user channel conditions and BS loads. Power allocation is used to ensure that users transmit with appropriate power levels to maintain link quality without imposing excessive interference on other users.

1.2 System Models

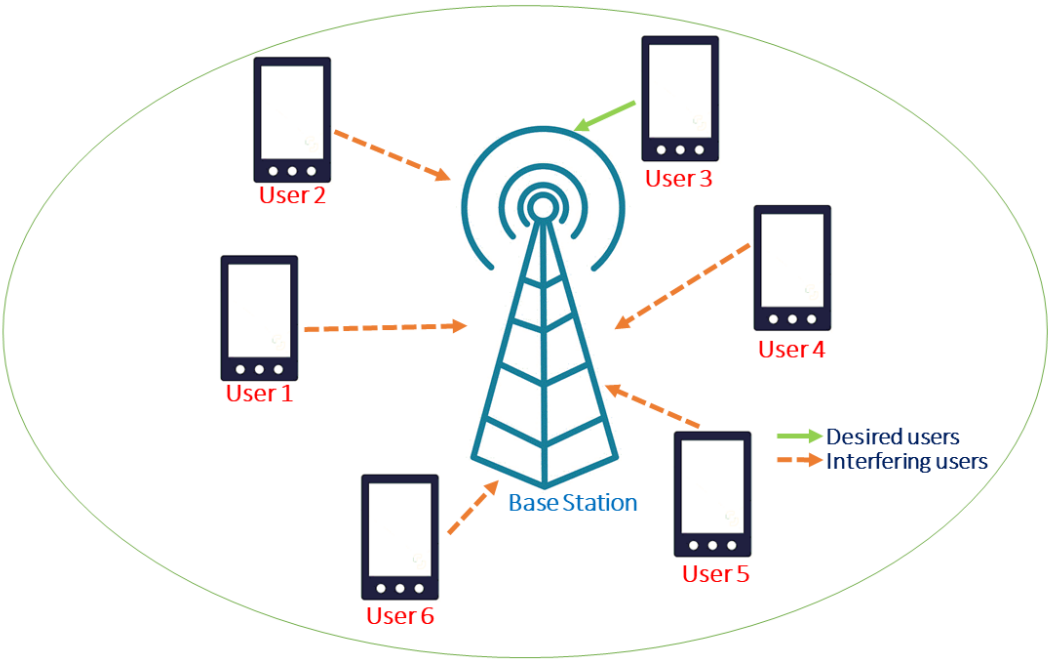

Figure 1.1: The system model.

Fig. 1.1 illustrates the system model where a single cell with one BS is located in the center and users are randomly distributed in the geographic area of the cell. It is assumed that every user has the same amount of resources and resources are shared so that there is mutual interference to the others due to concurrent transmission. With most power allocation schemes [12–15], only the channel path loss is considered, and the interference is assumed to be Gaussian distributed. However, wireless signals can be affected by multipath fading [16]. and the resulting channel variations should be considered in the power allocation scheme [17]. The Nakagami-m and Rayleigh distributions are commonly used to model fading [18]. The topography and objects obstructing the signal path cause shadowing [19] and this is typically modeled by a log normal distribution.

1.3 Power Allocation

The goal of power allocation is to reduce the power consumption of the system and increase the efficiency of the resource sharing strategies. Further, quality of service

(QoS) goals such as target signal to interference plus noise ratio (SINR) and outage probability should be achieved. The outage probability is the probability that the user SINR falls below a target SINR. Power allocation is conducted periodically depending on the channel conditions and the number of users. There are two types of power allocation, centralized power allocation (CPA) [20–22] and distributed power allocation (DPA) [23–25]. In CPA, the core network determines the optimal power levels for all users simultaneously using the channel state information (CSI) and target SINR. Therefore, CPA requires measurement of the channel gains which creates communication overhead between the core network and BSs. Thus, realization in a large system is challenging. With DPA, users determine their power levels using only local information and minimum feedback from the BSs. However, power levels may not be optimal, resulting in performance degradation. In general, DPA is preferred over CPA. There are three commonly used DPA schemes, single target SINR, variable SINR, and multiple target SINR.

Power allocation coordination can be implemented in a distributed manner using coordinated multi point (CoMP) joint transmission to further improve the cell edge performance and improve energy efficiency [26, 27]. In CoMP systems, coordinated base stations (BSs) are interconnected via a high speed network. In the case of joint transmission, the coordinated BSs share channel state information (CSI) and the information of all users [28]. Hence, the inter cell interference is reduced by using the signals transmitted from other cells to assist the transmission instead of acting as interference. Global coordination requires an enormous amount of feedback and backhaul overhead [29]. In order to reduce the inter BS communication overhead, power allocation with user grouping and clustering of BSs has been used [30]. With user grouping, only a subset of users with CoMP joint transmission is served. With clustering of BSs, the cell is divided into small subsystems and so clusters of BSs are considered.

1.4 Cell Association

There are three popular cell association schemes, max SINR based cell association, CRE, and CRE with ABS. With max SINR based cell association [31, 32], users are associated with the BS that provides the largest SINR, highest reference signal received power (RSRP) or maximum reference signal received quality (RSRQ). Then, most users may connect to MBSs due to transmit power differences between MBSs and

SBSs. This can cause overloaded MBSs and underutilized SBSs. With CRE [33], a positive bias is added to the SBS signal strengths, which make SBS more attractive to users. The drawback of this approach is that users in the CRE region can have a poor quality SBS channel and strong inter tier interference from MBSs. CRE with ABS uses time domain orthogonalization at the MBSs which leaves some subframes almost blank [34, 35]. This provides a window for SBSs to serve users in the CRE region with reduced inter tier interference. However, this solution wastes MBS subframes and thus throughput, and the blank to number of subframes ratio (ABS ratio) needs to be determined carefully.

This dissertation considers CAPA in cellular networks. Cell association is used to maintain good communication links and avoid BS overloading. Power allocation is used to manage user transmit power levels so that the interference to other users and the aggregate power consumption are reduced. Further, in a cellular network, there exist different types of users with various requirements. Thus, CAPA is investigated considering different user priorities and requirements. Users who require high and stable data rates, and active users, should have a high priority, and so are called priority users (PUs). Users who require low and variable data rates, and new users, are called normal users (NUs). To satisfy data rate requirements, reduce power consumption and avoid BS overloading, prioritized CAPA in cellular networks is employed. PU requirements should be satisfied first, and then as many NUs as possible should be satisfied with their target SINRs. PUs are assigned to BSs with small loads and good channel conditions while NUs adjust their transmit power given that PU requirements are met.

1.5 Contributions and Organization

The contributions of this dissertation are as follows.

1. The outage probability over Nakagami-m and Rayleigh fading channels is derived based on the normalized SINR. This characterizes how the normalized SINR affects the outage probability. The normalized SINR is the ratio of the average SINR to target SINR. Upper and lower bounds on the outage probability are also derived.

2. Two power allocation methods are proposed to minimize the outage probability. One is solved using interior point optimization with geometric programming

while the other is solved using Perron-Frobenius theory which is given in Algorithm 1.

3. Two power allocation methods are proposed to maximize the normalized SINR. One is solved using interior point optimization with geometric programming while the other is solved using Perron-Frobenius theory which is given in Algorithm 2.

4. A power allocation problem for power consumption minimization with an outage probability constraint is proposed. An upper bound on the outage probability is determined so that users are satisfied with their target SINRs. The proposed power allocation problem is then solved iteratively and is given in Algorithm 3.

5. A power allocation scheme with normalized SINR constraints is proposed and given in Algorithm 4. The outage probability and normalized SINR are used to determine which users should be removed.

6. Power allocation for throughput maximization with an outage probability constraint is proposed and given in Algorithm 5. The original problem is split into two subproblems using the Lagrangian method.

7. Power allocation for energy efficiency with an outage probability constraint is proposed and given in Algorithm 6. The original problem is a fractional programming problem, and so is converted into a linear form using parametric transformation.

8. A differential method to maximize the throughput is proposed and given in Algorithm 7. The original problem is logarithmic and so is split into two subproblems by introducing auxiliary functions. These subproblems are solved alternatively and iteratively using a differential method.

9. An approach to solve the energy efficiency problem is proposed and given in Algorithm 8. The original problem is a fractional programming problem and so is converted into a linear form using the Dinkelback transformation. An iterative approach using the Newton method is then used to solve this problem.

10. A prioritized and selective power allocation problem considering user priority is proposed. This problem is solved using the Lagrangian method and is given in Algorithm 9.

11. Finally, the CAPA problem in HetNets is examined. A two stage CAPA approach is proposed and given in Algorithm 10. The first stage considers the PUs and NUs while the second stage is employed by the BS. Unfortunately, the proposed optimization problem is nonconvex. Thus, a two loop algorithm is employed so that user transmit power and cell association are alternately optimized. Specifically, the outer loop performs cell association using Lagrange multipliers, and user transmit power is adjusted in the inner loop using a power update function (PUF). An exponential rule and the Nesterov subgradient method are used to accelerate inner and outer loop convergence, respectively.

The performance of the algorithms is evaluated using a MacBook Air with 1.6 GHz CPU (Intel Core i5, dual core, 4 threads, 4 MB cache), 8 GB RAM (2.133 MHz LPDDR3), and 128 GB memory (PCIe SSD). The remainder of the dissertation is organized as follows.

In Chapter 2, optimal power allocation in cellular networks based on outage probability and normalized SINR is discussed. Power allocation algorithms to maximize the normalized SINR and minimize power consumption are proposed assuming Rayleigh fading channels. Upper and lower bounds on the outage probability are determined using the normalized SINR considering path loss, shadowing, and fading.

In Chapter 3, power allocation for throughput and energy efficiency over Rayleigh fading channels in cellular networks is investigated. Power allocation problems to maximize the throughput and energy efficiency are derived and solved using parametric transformation and the Lagrangian method. Power allocation algorithms are proposed considering the outage probability constraint.

In Chapter 4, power allocation for throughput and energy efficiency over Nakagami-m fading channels in cellular networks is considered. A differential method is proposed to convert the logarithmic problem into a linear problem. Parametric transformation is then used to solve the throughput and energy efficiency problems. Upper and lower bounds on the outage probability are derived and shown to be tight.

In Chapter 5, prioritized and selective power allocation in cellular networks is examined. The power allocation is implemented considering user priority. Priority user (PU) requirements are satisfied first, and then as many normal users (NUs) as possible are satisfied with their target SINRs. If an NU is currently satisfied with their target SINR, they are not required to update their transmit power level. Conversely, NUs who are not satisfied update their power levels.

In Chapter 6, CAPA for HetNets is proposed based on user priority, channel

condition and BS traffic load. The goal is to improve network utility and reduce power consumption while considering user priority. PUs are associated with the BSs that provide good channel condition with a low number of users. NUs are connected to BSs so that the network utility is maximized. In addition, prioritized power allocation is used to reduce power consumption.

Finally, some concluding remarks and suggestions for future work are given in Chapter 7.

Chapter 2

Optimal Power Allocation in Cellular Networks based on Outage Probability and Normalized SINR

Power allocation is an important problem in wireless networks [36, 37]. The goal of power allocation is to reduce the power consumption of the system and increase the efficiency of the spectrum sharing. Power allocation to minimize the maximum (minmax) outage probability problems and maximize the minimum (maxmin) signal to interference plus noise ratio (SINR) problems in cellular networks were considered in [38–40]. These are known as outage probability and SINR maxmin fairness schemes. In [38], joint power control and resource allocation for outage balancing in a multicarrier network with femtocells and macrocells was considered. The objective is to minimize the maximum femtocell user outage probability constrained on the macrocell user outage requirements given the channel state information (CSI). In [39], maximizing the worst user SINR was proposed while in [40], a joint minmax outage probability and maxmin SINR algorithm was presented. Three power allocation schemes were proposed. The first maximizes the sum rate by selecting the base stations with good channel conditions for communications. The second minimizes the number of users in outage, while the third maximizes the minimum SINR considering the sum rate and outage probability.

In [41], two distributed power allocation schemes for high and low SINR scenarios were proposed and solved using geometric programming (GP). In [42], an iterative SINR tracking power control (ISPC) scheme for use with successive interference can-

cellation (SIC) in the presence of cancellation errors was proposed. Users increase their transmit power if the SINR is lower than a target SINR and vice versa. In [43], a distributed uplink power control (DUPC) scheme to address the uplink interference management problem in cellular networks was proposed so that the smallest number of users is removed to satisfy the target SINR requirements of all remaining users. In [44], a rate adaptive and opportunistic power control (RAPC) algorithm was proposed. This algorithm exploits channel variation and transmits opportunistically to maximize the system throughput. In RAPC, users increase their transmit power when the channel is good and decrease their power when the channel is poor. However, the user outage probability is not considered in ISPC and RAPC, which can lead to poor performance. In addition, the relationship between the normalized SINR and outage probability with path loss, shadowing and Rayleigh fading was not considered. The normalized SINR is the ratio of the average SINR to target SINR.

In this chapter, upper and lower bounds on the outage probability for a given normalized SINR are derived, and the upper bound is shown to be tight. Then, power allocation to minimize the outage probability or maximize the normalized SINR is considered. Two optimal approaches are proposed and solutions obtained by transforming the corresponding problems into nonlinear convex problems. One determines the optimum power levels using the interior point algorithm for GP problems. The other is based on Perron-Frobenius theory and is solved in a iterative manner. These solutions provide the global optimum for the outage probability and normalized SINR power allocation problems. Finally, two power allocation schemes to minimize the power consumption are proposed subject to constraints on the outage probability and normalized SINR.

The contributions of this chapter are as follows.

1. An expression for the outage probability is derived based on the normalized SINR. This shows that increasing the normalized SINR reduces the outage probability, and vice versa.

2. Two power allocation methods are proposed to minimize the outage probability. One is solved using the interior point algorithm for GP problems while the other is solved using Perron-Frobenius theory which is given in Algorithm 1.

3. Two power allocation methods are proposed to maximize the normalized SINR. One is solved using the interior point algorithm for GP problems while the other is solved using Perron-Frobenius theory which is given in Algorithm 2.

4. Two power allocation approaches with outage probability and target SINR constraints are given in Algorithms 3 and 4, respectively. The relationship between the outage probability and normalized SINR is used to adjust the user transmit power.

5. Simulation results are presented to compare the performance of the proposed algorithms with existing power allocation schemes.

The rest of the chapter is organized as follows. The system model is described in Section II. The problem formulation considering outage probability and normalized SINR is presented in Section III. The performance of the proposed approaches is evaluated in Section IV, and finally some concluding remarks are given in Section V.

2.1 System Model

Consider a system with k interfering users indexed $1, 2, \ldots, k$, and define the transmit power of user i as p_i, $i = 1, 2, \ldots, k$. The path loss for user i is given by [45]

$$h_i = \bar{h} d_i^{-\alpha},$$

where $\bar{h} = 0.97$ is a constant, d_i is the distance between user i and the BS, and α is the path loss exponent. A number of values for α have been proposed for different propagation environments. A value of $\alpha = 3$ is commonly used to model path loss in urban and suburban environments and so is employed here. The channel gain with log normal shadowing can be expressed as [46, 47]

$$g_i = h_i 10^{0.1\Xi},$$

where Ξ is a zero mean Gaussian random variable. The average received power is defined as [48]

$$\bar{p_i} = g_i \mathbb{E}\left[{X_i}^2\right] p_i = g_i p_i, \tag{2.1}$$

where X_i^2 denotes the fading of user i which is assumed to be an independent and identically distributed (i.i.d.) exponential random variable with unit mean [49, 50].

2.1.1 Normalized SINR and outage probability

The SINR of user i is given by

$$\gamma_i = \frac{g_i {X_i}^2 p_i}{\sum_{j \neq i} g_j {X_j}^2 p_j + \sigma_i^2}, \tag{2.2}$$

where σ_i^2 is the additive white Gaussian noise (AWGN) power of user i, and X_j^2 and g_j denote the fading and channel gain of the interference, respectively, from user j. Using (2.1), the average SINR for user i is given by

$$\bar{\gamma_i} = \frac{g_i \mathbb{E}[{X_i}^2] p_i}{\sum_{j \neq i} g_j \mathbb{E}[{X_j}^2] p_j + \sigma_i^2} = \frac{g_i p_i}{\sum_{j \neq i} g_j p_j + \sigma_i^2}, \tag{2.3}$$

and the normalized SINR is defined as

$$\overline{SINR}_i = \frac{\bar{\gamma_i}}{\hat{\gamma_i}} = \frac{g_i p_i}{\hat{\gamma_i} \left\{ \sum_{j \neq i} g_j p_j + \sigma_i^2 \right\}}, \tag{2.4}$$

where $\hat{\gamma_i}$ is the target SINR.

The outage probability for user i is defined as the probability that the target SINR is not achieved and can be expressed as

$$O_i = \mathbb{P}(\gamma_i \leq \hat{\gamma_i}) = \mathbb{P}(g_i {X_i}^2 p_i \leq \hat{\gamma_i} (\sum_{j \neq i} g_j {X_j}^2 p_j + \sigma_i^2)). \tag{2.5}$$

If the received signal power and interference power are exponentially distributed, then the outage probability is [51–53]

$$O_i = 1 - \exp(-\frac{\Lambda_i}{\bar{p_i}}) \phi_i(\frac{\hat{\gamma_i}}{\bar{p_i}}), \tag{2.6}$$

where $\Lambda_i = \sigma_i^2 \hat{\gamma_i}$, $\bar{p_i}$ is the mean received power and $\phi_i(\cdot)$ is the moment generating function (MGF) of the interference to user i which is given by

$$\phi_i(\frac{\hat{\gamma_i}}{\bar{p_i}}) = \prod_{j=1, j \neq i}^{k} \phi_j(\frac{\hat{\gamma_i}}{\bar{p_i}}) = \prod_{j=1, j \neq i}^{k} \frac{1}{1 + \bar{p_j} \frac{\hat{\gamma_i}}{\bar{p_i}}}, \tag{2.7}$$

where $\bar{p_j}$ is the mean received power of the interference to user i. The corresponding

outage probability is

$$O_i = 1 - \exp\left(-\frac{\sigma_i^2 \hat{\gamma}_i}{g_i p_i}\right) \prod_{j=1, j\neq i}^{k} \frac{1}{1 + \frac{\hat{\gamma}_i g_j p_j}{g_i p_i}}. \tag{2.8}$$

2.1.2 Upper and lower bounds on the outage probability

Upper and lower bounds on the outage probability can be obtained using the Maclaurin [54] and Weierstrass [55] inequalities

$$1 + a + \sum_{i=1}^{k} x_i \leq e^a \prod_{i=1}^{k} (1 + x_i) \leq e^{(a + \sum_{i=1}^{k}(x_i))}, \tag{2.9}$$

where $x_1, x_2, \ldots, x_k \geq 0$ and $a, k \geq 0$. The outage probability in (2.6) can be rewritten as

$$O_i = 1 - \left[\exp\left(\frac{\sigma_i^2 \hat{\gamma}_i}{g_i p_i}\right) \prod_{j=1, j\neq i}^{k} \left(1 + \frac{\hat{\gamma}_i g_j p_j}{g_i p_i}\right)\right]^{-1}.$$

Using the right hand inequality in (2.9), the upper bound on the outage probability is

$$\begin{aligned}
O_i &\leq 1 - \left[\exp\left(\frac{\sigma_i^2 \hat{\gamma}_i}{g_i p_i} + \sum_{j=1, j\neq i}^{k} \frac{\hat{\gamma}_i g_j p_j}{g_i p_i}\right)\right]^{-1} \\
&= 1 - \left[\exp\left(\frac{\hat{\gamma}_i}{g_i p_i}\left(\sigma_i^2 + \sum_{j=1, j\neq i}^{k} g_j p_j\right)\right)\right]^{-1} \\
&= 1 - \left[\exp\left(\frac{1}{\overline{SINR_i}}\right)\right]^{-1} \\
&= 1 - \left[\exp\left(-\frac{1}{\overline{SINR_i}}\right)\right] \\
&= O_u,
\end{aligned}$$

and using the left side inequality gives the lower bound

$$\begin{aligned} O_i &\geq 1 - \left[1 + \frac{\sigma_i^2 \hat{\gamma}_i}{g_i p_i} + \sum_{j=1, j\neq i}^{k} \left(\frac{\hat{\gamma}_i g_j p_j}{g_i p_i}\right)\right]^{-1} \\ &= 1 - \left[1 + \frac{1}{\overline{SINR_i}}\right]^{-1} \\ &= \frac{1}{\left(1 + \overline{SINR_i}\right)} \\ &= O_l. \end{aligned}$$

Thus we have that

$$\frac{1}{\left(1 + \overline{SINR_i}\right)} \leq O_i \leq 1 - \left[\exp\left(-\frac{1}{\overline{SINR_i}}\right)\right]. \tag{2.10}$$

2.2 Problem Formulation

In this section, the power allocation problems to minimize the outage probability or maximize the normalized SINR are considered. Then, iterative power allocation schemes using Perron-Frobenius theory and the interior point algorithm are proposed to solve these problems. A power allocation algorithm to minimize power consumption with outage probability constraints is also proposed. Users with an outage probability above a threshold O_{th} adjust their transmit power levels to reduce the interference to other users. Finally, a power allocation algorithm with a normalized SINR constraint is proposed. The outage probability is used as the removal criteria.

2.2.1 Outage probability minimization

The power allocation problem for outage probability minimization is as follows

$$\begin{aligned} &\text{minimize} && O_{\max} \\ &\text{subject to} && p_{\min} \leq p_i \leq p_{\max}, \end{aligned} \tag{2.11}$$

where $p_{\max}$ and $p_{\min}$ are the maximum and minimum transmit power, respectively, and $O_{\max}$ is the maximum outage probability over all users which is given by

$$O_{\max} = \max_i O_i = \max_i \left\{ 1 - \left[\exp\left(\frac{\sigma_i^2 \hat{\gamma}_i}{g_i p_i} \right) \prod_{j=1, j\neq i}^{k} \left(1 + \frac{\hat{\gamma}_i g_j p_j}{g_i p_i} \right) \right]^{-1} \right\}.$$

This can be written as

$$1 - \left[\exp\left(\frac{\sigma_i^2 \hat{\gamma}_i}{g_i p_i} \right) \prod_{j=1, j\neq i}^{k} \left(1 + \frac{\hat{\gamma}_i g_j p_j}{g_i p_i} \right) \right]^{-1} \leq O_{\max}$$

$$\exp\left(\frac{\sigma_i^2 \hat{\gamma}_i}{g_i p_i} \right) \prod_{j=1, j\neq i}^{k} \left(1 + \frac{\hat{\gamma}_i g_j p_j}{g_i p_i} \right) \leq \frac{1}{1 - O_{\max}}.$$

Let $\zeta = \frac{1}{1-O_{\max}}$. The power allocation problem for outage probability minimization is equivalent to minimizing ζ, so it can be reformulated as

$$\begin{aligned} \text{minimize} \quad & \zeta \\ \text{subject to} \quad & \frac{p_{\min}}{p_i} \leq 1 \\ & \frac{p_i}{p_{\max}} \leq 1 \\ & \exp\left(\frac{\sigma_i^2 \hat{\gamma}_i}{g_i p_i} \right) \prod_{j=1, j\neq i}^{k} \left(1 + \frac{\hat{\gamma}_i g_j p_j}{g_i p_i} \right) \leq \zeta. \end{aligned} \tag{2.12}$$

This is a geometric programming optimization problem with variables $p_1, p_2, \ldots, p_k$ and ζ. Therefore, it can be solved using the interior point algorithm for convex optimization (CVX).

The transmit power of user i which achieves the minimum in (2.12) corresponds to the power level in which the last constraint in (2.12) is satisfied with equality [56,57]. Thus, the goal is to determine the minimum outage probability which achieves this [58]. This outage probability is given by

$$\psi = 1 - \left[\exp\left(\frac{\sigma_i^2 \hat{\gamma}_i}{g_i p_i} \right) \prod_{j=1, j\neq i}^{k} \left(1 + \frac{\hat{\gamma}_i g_j p_j}{g_i p_i} \right) \right]^{-1},$$

so the problem can be rewritten as

$$\begin{aligned} &\text{minimize} && \psi \\ &\text{subject to} && p_{\min} \le p_i \le p_{\max} \\ & && 1 - \left[\exp\left(\frac{\sigma_i^2 \hat{\gamma}_i}{g_i p_i} \right) \prod_{j=1, j \neq i}^{k} \left(1 + \frac{\hat{\gamma}_i g_j p_j}{g_i p_i} \right) \right]^{-1} = \psi. \end{aligned} \tag{2.13}$$

The last constraint is equivalent to

$$\exp\left(\frac{\sigma_i^2 \hat{\gamma}_i}{g_i p_i} \right) \prod_{j=1, j \neq i}^{k} \left(1 + \frac{\hat{\gamma}_i g_j p_j}{g_i p_i} \right) = \frac{1}{1 - \psi}.$$

Taking the logarithm of both sides gives

$$\log \left[\exp\left(\frac{\sigma_i^2 \hat{\gamma}_i}{g_i p_i} \right) \prod_{j=1, j \neq i}^{k} \left(1 + \frac{\hat{\gamma}_i g_j p_j}{g_i p_i} \right) \right] = \log \left(\frac{1}{1 - \psi} \right),$$

which can be expressed as

$$\frac{\sigma_i^2 \hat{\gamma}_i}{g_i p_i} + \sum_{j=1, j \neq i}^{k} \log \left(1 + \frac{\hat{\gamma}_i g_j p_j}{g_i p_i} \right) = \log \left(\frac{1}{1 - \psi} \right).$$

After some manipulation this becomes

$$\sum_{j=1, j \neq i}^{k} \left[\log \left(1 + \frac{\hat{\gamma}_i g_j p_j}{g_i p_i} \right) + \frac{\sigma_i^2 \hat{\gamma}_i}{(k-1) g_i p_i} \right] = \log \left(\frac{1}{1 - \psi} \right),$$

which is equivalent to

$$\sum_{j=1, j \neq i}^{k} \frac{p_i}{p_j} \left[\log \left(1 + \frac{\hat{\gamma}_i g_j p_j}{g_i p_i} \right) + \frac{\sigma_i^2 \hat{\gamma}_i}{(k-1) g_i p_i} \right] p_j = \left[\log \left(\frac{1}{1 - \psi} \right) \right] p_i.$$

This can be written as $U(p_j) p_j = \chi p_i$ where $\chi = \log(\frac{1}{1-\psi})$ and the matrix $U(p_j)$ is given by

$$U(p_j) = \frac{p_i}{p_j} \left[\log \left(1 + \frac{\hat{\gamma}_i g_j p_j}{g_i p_i} \right) + \frac{\sigma_i^2 \hat{\gamma}_i}{(k-1) g_i p_i} \right]. \tag{2.14}$$

The optimization problem with respect to ψ is then equivalent to minimizing χ.

The variables for the power allocation problem (2.13) are $p_1, p_2, \ldots, p_k$ and χ. This problem can be solved efficiently using the iterative Perron-Frobenius method [59,60]. The objective is to determine the minimum χ such that the criterion $U(p_j)p_j = \chi p_i$ is satisfied. The proposed algorithm for outage probability minimization is summarized in Algorithm 1. First, $U(p_j)$ is determined using (2.14). This characterizes the effect of the target SINR, interference and noise on user i. Then, the transmit power for user i is adjusted based on $U(p_j)$ until the algorithm converges. The optimal power allocation for user i then corresponds to the Perron-Frobenius eigenvector of $U(p_j)$, and χ is the eigenvalue of $U(p_j)$.

Algorithm 1 Iterative Perron-Frobenius Algorithm for Outage Probability Minimization

---

Step 1: Initialize the iteration index $t = 1$, the transmit power $p_i(t) = p_{\min}$ and set the target SINRs $\hat{\gamma}_i$.

Step 2: Determine $U(p_j(t))$ using

$$U(p_j(t)) = \frac{p_i(t)}{p_j(t)} \left[\log\left(1 + \frac{\hat{\gamma}_i(t) g_j p_j(t)}{g_i p_i(t)}\right) + \frac{\sigma_i^2 \hat{\gamma}_i}{(k-1) g_i p_i(t)} \right], \quad i = 1, 2, \ldots, k \text{ and } j \neq i.$$

Step 3: Update $p_i(t)$ using

$$U(p_j(t))p_j(t) = \chi p_i(t+1).$$

Step 4: Terminate when

$$\max_i |p_i(t+1) - p_i(t)| \leq \epsilon,$$

otherwise go to **Step 2**.

2.2.2 Normalized SINR maximization

The power allocation problem for normalized SINR maximization is

$$\begin{aligned} &\text{maximize} && \overline{SINR}_{\min} \\ &\text{subject to} && p_{\min} \leq p_i \leq p_{\max}, \end{aligned} \tag{2.15}$$

where $\overline{SINR}_{\min}$ is the minimum normalized SINR over all users given by

$$\overline{SINR}_{\min} = \min_i \overline{SINR}_i = \min_i \left[\frac{g_i p_i}{\hat{\gamma}_i \left(\sum_{j \neq i} g_j p_j + \sigma_i^2 \right)} \right].$$

This expression is equivalent to

$$\frac{g_i p_i}{\hat{\gamma}_i \left(\sum_{j \neq i} g_j p_j + \sigma_i^2 \right)} \geq \overline{SINR}_{\min},$$

or

$$\frac{\hat{\gamma}_i \left(\sum_{j \neq i} g_j p_j + \sigma_i^2 \right)}{g_i p_i} \leq \frac{1}{\overline{SINR}_{\min}}.$$

Let $\tau = \frac{1}{\overline{SINR}_{\min}}$. The power allocation problem (2.15) is equivalent to minimizing τ, so it can be reformulated as

$$\begin{aligned} \text{minimize} \quad & \tau \\ \text{subject to} \quad & \frac{p_{\min}}{p_i} \leq 1 \\ & \frac{p_i}{p_{\max}} \leq 1 \\ & \frac{\hat{\gamma}_i \left(\sum_{j \neq i} g_j p_j + \sigma_i^2 \right)}{g_i p_i} \leq \tau. \end{aligned} \tag{2.16}$$

This is a geometric programming optimization problem with variables $p_1, p_2, \ldots, p_k$ and τ and so can be solved using the interior point algorithm for GP problems.

The transmit power of user i which achieves the minimum in (2.16) corresponds to the user transmit power level in which the last constraint in (2.16) is satisfied with equality [56, 57]. Thus, the goal is to determine the minimum τ which achieves this [58]. The optimal solution of (2.16) is given by

$$\vartheta = \frac{\hat{\gamma}_i}{g_i p_i} \left(\sum_{j \neq i} g_j p_j + \sigma_i^2 \right).$$

Thus, the power allocation problem for normalized SINR maximization can be rewrit-

ten as

$$\begin{aligned} \text{minimize} \quad & \vartheta \\ \text{subject to} \quad & p_{\min} \leq p_i \leq p_{\max} \\ & \frac{\hat{\gamma}_i \left(\sum_{j \neq i} g_j p_j + \sigma_i^2 \right)}{g_i p_i} = \vartheta. \end{aligned} \tag{2.17}$$

Multiplying both sides of the last constraint in (2.17) by p_i gives

$$\sum_{j \neq i} \frac{\hat{\gamma}_i}{g_i} \left(g_j p_j + \frac{\sigma_i^2}{k} \right) = \vartheta p_i,$$

which is equivalent to

$$\sum_{j \neq i} \frac{\hat{\gamma}_i}{g_i} \left(g_j + \frac{\sigma_i^2}{k p_j} \right) p_j = \vartheta p_i.$$

This can be expressed as $V(p_j)p_j = \vartheta p_i$ where

$$V(p_j) = \frac{\hat{\gamma}_i}{g_i} \left(g_j + \frac{\sigma_i^2}{k p_j} \right). \tag{2.18}$$

The power allocation problem in (2.17) has variables $p_1, p_2, \ldots, p_k$ and ϑ. This can be solved efficiently using the iterative Perron-Frobenius method [59, 60]. The objective is to determine the minimum ϑ such that the criterion $V(p_j)p_j = \vartheta p_i$ is satisfied. The corresponding algorithm for SINR maximization is summarized in Algorithm 2. First, $V(p_j)$ is determined using (2.18). $V(p_j)$ characterizes the effect of noise and interference on user i. Then, the transmit power for user i is adjusted based on $V(p_j)$ until the algorithm converges. The optimal power allocation for user i corresponds to the Perron-Frobenius eigenvector of $V(p_j)$, and ϑ is determined using the eigenvalue of $V(p_j)$.

Algorithm 2 Iterative Perron-Frobenius Algorithm for SINR Maximization

Step 1: Initialize the iteration index $t = 1$, and the transmit power $p_i(t) = p_{\min}$ and set the target SINR $\hat{\gamma}_i$.

Step 2: Determine $V(p_j(t))$ using

$$V(p_j(t)) = \frac{\hat{\gamma}_i(t)}{g_i}\left(g_j + \frac{\sigma_i^2}{kp_j(t)}\right), \quad i = 1, 2, \ldots, k \text{ and } j \neq i.$$

Step 3: Update $p_i(t)$ using

$$V(p_j(t+1))p_j(t) = \vartheta p_i(t).$$

Step 4: Terminate when

$$\max_i |p_i(t+1) - p_i(t)| \leq \epsilon,$$

otherwise go to **Step 2**.

2.2.3 Power allocation with an outage probability constraint

The power consumption problem subject to outage probability and transmit power constraints can be formulated as

$$\begin{aligned} \text{minimize} \quad & \sum_{i=1}^{k} p_i \\ \text{subject to} \quad & p_{\min} \leq p_i \leq p_{\max} \\ & 1 - \left[\exp\left(\frac{\sigma_i^2 \hat{\gamma}_i}{g_i p_i} \right) \prod_{j=1, j\neq i}^{k} \left(1 + \frac{\hat{\gamma}_i g_j p_j}{g_i p_i} \right) \right]^{-1} \leq O_{th}, \end{aligned} \tag{2.19}$$

where O_{th} is the outage probability threshold. This problem is equivalent to

$$\begin{aligned} \text{minimize} \quad & \sum_{i=1}^{k} p_i \\ \text{subject to} \quad & \frac{p_{\min}}{p_i} \leq 1 \\ & \frac{p_i}{p_{\max}} \leq 1 \\ & \left[\exp\left(\frac{\sigma_i^2 \hat{\gamma}_i}{g_i p_i} \right) \prod_{j=1, j\neq i}^{k} \left(1 + \frac{\hat{\gamma}_i g_j p_j}{g_i p_i} \right) \right] (1 - O_{th}) \leq 1. \end{aligned} \tag{2.20}$$

This is a geometric programming optimization problem with variables $p_1, p_2, \ldots, p_k$. Therefore, it can be solved using the interior point algorithm for GP.

Using the upper bound in (2.10) with the last constraint in (2.20) gives

$$1 - \left[\exp\left(\frac{\sigma_i^2 \hat{\gamma}_i}{g_i p_i} \right) \prod_{j=1, j\neq i}^{k} \left(1 + \frac{\hat{\gamma}_i g_j p_j}{g_i p_i} \right) \right]^{-1} \leq 1 - \left[\exp\left(-\frac{1}{\overline{SINR_i}} \right) \right] \leq O_{th}.$$

Thus, this constraint is satisfied when this bound is less than O_{th}

$$1 - \left[\exp\left(-\frac{1}{\overline{SINR_i}} \right) \right] \leq O_{th},$$

where $\overline{SINR}_i = \frac{\bar{\gamma}_i}{\hat{\gamma}_i}$. After some manipulation, this inequality can be written as

$$\bar{\gamma}_i \geq -\frac{\hat{\gamma}_i}{\log\left(1 - O_{th}\right)}.$$

The power allocation problem then becomes

$$\begin{aligned} \text{minimize} \quad & \sum_{i=1}^{k} p_i \\ \text{subject to} \quad & \frac{p_{\min}}{p_i} \leq 1 \\ & \frac{p_i}{p_{\max}} \leq 1 \\ & \bar{\gamma}_i \geq -\frac{\hat{\gamma}_i}{\log\left(1 - O_{th}\right)}. \end{aligned} \tag{2.21}$$

This can be solved using the following power update function

$$p_i(t+1) = -\frac{1}{\log\left(1 - O_{th}\right)} \frac{\hat{\gamma}_i(t)}{\bar{\gamma}_i} p_i(t). \tag{2.22}$$

The proposed power control algorithm based on (2.22) is given in Algorithm 3.

Algorithm 3 Power Allocation Algorithm With an Outage Probability Constraint

Step 1: Initialize the iteration index $t = 1$. User i obtain the outage probability threshold O_{th} from the BS and determines the average SINR $\bar{\gamma}_i$. Sets the target SINR $\hat{\gamma}_i$.

Step 2: Users update their transmit power using

$$p_i(t+1) = -\frac{1}{\log\left(1 - O_{th}\right)} \frac{\hat{\gamma}_i(t)}{\bar{\gamma}_i} p_i(t), \quad i = 1, 2, \ldots, k.$$

Step 3: Terminate when

$$\max_i \left| p_i(t+1) - p_i(t) \right| \leq \epsilon,$$

otherwise go to **Step 2**.

2.2.4 Power allocation with normalized SINR constraints

The power allocation problem with a normalized SINR constraint is

$$\begin{aligned} \text{minimize} \quad & \sum_{i=1}^{k} p_i \\ \text{subject to} \quad & \frac{p_{\min}}{p_i} \leq 1 \\ & \frac{p_i}{p_{\max}} \leq 1 \\ & \overline{SINR_i} \geq \beta_i, \end{aligned} \tag{2.23}$$

where $\overline{SINR_i} = \frac{\bar{\gamma}_i}{\hat{\gamma}_i}$ and β_i is a constant which is used as a control parameter. The higher the value of β_i, the greater the target SINR of user i. This problem can be solved using the following power update function

$$p_i(t+1) = \beta_i \frac{\hat{\gamma}_i(t)}{\bar{\gamma}_i} p_i(t). \tag{2.24}$$

A power allocation algorithm is now obtained using the outage probability threshold. Users increase their power level if their outage probability is less than the outage probability threshold, and the level is reduced if the outage probability is greater than the threshold. Therefore, if the outage probability of user i is above O_{th}, β_i is reduced, giving a lower target SINR. If the outage probability of user i is less than O_{th}, β_i is increased, giving a higher target SINR. β_i can then be defined as

$$\beta_i = \kappa(1 - O_i), \tag{2.25}$$

where $\kappa = \frac{1}{1-O_{th}}$. Thus, if the outage probability is equal to the outage probability threshold, the transmit power does not change. The proposed power control algorithm based on (2.24) and (2.25) is given in Algorithm 4.

2.3 Numerical Results

In this section, Monte Carlo simulation is used to evaluate the performance of the proposed power allocation schemes. As in [61–63], the channel gain is $g_i = \bar{h} d_i^{\alpha} 10^{0.1\Xi} {X_i}^2$ where $\bar{h} = 0.97$ is a constant, and $\alpha = 3$ is the path loss exponent which corresponds to typical urban and suburban environments. The stopping criteria is $\epsilon = 10^{-10}$. The

Algorithm 4 Power Allocation Algorithm With Normalized SINR Constraints

Step 1: Initialize the iteration index $t = 1$. User i obtain the outage probability threshold O_{th} from the BS and determines the average SINR $\bar{\gamma}_i$. Sets the target SINR $\hat{\gamma}_i$.

Step 2: User i determine β_i using

$$\beta_i(t) = \kappa(1 - O_i(t)).$$

Step 3: Users update their transmit power using

$$p_i(t+1) = \beta_i(t)\frac{\hat{\gamma}_i(t)}{\bar{\gamma}_i}p_i(t).$$

Step 3: Terminate when

$$\max_i |p_i(t+1) - p_i(t)| \leq \epsilon,$$

otherwise go to **Step 2**.

noise power is $\sigma^2 = 0.01$ W and the initial power level for all users is set to 1 W. The maximum transmit power is $p_{\max} = 2$ W. The number of taps for the Rayleigh fading channel is set to 4 [64]. The real and imaginary parts of the channel coefficients are randomly chosen from a Gaussian distribution. The magnitude is then Rayleigh distributed and the phase is uniformly distributed between 0 and 2π. The users are uniformly distributed in a 500 m $\times$ 500 m geographic area with the BS located at the center. Results are obtained for 10000 trials for each number of users with the user locations changed each trial.

Fig. 2.1 presents the exact average outage probability from (2.8) and the upper and lower bounds from (2.10) with 8, 16, 32, and 64 users, respectively. These results show that the upper bound is tight and is a better approximation than the lower bound, particularly for high SINRs and a large number of users. The maximum gap between the exact outage probability and the lower bound is 1.9% for 8 users, 5.8% for 16 users, 10.4% for 32 users, and 19.3% for 64 users. The maximum gap between the exact outage probability and the upper bound is 0.7% for 8 users, 1.1% for 16 users, 0.8% for 32 users, and 0.7% for 64 users. Thus, the upper bound is a suitable estimate for the outage probability in cellular networks.

Fig. 2.2 shows the average outage probability obtained via the GP problem in (2.12) and Algorithm 1 with 32 users. The outage probability is not determined directly by Algorithm 2 so (2.10) is used to obtain bounds on the outage probability. The average initial outage probability is the average outage probability without using any algorithm and varies from 12.0% to 19.1%. At 30 dB, the gap between the average outage probability for Algorithm 1 and the initial outage probability is 5.2%, which is the lowest, and at 10 dB, this gap is 11.7%, which is the highest. The average outage probabilities with Algorithm 1 and the GP method are almost identical. The gap between the average outage probability with Algorithm 1 and the upper bound using Algorithm 2 is almost 0, while the gap with the lower bound is large for a target SINR greater than 10 dB. The average computation time using Algorithm 1 and Algorithm 2 is 0.016 s and 0.013 s, respectively. The corresponding average time with GP is 1280 s, so this algorithm is much slower.

Fig. 2.3 gives the average outage probability with Algorithms 1 and 2 for 128 users. The bounds on outage probability for Algorithm 2 are also shown. The average initial outage probability varies from 19.0% to 99%. At 1 dB, the gap between the average outage probability for Algorithm 1 and the initial outage probability is 12%, which is the lowest, and at 9 dB, this gap is 41%, which is the highest. At 1 dB,

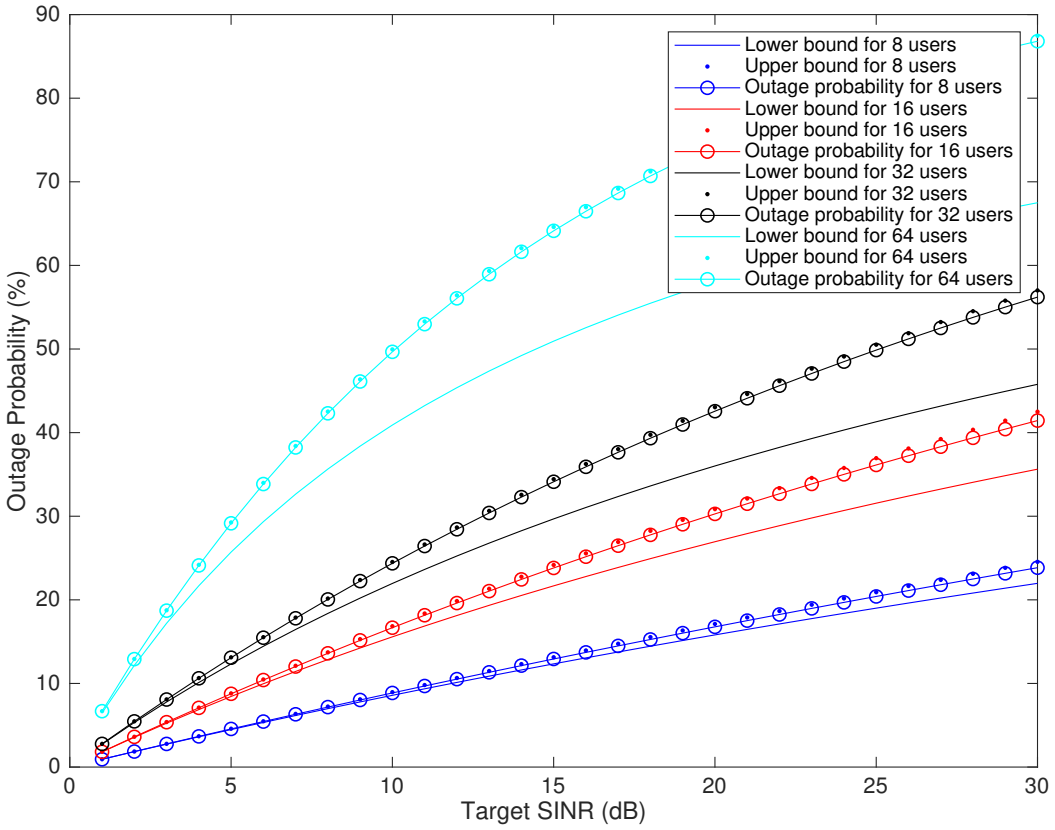

Figure 2.1: Upper and lower bounds on the average outage probability with different numbers of users.

the gap between Algorithm 1 and the lower bound using Algorithm 2 is 0.2% but this increases to 19.0% at 30 dB. The average outage probabilities with the upper bound using Algorithm 2 and Algorithm 1 are almost identical. In general, the higher the target SINR, the greater the outage probability. The average computation time using Algorithms 1 and 2 is 0.024 s and 0.015 s, respectively, so they have similar complexity.

Fig. 2.4 shows the average normalized SINR for theiterative SINR tracking power control (ISPC), distributed uplink power control (DUPC), rate adaptive opportunistic power control (RAPC) schemes and Algorithms 1 and 2, with 128 users. This shows that the results using outage probability and normalized SINR optimization in Algorithms 1 and 2 are similar and much better than with ISPC and DUPC. Algorithms 1 and 2 are slightly better than RAPC. Algorithm 2 gives the best performance as

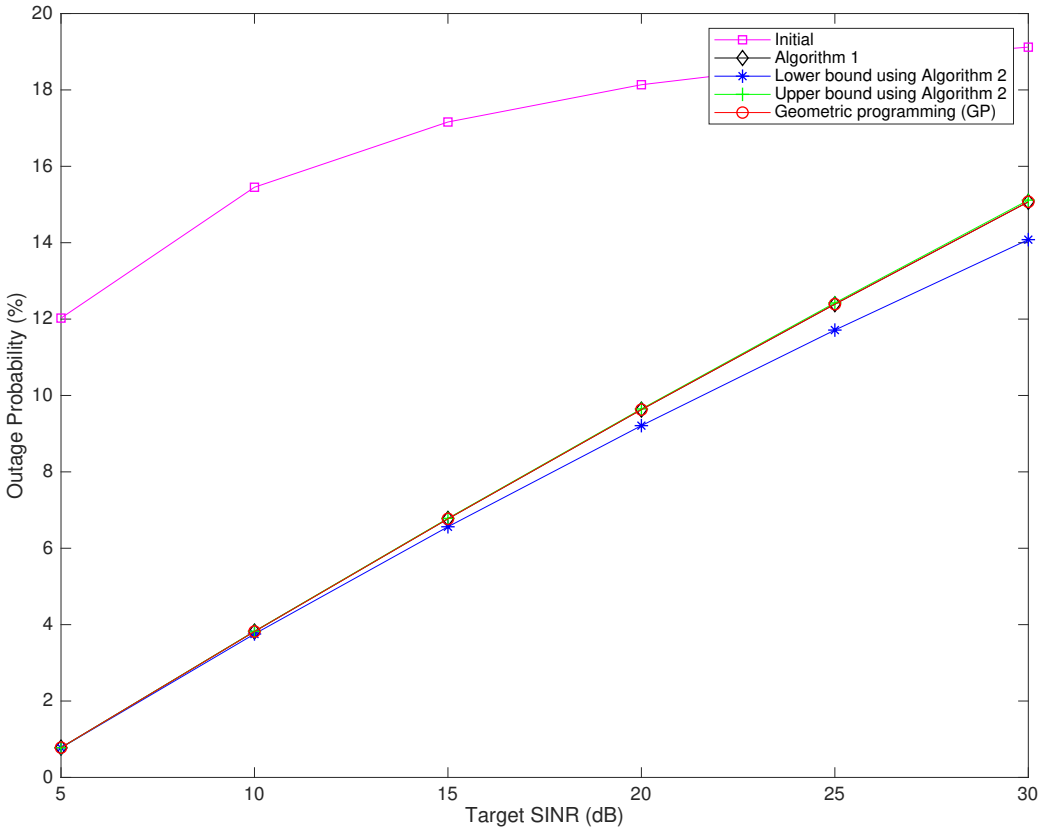

Figure 2.2: Average outage probability using geometric programming (GP) and Algorithms 1 and 2 with 32 users.

this is the algorithm criterion. The average normalized SINR is the worst with ISPC, followed by DUPC, and then RAPC. They are similar for a target SINR greater than 10 dB. Note that the average normalized SINR is not monotonic using DUPC and RAPC.

Fig. 2.5 shows the outage probability, transmit power and SINR for the distributed uplink power control (DUPC) scheme with 8 users for 1 trial. The target SINRs were chosen randomly in the range $[0.1, 0.5]$ dB and are

$$\hat{\gamma}_k = [0.18 \quad 0.32 \quad 0.48 \quad 0.16 \quad 0.15 \quad 0.20 \quad 0.16 \quad 0.11] \text{ dB}.$$

With DUPC, a higher outage probability results in a higher transmit power. These results show that the transmit power for user 2 is the highest since the corresponding

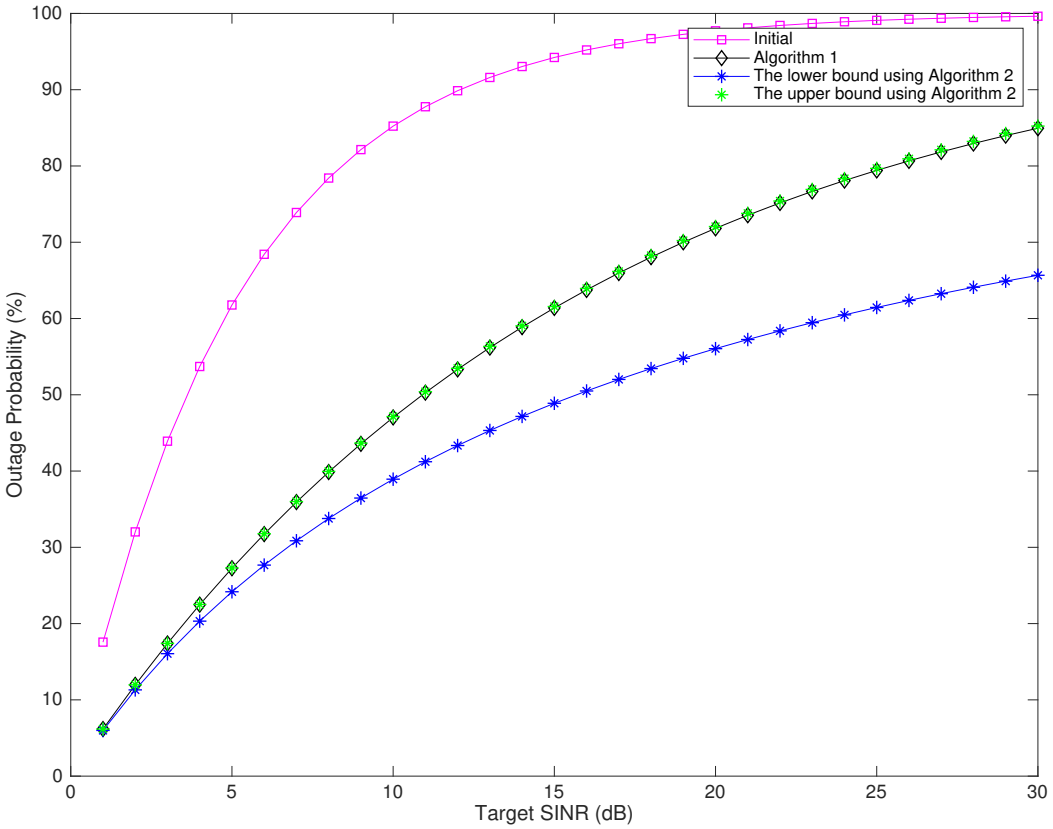

Figure 2.3: Average outage probability using Algorithms 1 and 2 with 128 users.

outage probability is the highest. This is followed by users 3 and 5. After 30 iterations, the average outage probability is 0.61, and the average required power is 0.62 W.

Fig. 2.6 shows the corresponding outage probability, transmit power and SINR for the iterative SINR tracking power control (ISPC) scheme. With ISPC, a higher target SINR results in a higher transmit power. As a high outage probability implies a poor SINR, user 7 requires more power to attain the target SINR compared to the other users. Next is user 3 which has the highest target SINR followed by user 2. The required power for users 5 and 8 is the lowest since their target SINRs are the lowest. After 30 iterations, the average outage probability is 0.58 and the average required power is 0.53 W, which are lower than with DUPC.

Fig. 2.7 shows the corresponding outage probability, transmit power and SINR for the rate adaptive and opportunistic power control (RAPC) scheme. With RAPC, a higher outage probability results in a lower SINR. These results show that the

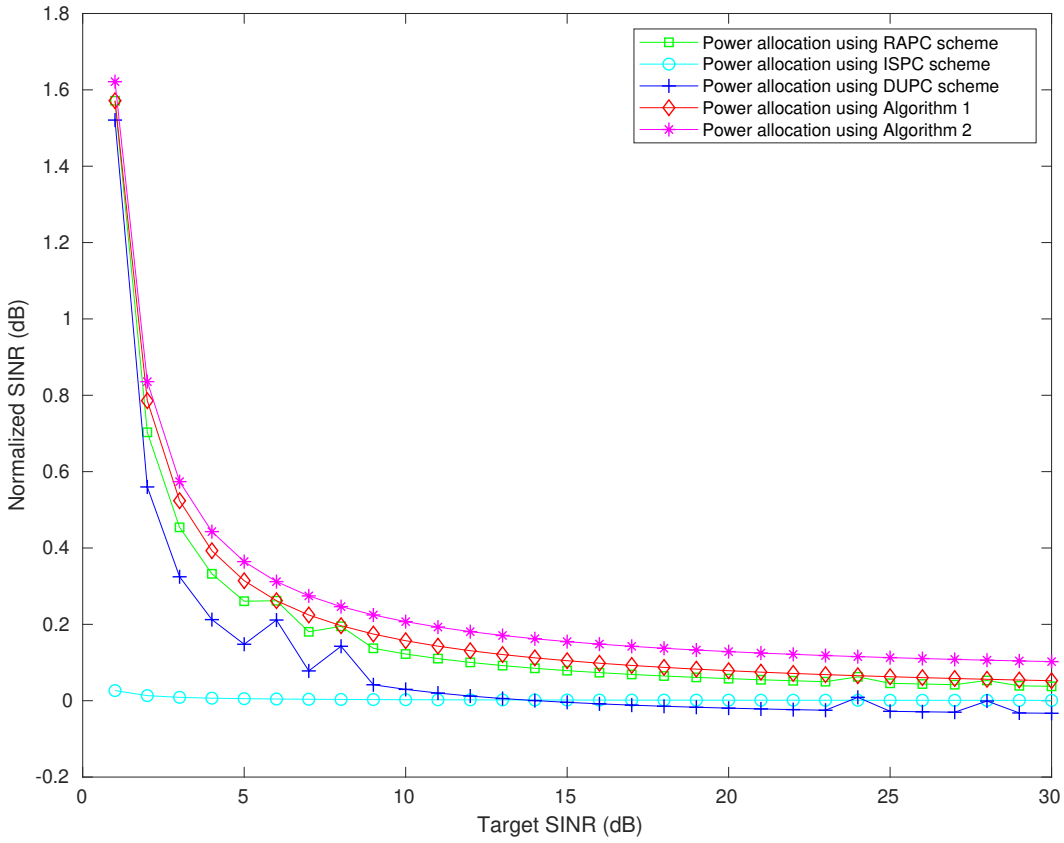

Figure 2.4: Average normalized SINR using ISPC, DUPC, RAPC, and Algorithms 1 and 2 with 128 users.

transmit power for user 3 is minimum since the outage probability for user 3 is the highest, which is 0.8. The outage probability for user 5 is the lowest, and thus the transmit power for user 5 is the highest, which is 0.39 W. After 30 iterations, the target SINRs for users 1, 3, and 5 were not met. The average outage probability is 0.57 and the average required power is 0.35 W, which are lower than with DUPC and ISPC.

Fig. 2.8 shows the outage probability, transmit power and SINR for the proposed power allocation scheme based on outage probability in Algorithm 3 with 8 users for 1 trial and 30 iterations. The target SINRs were chosen randomly in the range $[0.1, 0.5]$ dB and are the same as for DUPC, ISPC and RAPC. These results show that the outage probability and SINR for user 4 is the highest. Thus, the power required to obtain a target SINR for user 4 is the highest. Next is user 2 since the target SINR for

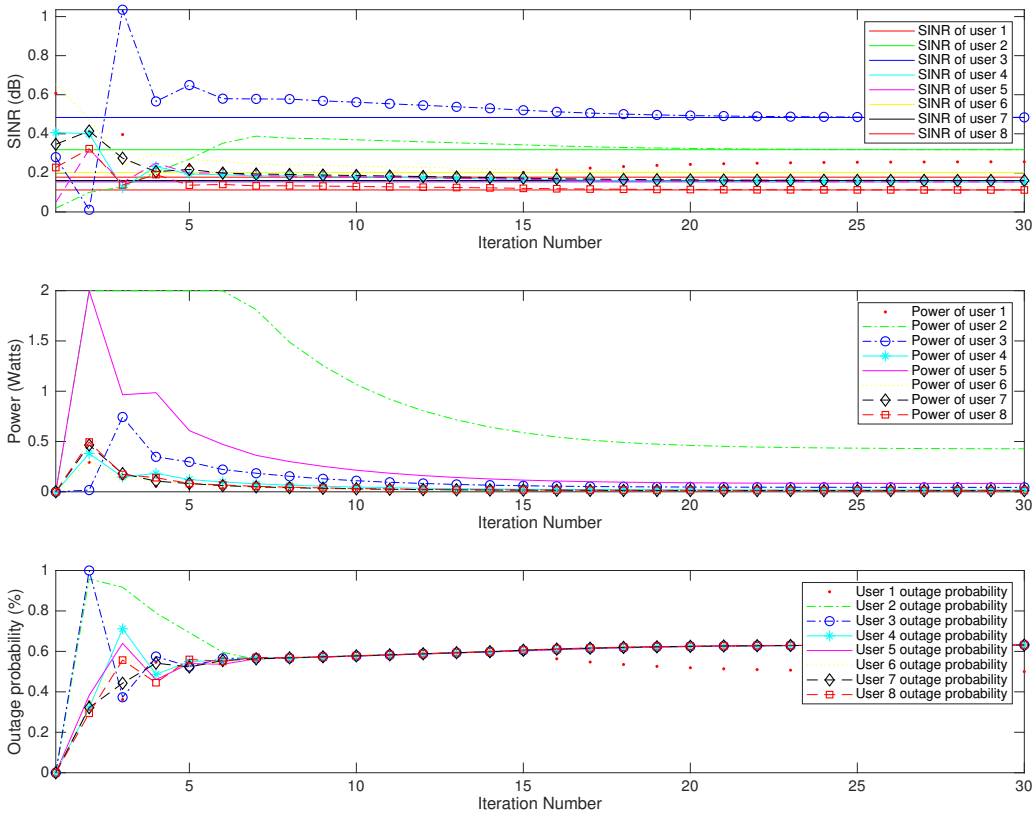

Figure 2.5: Normalized SINR, transmit power and outage probability for 8 users with DUPC.

user 2 is the second highest. The required powers for users 5 and 8 are the lowest since their target SINRs are the lowest. After 30 iterations, the average outage probability is 0.47, and the average required power is 0.14 W. These values are much lower than with DUPC, ISPC and RAPC. Fig. 2.9 shows the corresponding transmit power and SINR for 30 iterations with Algorithm 4 with fixed control parameter $\beta_i = 0.05$. These results show that after 30 iterations, all users have SINRs higher than their target SINRs. User 2 has the highest transmit power and the second highest target SINR. Further, this user has the highest initial outage probability, which explains why their transmit power is so high. After 30 iterations, the average outage probability is 0.57, and the average required power is 0.11 W. Fig. 2.10 shows the corresponding transmit power and SINR for 30 iterations with Algorithm 4. The dynamic control

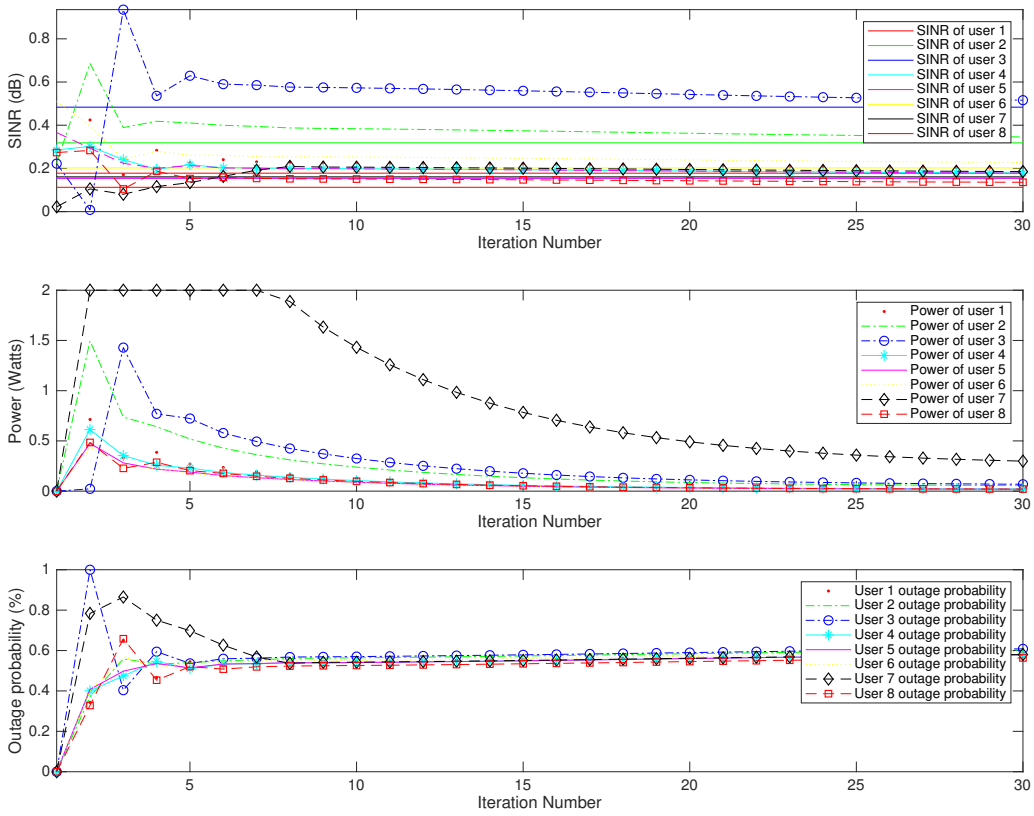

Figure 2.6: Normalized SINR, transmit power and outage probability for 8 users with ISPC.

parameter β_i was determined using (2.25) which gives

$$\beta_i = [0.29 \quad 0.09 \quad 0.12 \quad 0.04 \quad 0.27 \quad 0.03 \quad 0.01 \quad 0.15].$$

This figure shows that the outage probability for users 1, 5, and 8 is lower than that of the other users. Thus, the gap between the SINRs achieved and the corresponding targets is greater. These differences are

$$[0.13 \quad 0.03 \quad 0.07 \quad 0.01 \quad 0.16 \quad 0.01 \quad 0 \quad 0.15] \text{ dB}.$$

The outage probability for users 6 and 7 is the highest. Thus, their requirements are harder to satisfy and so the SINRs achieved are lower than those of the remaining users, except user 4. After 30 iterations, users with a low outage probability achieved

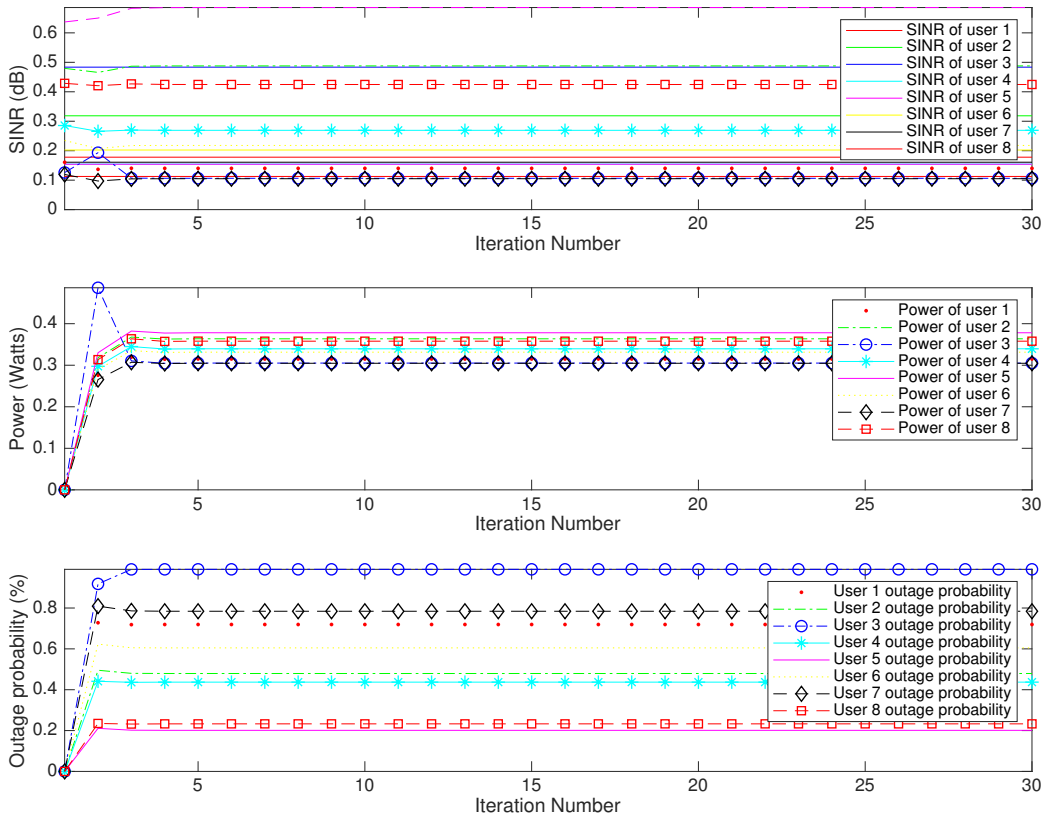

Figure 2.7: Normalized SINR, transmit power and outage probability for 8 users with RAPC.

higher SINRs compared to the others. The average outage probability is 0.51, and the average required power is 0.13 W.

2.4 Conclusion

In this chapter, power allocation schemes considering the outage probability and normalized signal to interference plus noise ratio (SINR) were proposed. The goal is to reduce the outage probability and increase the normalized SINR. Algorithm 1 is based on minimizing the outage probability and Algorithm 2 is based on maximizing the SINR. Results were presented which show that Algorithm 1, Algorithm 2 and geometric programming (GP) produce similar results, but the computation time with Algorithms 1 and 2 is much lower. Further, Algorithms 1 and 2 provide a higher

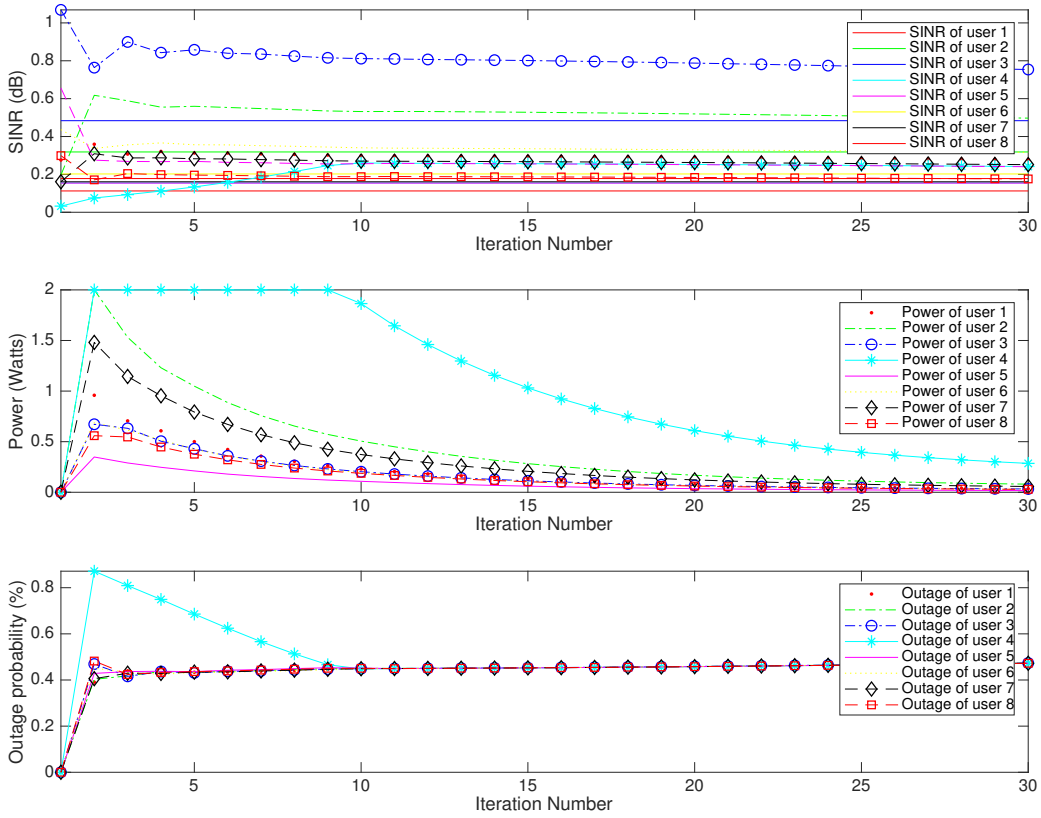

Figure 2.8: Normalized SINR, transmit power and outage probability for 8 users with Algorithm 3.

normalized SINR than the rate adaptive and opportunistic power control (RAPC) and distributed uplink power control (DUPC) schemes, while iterative SINR tracking power control (ISPC) is the worst. Power allocation schemes were also given to reduce the power consumption (Algorithm 3) and satisfy user SINR requirements (Algorithm 4). Algorithm 3 provides the best average outage probability, followed by Algorithm 4, RAPC and then ISPC, while DUPC is the worst. Algorithm 4 requires the lowest average power, followed by Algorithm 3, RAPC, ISPC, and finally DUPC.

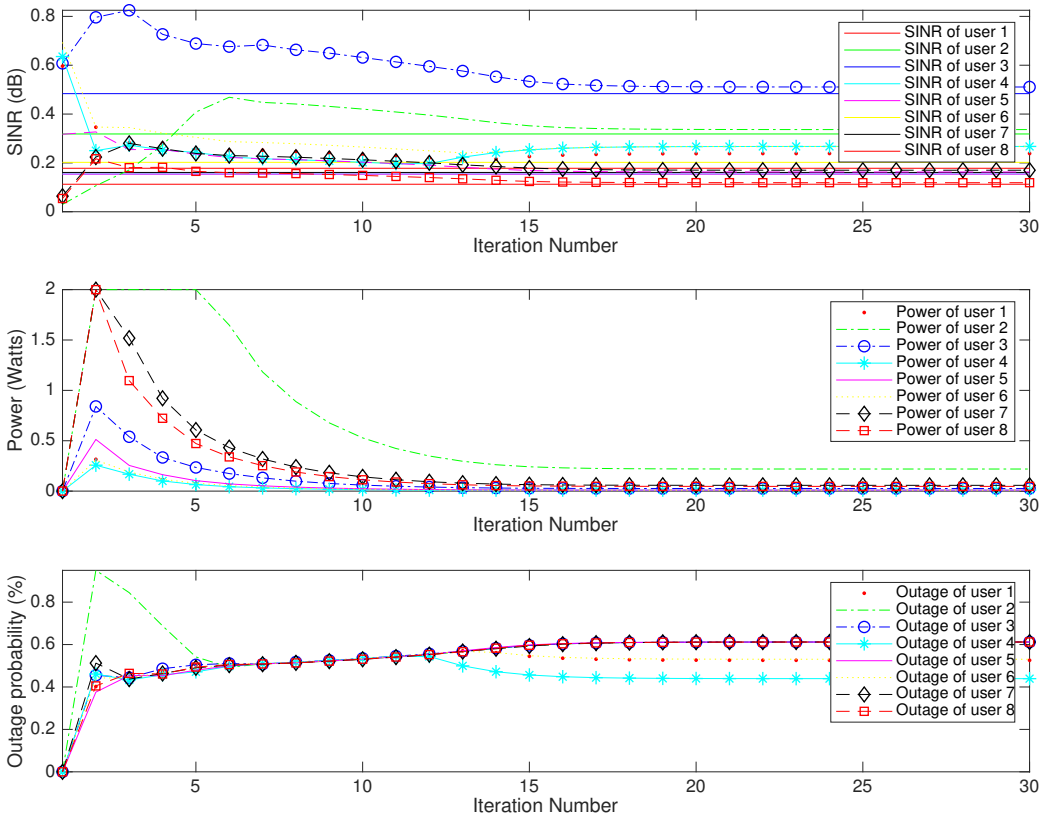

Figure 2.9: Normalized SINR, transmit power and outage probability for 8 users with Algorithm 4 and fixed control parameter $\beta_i = 0.05$.

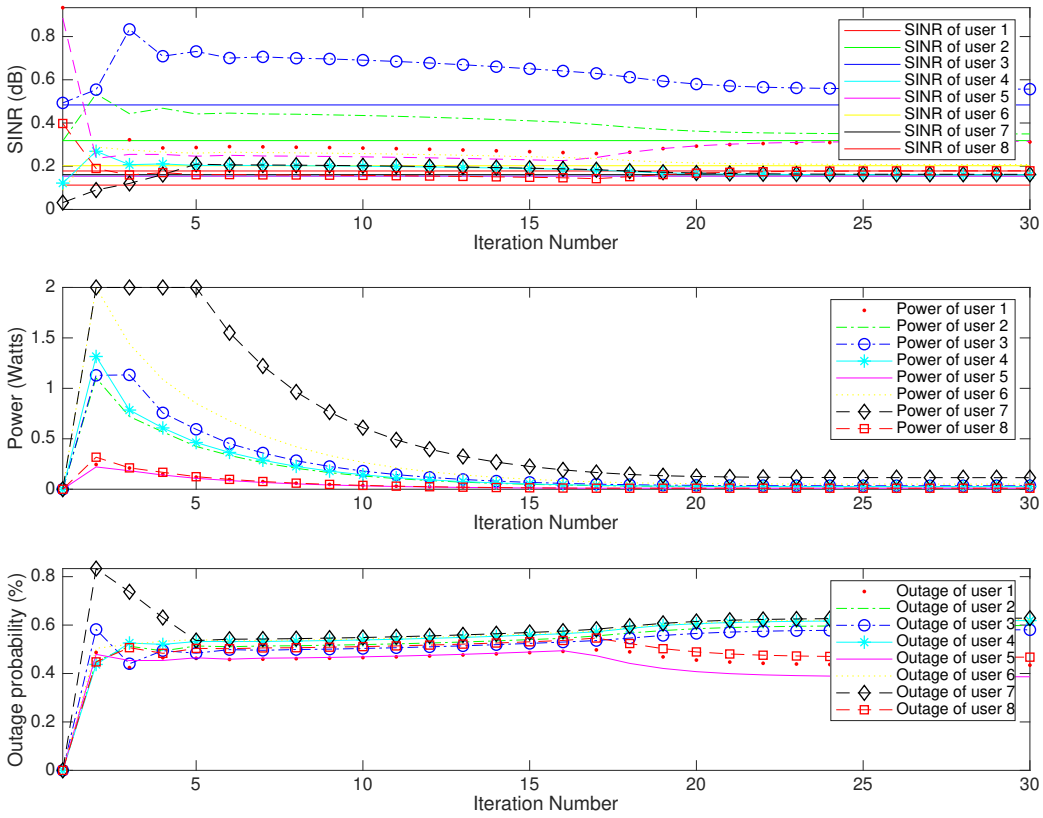

Figure 2.10: Normalized SINR, transmit power and outage probability for 8 users with Algorithm 4 and dynamic control parameter β_i.

Chapter 3

Power Allocation for Normalized Throughput and Energy Efficiency over Rayleigh Fading Channels in Cellular Networks

To accommodate the demand for high spectrum efficiency, cellular networks are consuming more energy, which increases the operating costs of mobile operators. Power control to improve the throughput [65–67] or energy efficiency [68,69] have both been considered for cellular networks. In [65], a power allocation scheme was proposed to find the power levels that maximize the aggregate throughput considering individual throughput. An iterative distributed power control (IDPC) scheme in cellular radio systems was proposed in [66]. The user transmit power is multiplied by a factor which is equal to the ratio of its obtained signal to interference plus noise ratio (SINR) and the target SINR. So power is increased or decreased based on the obtained SINR. In [67], a target SINR and opportunistic based power control (TOPC) scheme was proposed. If the user target SINR is below a threshold, then target SINR tracking power control (TPC) is used. If the user target SINR is above a threshold, then opportunistic power control (OPC) is used. A fixed step power control (FSPC) scheme with quantization and active link quality protection for energy efficiency was proposed in [68]. The target SINRs for users were determined based on user priority. In [69], a non-cooperative game theory based power allocation scheme for small cell networks was presented. Each base station maximizes its energy efficiency using distributed

power allocation.

The relationship between normalized SINR and outage probability has not been considered in solving the power allocation problem. In this chapter, upper and lower bounds on the outage probability for a given normalized SINR are determined. Power allocation schemes for energy efficiency and throughput maximization are then proposed subject to constraints on the outage probability and normalized SINR. Solutions to the resulting optimization problems are obtained using Lagrangian and parametric transformation methods. The contributions of this chapter are as follows.

1. The outage probability is obtained based on the normalized SINR and upper and lower bounds on the outage probability are derived. It is shown that if the normalized SINR increases, the outage probability decreases.

2. A distributed power allocation approach for normalized throughput maximization considering the outage probability and target SINR constraints is proposed and given in Algorithm 5.

3. A power allocation scheme for energy efficiency is presented and given in Algorithm 6. The relationship between outage probability and the normalized SINR is used to adjust the user transmit power.

4. Results are presented which show that the proposed power allocation approaches outperform the iterative distributed power control (IDPC), target SINR and opportunistic based power control (TOPC), and prioritized and selective power allocation (FSPC) schemes in terms of power consumption, throughput and energy efficiency.

The rest of the chapter is organized as follows. The channel model is described in Section II. Expressions for the outage probability, normalized throughput and energy efficiency are presented in Section III. The power allocation problems considering normalized SINR and outage probability are presented in Section III. The performance of the proposed power allocation approaches is evaluated in Section IV, and finally some concluding remarks are given in Section V.

3.1 Channel Model

Assume there are k users indexed $1, 2, \ldots, k$ and define the transmit power level of user i as p_i, $i = 1, 2, \ldots, k$. The signal attenuation due to path loss is given by

$$h_i = \bar{h} d_i^{\alpha},$$

where $\bar{h} = 0.97$ is a constant, d_i is the distance between user i and the corresponding BS, and α is the path loss exponent. The value of α depends on the propagation environment. Buildings, mountains and other objects block the wireless signals. This is often the case in large urban areas. The log normal shadowing can be expressed as

$$10^{0.1\Xi},$$

where Ξ is a Gaussian random variable so the channel loss due to path loss and shadowing is

$$g_i = h_i 10^{0.1\Xi},$$

A Rayleigh distribution is commonly used to describe the statistical time varying nature of the received envelope of a flat fading signal. This distribution has probability density function (PDF)

$$f(x) = \begin{cases} \frac{x}{\bar{x}^2} \exp\left(-\frac{x^2}{2\bar{x}^2}\right), \text{if } x \geq 0 \\ 0, \text{if } x < 0, \end{cases} \tag{3.1}$$

where x is the random variable, $\bar{x} = \mathbb{E}[x]$, and $\bar{x}^2$ is the signal envelope. Then the received power for user i is [70, 71]

$$h_i {x_i}^2 p_i,$$

where x_i is the associated Rayleigh fading component of user i. Thus, the received power for user i is exponentially distributed with mean [48]

$$g_i \mathbb{E}[{x_i}^2] p_i = g_i p_i.$$

3.2 Normalized Throughput, Energy Efficiency and Outage Probability

3.2.1 Normalized throughput

The SINR of user i is given by

$$\gamma_i = \frac{g_i {x_i}^2 p_i}{\sum_{j \neq i} g_j {x_j}^2 p_j + \sigma_i^2}, \tag{3.2}$$

where σ_i^2 is the additive white Gaussian noise (AWGN) power of user i, x_j denotes the signal from user j with PDF given by (3.1), and g_j denotes the interference from user j. The average SINR is

$$\bar{\gamma_i} = \frac{g_i p_i}{\sum_{j \neq i} g_j p_j + \sigma_i^2}, \tag{3.3}$$

so then the normalized SINR of user i is

$$\overline{S}_i = \frac{\bar{\gamma_i}}{\hat{\gamma_i}} = \frac{g_i p_i}{\hat{\gamma_i} \left(\sum_{j \neq i} g_j p_j + \sigma_i^2 \right)}, \tag{3.4}$$

where $\hat{\gamma_i}$ is the target SINR for user i. The normalized throughput of user i is defined as

$$R_i = \log \left(1 + \overline{S}_i \right). \tag{3.5}$$

3.2.2 Energy efficiency and outage probability

The power consumption of user i can be expressed as [72]

$$P_i = \xi p_i + p_{iap} + p_{icp}, \tag{3.6}$$

where $\xi \geq 0$ is the drain efficiency reciprocal of the power amplifier which denotes the amplifier inefficiency, p_{iap} is the power consumed by the power amplifier, and p_{icp} is the circuit power consumption due to signal processing and related functions. The energy efficiency of user i is defined as

$$\eta_i = \frac{R_i}{P_i},$$

and the system energy efficiency is

$$\eta = \sum_{i=1}^{k} \frac{R_i}{P_i}. \tag{3.7}$$

The outage probability is defined as the probability that the target SINR is not achieved. Thus, the outage probability for user i can be expressed as

$$O_i = \mathbb{P}\left[\gamma_i \leq \hat{\gamma_i}\right] = \mathbb{P}\left[g_i {x_i}^2 p_i \leq \hat{\gamma_i}\left(\sum_{j\neq i} g_j {x_j}^2 p_j + \sigma_i^2\right)\right].$$

Assuming that the received power and interference follow an exponential distribution gives [73–75]

$$O_i = 1 - \exp\left(-\frac{\Lambda_i}{\bar{p_i}}\right)\phi_I\left(\frac{\hat{\gamma_i}}{\bar{p_i}}\right), \tag{3.8}$$

where $\Lambda_i = \sigma_i^2\hat{\gamma_i}$, $\bar{p_i} = \mathbb{E}[g_i {x_i}^2 p_i] = g_i p_i$, and $\phi_I\left(\frac{\hat{\gamma_i}}{\bar{p_i}}\right)$ denotes the moment generating function (MGF) of the interference. In Rayleigh fading, the MGF of the interference is

$$\phi_I\left(\frac{\hat{\gamma_i}}{\bar{p_i}}\right) = \prod_{j=1,j\neq i}^{k} \phi_j\left(\frac{\hat{\gamma_i}}{\bar{p_i}}\right) = \prod_{j=1,j\neq i}^{k} \frac{1}{1+\bar{p_j}\frac{\hat{\gamma_i}}{\bar{p_i}}}, \tag{3.9}$$

where $\bar{p_j} = \mathbb{E}[g_j {x_j}^2 p_j] = g_j p_j$. Thus, (3.9) can be reformulated as

$$O_i = 1 - \exp\left(-\frac{\sigma_i^2\hat{\gamma_i}}{g_i p_i}\right)\prod_{j=1,j\neq i}^{k} \frac{1}{1+\frac{\hat{\gamma_i} g_j p_j}{g_i p_i}}. \tag{3.10}$$

Let $G_j = \frac{g_j}{g_i}$ and $\bar{\sigma_i} = \frac{\sigma_i^2}{g_i}$. Then, (3.10) can be rewritten as

$$O_i = 1 - \exp\left(-\frac{\bar{\sigma_i}\hat{\gamma_i}}{p_i}\right)\prod_{j=1,j\neq i}^{k} \frac{1}{1+\frac{\hat{\gamma_i} G_j p_j}{p_i}}. \tag{3.11}$$

Upper and lower bounds on the outage probability can be obtained using the following inequality [54, 55]

$$1 + a + \sum_{i=1}^{k} x_i \leq e^a \prod_{i=1}^{k}(1+x_i) \leq e^{\left(a+\sum_{i=1}^{k} x_i\right)}, \tag{3.12}$$

where $x_1, x_2, \ldots, x_k \geq 0$ and $a, k \geq 0$. The left hand side is obtained using the Weierstrass product inequality and the right hand side using the linear and exponential inequalities. The outage probability in (3.11) can be rewritten as

$$O_i = 1 - \left[\exp\left(\frac{\bar{\sigma}_i \hat{\gamma}_i}{p_i} \right) \prod_{j=1, j\neq i}^{k} \left(1 + \frac{\hat{\gamma}_i G_j p_j}{p_i} \right) \right]^{-1}.$$

The upper bound on the outage probability is obtained from the right hand side inequality as

$$\begin{aligned} O_i &\leq 1 - \left[\exp\left(\frac{\bar{\sigma}_i \hat{\gamma}_i}{p_i} + \sum_{j=1, j\neq i}^{k} \frac{\hat{\gamma}_i G_j p_j}{p_i} \right) \right]^{-1} \\ &= 1 - \left\{ \exp\left[\frac{\hat{\gamma}_i}{p_i} \left(\bar{\sigma}_i + \sum_{j=1, j\neq i}^{k} G_j p_j \right) \right] \right\}^{-1} \\ &= 1 - \left[\exp\left(\frac{1}{\overline{S}_i} \right) \right]^{-1} \\ &= 1 - \left[\exp\left(-\frac{1}{\overline{S}_i} \right) \right]. \end{aligned}$$

The lower bound obtained from the left hand side inequality is

$$\begin{aligned} O_i &\geq 1 - \left[1 + \frac{\bar{\sigma}_i \hat{\gamma}_i}{p_i} + \sum_{j=1, j\neq i}^{k} \left(\frac{\hat{\gamma}_i G_j p_j}{p_i} \right) \right]^{-1} \\ &= 1 - \left(1 + \frac{1}{\overline{S}_i} \right)^{-1} \\ &= \frac{1}{\left(1 + \overline{S}_i \right)}. \end{aligned}$$

The bounds on the outage probability are thus

$$\frac{1}{\left(1 + \overline{S}_i \right)} \leq O_i \leq 1 - \left[\exp\left(-\frac{1}{\overline{S}_i} \right) \right]. \tag{3.13}$$

3.3 Problem Formulation

In this section, the transmit power allocating problem is derived considering the normalized throughput and energy efficiency. This problem is solved using the Lagrangian and parametric transformation methods. Two distributed iterative power allocation schemes for normalized throughput and energy efficiency are proposed. Then an algorithm is presented in which users with an outage probability above a threshold O_{th} do not transmit or adjust their transmit power levels to restrict the interference to the remaining users.

3.3.1 Distributed power allocation for normalized throughput maximization with an outage probability threshold

In this section, the normalized throughput maximization problem is considered subject to outage probability and transmit power constraints. This can be formulated as

$$\begin{aligned} \text{maximize} \quad & \sum_{i=1}^{k} R_i = \sum_{i=1}^{k} \log\left(1+\overline{S}_i\right) \\ \text{subject to} \quad & p_{\min} \le p_i \le p_{\max} \\ & 1 - \left[\exp\left(\frac{\bar{\sigma}_i\hat{\gamma}_i}{p_i}\right) \prod_{j=1,j\neq i}^{k} \left(1+\frac{\hat{\gamma}_i G_j p_j}{p_i}\right)\right]^{-1} \le O_{th}, \end{aligned} \tag{3.14}$$

where $\overline{S}_i = \frac{\bar{\gamma}_i}{\hat{\gamma}_i} = \frac{p_i}{\hat{\gamma}_i\left(\sum_{j\neq i} G_j p_j + \bar{\sigma}_i\right)}$, $p_{\max}$ and $p_{\min}$ are the maximum and minimum transmit power, respectively. Using (3.13), the last constraint in (3.14) can be approximated by

$$\overline{S}_i \ge -\frac{1}{\log\left(1-O_{th}\right)}.$$

After some manipulation, (3.14) becomes

$$\begin{aligned} \text{maximize} \quad & \sum_{i=1}^{k} R_i = \sum_{i=1}^{k} \log\left[1+\frac{p_i}{\hat{\gamma}_i\left(\sum_{j\neq i} G_j p_j + \bar{\sigma}_i\right)}\right] \\ \text{subject to} \quad & p_{\min} \le p_i \le p_{\max} \\ & \frac{p_i}{\hat{\gamma}_i\left(\sum_{j\neq i} G_j p_j + \bar{\sigma}_i\right)} \ge -\frac{1}{\log\left(1-O_{th}\right)}. \end{aligned} \tag{3.15}$$

Introducing a new variable Ω_i to replace each term inside the logarithm, (3.15) can be rewritten as

$$\begin{aligned} \text{maximize} \quad & \sum_{i=1}^{k} R_i = \sum_{i=1}^{k} \log\left(\Omega_i\right) \\ \text{subject to} \quad & p_{\min} \le p_i \le p_{\max} \\ & 1 - \frac{1}{\log\left(1 - O_{th}\right)} \le \Omega_i \le 1 + \frac{p_i}{\hat{\gamma}_i \left(\sum_{j \neq i} G_j p_j + \bar{\sigma}_i\right)}. \end{aligned} \tag{3.16}$$

This can be considered as an outer optimization over p_i and an inner optimization over Ω_i with fixed p_i. The inner optimization problem is

$$\begin{aligned} \text{maximize} \quad & \sum_{i=1}^{k} R_i = \sum_{i=1}^{k} \log\left(\Omega_i\right) \\ \text{subject to} \quad & p_{\min} \le p_i \le p_{\max} \\ & \Omega_i \le 1 + \frac{p_i}{\hat{\gamma}_i \left(\sum_{j \neq i} G_j p_j + \bar{\sigma}_i\right)}. \end{aligned} \tag{3.17}$$

The solution to this problem is that Ω_i should satisfy the constraint with equality. This problem can be expressed as follows. Note that this is a convex optimization problem in Ω_i so strong duality holds. Introduce the dual variable λ_i for each inequality constraint in the above optimization problem and form the Lagrangian function

$$\mathcal{L}(\Omega_i, \lambda_i) = \sum_{i=1}^{k} \log\left(\Omega_i\right) - \sum_{i=1}^{k} \lambda_i \left[\Omega_i - 1 - \frac{p_i}{\hat{\gamma}_i \left(\sum_{j \neq i} G_j p_j + \bar{\sigma}_i\right)}\right].$$

Due to strong duality, (3.17) is equivalent to the dual problem

$$\min_{\lambda_i \ge 0} \quad \max_{\Omega_i} \quad \mathcal{L}(\Omega_i, \lambda_i).$$

Let $(\lambda_i^*, \Omega_i^*)$ be the saddle point of this problem. It must satisfy the first order derivative condition $\frac{\partial \mathcal{L}}{\partial \Omega_i} = 0$ which gives

$$\lambda_i^* = \frac{1}{\Omega_i^*},$$

so that

$$\mathcal{L}(\Omega_i, \lambda_i) = \sum_{i=1}^{k} \left[\log(\Omega_i) - \Omega_i + 1 + \frac{p_i}{p_i \hat{\gamma}_i \left(\sum_{j \neq i} G_j p_j + \bar{\sigma}_i \right)} \Omega_i \right].$$

The power allocation problem (3.17) is equivalent to

$$\begin{aligned} \text{maximize} \quad & \sum_{i=1}^{k} R_i = \sum_{i=1}^{k} \left[\log(\Omega_i) - \Omega_i + 1 + \frac{p_i}{p_i + \hat{\gamma}_i \left(\sum_{j \neq i} G_j p_j + \bar{\sigma}_i \right)} \Omega_i \right] \\ \text{subject to} \quad & p_{\min} \leq p_i \leq p_{\max}. \end{aligned} \tag{3.18}$$

Taking the derivative of R_i with respect to Ω_i

$$\frac{\partial R_i}{\partial \Omega_i} = \frac{1}{\Omega_i} - 1 + \frac{p_i}{p_i + \hat{\gamma}_i \left(\sum_{j \neq i} G_j p_j + \bar{\sigma}_i \right)},$$

and setting this to 0 gives

$$\Omega_i = 1 + \frac{p_i}{\hat{\gamma}_i \left(\sum_{j \neq i} G_j p_j + \bar{\sigma}_i \right)}. \tag{3.19}$$

A subtractive form of (3.18) can be obtained using parametric transformation with an additional variable u_i. The outer optimization is then

$$\begin{aligned} \text{maximize} \quad & \sum_{i=1}^{k} R_i = \sum_{i=1}^{k} \left\{ \log(\Omega_i) - \Omega_i + 1 + 2\sqrt{u_i} p_i \Omega_i - u_i \left[p_i + \hat{\gamma}_i \left(\sum_{j \neq i} G_j p_j + \bar{\sigma}_i \right) \right]^2 \right\} \\ \text{subject to} \quad & p_{\min} \leq p_i \leq p_{\max}. \end{aligned} \tag{3.20}$$

The variable u_i is determined by taking the derivative of R_i with respect u_i and setting $\frac{\partial R_i}{\partial u_i}$ to 0 which gives

$$u_i = \frac{(p_i \Omega_i)^2}{\left[p_i + \hat{\gamma}_i \left(\sum_{j \neq i} G_j p_j + \bar{\sigma}_i \right) \right]^4}. \tag{3.21}$$

Then taking the derivative of R_i with respect to p_i and setting $\frac{\partial R_i}{\partial p_i}$ to 0 gives

$$p_i = \frac{\Omega_i^2}{u_i\Big(1+\hat{\gamma}_i\sum_{j\neq i}G_j\Big)^2}. \tag{3.22}$$

The proposed distributed power allocation algorithm based on (3.19), (3.21) and (3.22) is given in Algorithm 5.

Algorithm 5 Distributed Power Allocation For Normalized Throughput Maximization

---

Step 1: Initialize the iteration index $t = 1$. User i obtains the outage probability threshold O_{th} from the BS and determines the average SINR $\bar{\gamma}_i$. Set the target SINR $\hat{\gamma}_i$ and the convergence threshold ϵ.

Step 2: User i determines $\Omega_i(t)$ using

$$\Omega_i(t) = 1 + \frac{p_i(t)}{\hat{\gamma}_i\left[\sum_{j\neq i}G_j p_j(t) + \bar{\sigma}_i\right]}.$$

Step 3: User i determines $u_i(t)$ using

$$u_i(t) = \frac{\big[p_i(t)\Omega_i(t)\big]^2}{\left\{p_i(t) + \hat{\gamma}_i\left[\sum_{j\neq i}G_j p_j(t) + \bar{\sigma}_i\right]\right\}^4}.$$

Step 4: Users update their transmit power as

$$p_i(t+1) = \frac{\Omega_i^2(t)}{u_i(t)\Big(1+\hat{\gamma}_i\sum_{j\neq i}G_j\Big)^2}.$$

Step 5: Terminate when

$$\max_i |p_i(t+1) - p_i(t)| \leq \epsilon,$$

otherwise go to **Step 2**.

3.3.2 Distributed power allocation for energy efficiency with an outage probability threshold

The energy efficiency problem subject to outage probability and transmit power constraints is presented. This problem can be formulated as

$$\begin{aligned} \text{maximize} \quad & \eta = \sum_{i=1}^{k} \frac{R_i}{P_i} \\ \text{subject to} \quad & p_{\min} \leq p_i \leq p_{\max} \\ & 1 - \left[\exp\left(\frac{\bar{\sigma}_i \hat{\gamma}_i}{p_i} \right) \prod_{j=1, j\neq i}^{k} \left(1 + \frac{\hat{\gamma}_i G_j p_j}{p_i} \right) \right]^{-1} \leq O_{th}. \end{aligned} \tag{3.23}$$

This is equivalent to

$$\begin{aligned} \text{maximize} \quad & \eta = \sum_{i=1}^{k} \frac{R_i}{P_i} \\ \text{subject to} \quad & \frac{p_{\min}}{p_i} \leq 1 \\ & \frac{p_i}{p_{\max}} \leq 1 \\ & \left[\exp\left(\frac{\bar{\sigma}_i \hat{\gamma}_i}{p_i} \right) \prod_{j=1, j\neq i}^{k} \left(1 + \frac{\hat{\gamma}_i G_j p_j}{p_i} \right) \right] (1 - O_{th}) \leq 1, \end{aligned} \tag{3.24}$$

which is a geometric programming problem with variables $p_1, p_2, \ldots, p_k$. Therefore, the power allocation problem can be solved using the interior point method with convex optimization (CVX) geometry programming.

A subtractive form of (3.24) can be obtained using parametric transformation

with an additional variable v_i which gives

$$\begin{aligned} \text{maximize} \quad & \eta = \sum_{i=1}^{k} 2\sqrt{v_i}R_i - v_i(P_i)^2 \\ \text{subject to} \quad & \frac{p_{\min}}{p_i} \leq 1 \\ & \frac{p_i}{p_{\max}} \leq 1 \\ & 1 - \left[\exp\left(\frac{\bar{\sigma_i}\hat{\gamma_i}}{p_i}\right) \prod_{j=1, j\neq i}^{k} \left(1 + \frac{\hat{\gamma_i} G_j p_j}{p_i}\right)\right]^{-1} \leq O_{th}. \end{aligned} \tag{3.25}$$

Using (3.5), (3.20) and (3.25), the power allocation problem (3.18) can be rewritten as

$$\begin{aligned} \text{maximize} \quad \eta = \quad & \sum_{i=1}^{k} 2\sqrt{v_i} \left\{ \log\left(\Omega_i\right) - \Omega_i + 1 + 2\sqrt{u_i} p_i \Omega_i - u_i \left[p_i + \hat{\gamma_i} \left(\sum_{j\neq i} G_j p_j + \bar{\sigma_i} \right) \right]^2 \right\} \\ & - \sum_{i=1}^{k} v_i (\xi p_i + p_{iap} + p_{icp})^2 \\ \text{subject to} \quad & \frac{p_{\min}}{p_i} \leq 1 \\ & \frac{p_i}{p_{\max}} \leq 1 \\ & \bar{\gamma_i} \geq -\frac{\hat{\gamma_i}}{\log\left(1 - O_{th}\right)}. \end{aligned} \tag{3.26}$$

Similar to (3.19), Ω_i is determined as

$$\Omega_i = 1 + \frac{p_i}{\hat{\gamma_i}\left(\sum_{j\neq i} G_j p_j + \bar{\sigma_i}\right)}.$$

The variable u_i is determined by taking the derivative of η with respect to u_i and setting $\frac{\partial \eta}{\partial u_i}$ to 0 which gives

$$u_i = \frac{\left(p_i \Omega_i\right)^2}{\left[p_i + \hat{\gamma_i}\left(\sum_{j\neq i} G_j p_j + \bar{\sigma_i}\right)\right]^4}. \tag{3.27}$$

The additional variable v_i is determined by taking the derivative of η with respect to v_i and setting $\frac{\partial R_i}{\partial v_i}$ to 0 which gives

$$v_i = \frac{R_i^2}{P_i^4} = \frac{\left[\log\left(1+\overline{S}_i\right)\right]^2}{\left(\xi p_i + p_{iap} + p_{icp}\right)^4}. \tag{3.28}$$

Taking the derivative of η with respect to p_i and setting $\frac{\partial \eta}{\partial p_i}$ to 0 gives

$$p_i = \frac{4u_i v_i \Omega_i^2}{\left[v_i + 2u_i\sqrt{v_i}\left(1+\hat{\gamma}_i \sum_{j\neq i} G_j\right)\right]^2}. \tag{3.29}$$

The minimum transmit power to reach a target SINR is obtained from the last constraint in (3.23) and the upper bound on outage probability in (3.13) as

$$1 - \left[\exp\left(\frac{\bar{\sigma}_i\hat{\gamma}_i}{p_i}\right)\prod_{j=1,j\neq i}^{k}\left(1+\frac{\hat{\gamma}_i G_j p_j}{p_i}\right)\right]^{-1} \leq 1 - \left[\exp\left(-\frac{1}{\overline{S}_i}\right)\right] \leq O_{th}.$$

This is satisfied as long as the upper bound on the outage probability is less than O_{th}, which means

$$1 - \left[\exp\left(-\frac{1}{\overline{S}_i}\right)\right] \leq O_{th},$$

where $\overline{S}_i = \frac{\bar{\gamma}_i}{\hat{\gamma}_i}$. After some manipulation, this inequality can be rewritten as

$$\bar{\gamma}_i \geq -\frac{\hat{\gamma}_i}{\log\left(1-O_{th}\right)}.$$

Thus, the minimum transmit power required to attain the target SINR is

$$p_i \geq -\left(\sum_{j\neq i} G_j p_j + \bar{\sigma}_i\right)\left[\frac{\hat{\gamma}_i}{\log\left(1-O_{th}\right)}\right]. \tag{3.30}$$

A power allocation algorithm is obtained by defining the control parameter

$$\alpha_i = \kappa(1-O_i), \tag{3.31}$$

where $\kappa = \frac{1}{1-O_{th}}$. The transmit power is increased if the outage probability is less than the threshold, and decreased if greater than the threshold. Thus if the outage probability of user i is more than O_{th}, α_i is reduced resulting in a lower transmit power. The user transmit power is then given by

$$p_i = \frac{4\alpha_i(t)u_i(t)v_i(t)\Omega_i^2}{\left[v_i(t) + 2u_i(t)\sqrt{v_i(t)}\left(1 + \hat{\gamma}_i \sum_{j\neq i} G_j\right)\right]^2}. \tag{3.32}$$

The proposed distributed power allocation algorithm is based on (3.19), (3.27), (3.28), (3.30) and (3.32), and is given in Algorithm 6.

3.4 Numerical Results

In this chapter, Monte Carlo simulation is used to evaluate the performance of the proposed power allocation schemes. The channel gain is $g_i = \bar{h} d_i^{\alpha} 10^{0.1\Xi} {x_i}^2$ where $\bar{h} = 0.97$ is a constant, and $\alpha = 3$ is the path loss exponent which corresponds to urban and suburban environments [76–78]. The stopping criteria for the algorithms is set to $\epsilon = 10^{-20}$. The noise power is $\sigma^2 = 0.01$ W, the initial power level for all users is set to 0.01 W, and the maximum transmit power is $p_{\max} = 2$ W. The number of taps for the Rayleigh fading channel is set to 4. The real and imaginary parts of the channel coefficients are randomly chosen from a Gaussian distribution with zero mean and variance $\frac{1}{\sqrt{2}}$. The magnitude is then Rayleigh distributed and the phase is uniformly distributed between 0 and 2π. The performance of the proposed power allocation schemes is compared with that of the iterative distributed power control (IDPC), target SINR and opportunistic based power control (TOPC), and fixed step power control (FSPC) algorithms. Power consumption, throughput, and energy efficiency are the comparison criteria. The users are uniformly distributed in the geographic areas of the cells. In the first and second scenarios, there is one femtocell with 4 and 8 users, respectively. The femtocell is located at the center of a square geographic area with dimensions 20 m $\times$ 20 m. In the third and fourth scenarios, there is one picocell with 16 and 32 users, respectively. The picocell is located at the center of a square geographic area with dimensions 200 m $\times$ 200 m. The results are obtained for 1000 trials for each number of users with the user locations changed each trial.

Fig. 3.1 presents the exact average outage probability from (3.11) and the corresponding upper and lower bounds from (3.13) with 4, 8, 16, and 32 users versus

Algorithm 6 Distributed Power Allocation For Energy Efficiency with an Outage Probability Constraint

Step 1: Initialize the iteration index $t = 1$. User i obtain the outage probability threshold O_{th} from the BS and determines the average SINR $\bar{\gamma}_i$. Set the target SINR $\hat{\gamma}_i$.

Step 2: User i determines $\Omega_i(t)$ using

$$\Omega_i(t) = 1 + \frac{p_i(t)}{\hat{\gamma}_i \left[\sum_{j \neq i} G_j p_j(t) + \bar{\sigma}_i\right]}.$$

Step 3: User i determines $u_i(t)$ using

$$u_i(t) = \frac{\left[p_i(t)\Omega_i(t)\right]^2}{\left\{p_i(t) + \hat{\gamma}_i \left[\sum_{j \neq i} G_j p_j(t) + \bar{\sigma}_i\right]\right\}^4}.$$

Step 4: User i determines $v_i(t)$ using

$$v_i(t) = \frac{\left\{\log\left[1 + \overline{S}_i(t)\right]\right\}^2}{\left[\xi p_i(t) + p_{iap} + p_{icp}\right]^4}.$$

Step 5: Users update their transmit power using (3.29), (3.30) and (3.31)

$$p_i(t+1) = \max\left\{ \quad - \left[\sum_{j \neq i} G_j p_j(t) + \bar{\sigma}_i\right] \left[\frac{\hat{\gamma}_i}{\log\left(1 - O_{th}\right)}\right], \right.$$
$$\left. \frac{4\alpha_i(t) u_i(t) v_i(t) \Omega_i^2}{\left[v_i(t) + 2u_i(t)\sqrt{v_i(t)}\left(1 + \hat{\gamma}_i \sum_{j \neq i} G_j\right)\right]^2} \right\}.$$

Step 6: Terminate when

$$\max_i |p_i(t+1) - p_i(t)| \leq \epsilon,$$

otherwise go to **Step 2**.

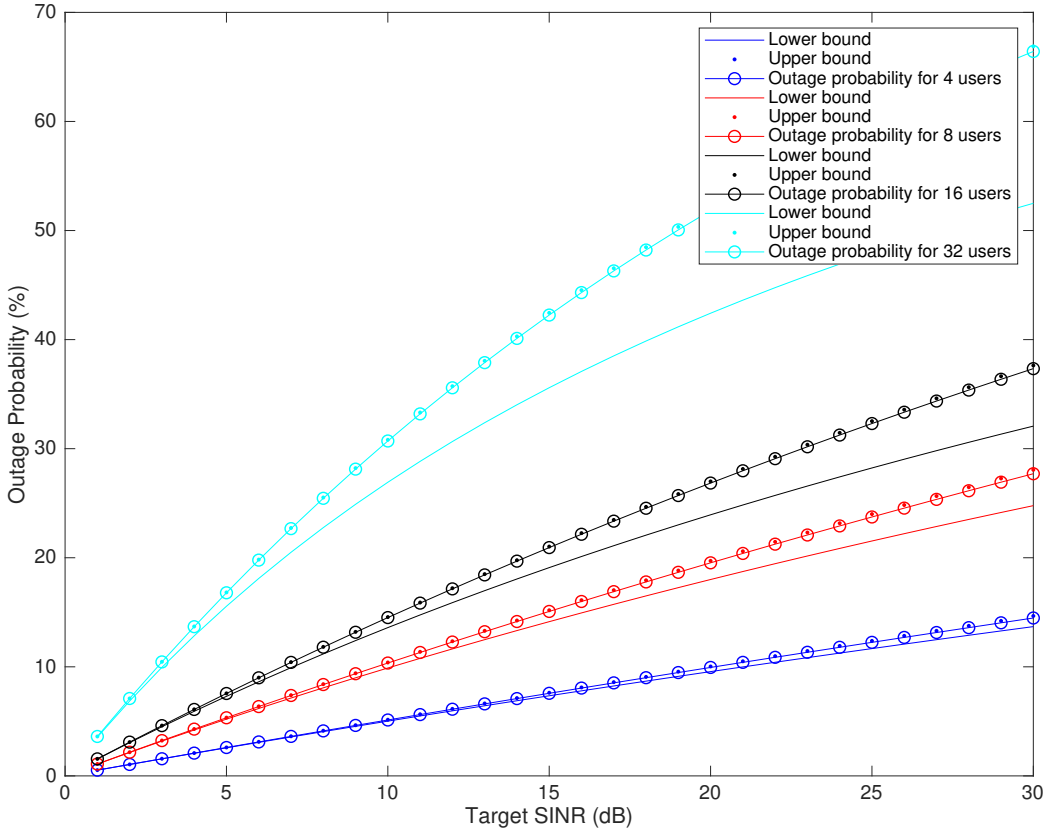

Figure 3.1: Upper and lower bounds on the average outage probability with different numbers of users.

the target SINR. This shows that the upper bound is a better approximation than the lower bound, particularly at high target SINRs. Therefore, the upper bound is suitable to estimate the outage probability in cellular networks.

Fig. 3.2 presents the average power for the IDPC, TOPC, FSPC and proposed power allocation schemes for the four scenarios. This shows that the average power for IDPC is the highest, followed by FSPC. The proposed approaches have the least average power. In the first scenario, the average power for FSPC is the highest, which is approximately 2.5 W. In the second scenario, the average power for IDPC and FSPC is the highest, which is approximately 4 W. The lowest average power is obtained with the proposed schemes, which is approximately 0.5 W. In the third and fourth scenarios, the average power of IDPC is the worst, followed by TOPC, FSPC and the first proposed scheme. The average power of IDPC for these scenarios is

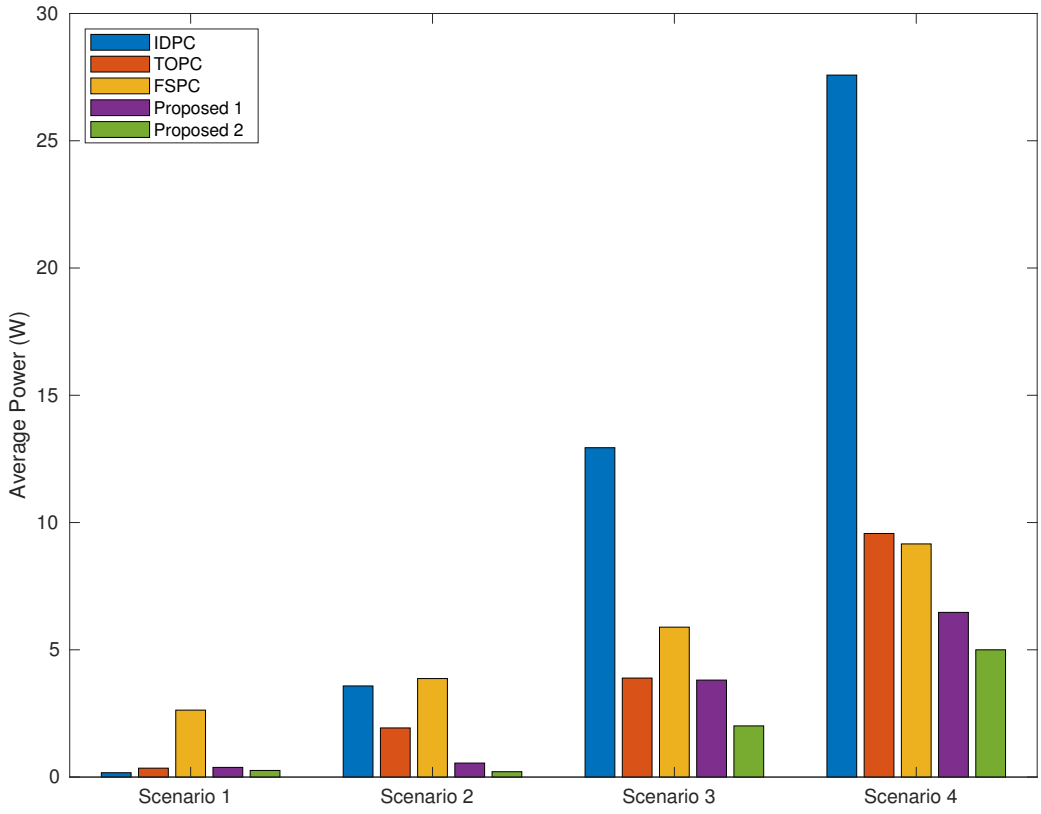

Figure 3.2: The average power for four scenarios with five power allocation schemes.

approximately 10 W and 15 W, respectively. The second proposed scheme provides the best performance in all cases.

Fig. 3.3 presents the average normalized throughput from (3.5) (Mbps) for the IDPC, TOPC, FSPC and proposed power allocation schemes for the four scenarios. This shows that the first proposed scheme has the highest average throughput in all but the first scenario. Further, the average normalized throughput of the IDPC, TOPC, FSPC, and second proposed schemes are almost identical. Fig. 3.4 presents the average system energy efficiency from (3.7) (Mbps/W) for the IDPC, TOPC, FSPC and proposed power allocation schemes for the scenarios. The second proposed scheme has the highest efficiency in all but the first scenario. In the first scenario, the average system energy efficiency of IDPC is the highest at 19.2 Mbps/W, followed by the second proposed scheme which is 17.3 Mbps/W. In the second, third and fourth scenarios, the proposed approaches are much better than IDPC, TOPC, and

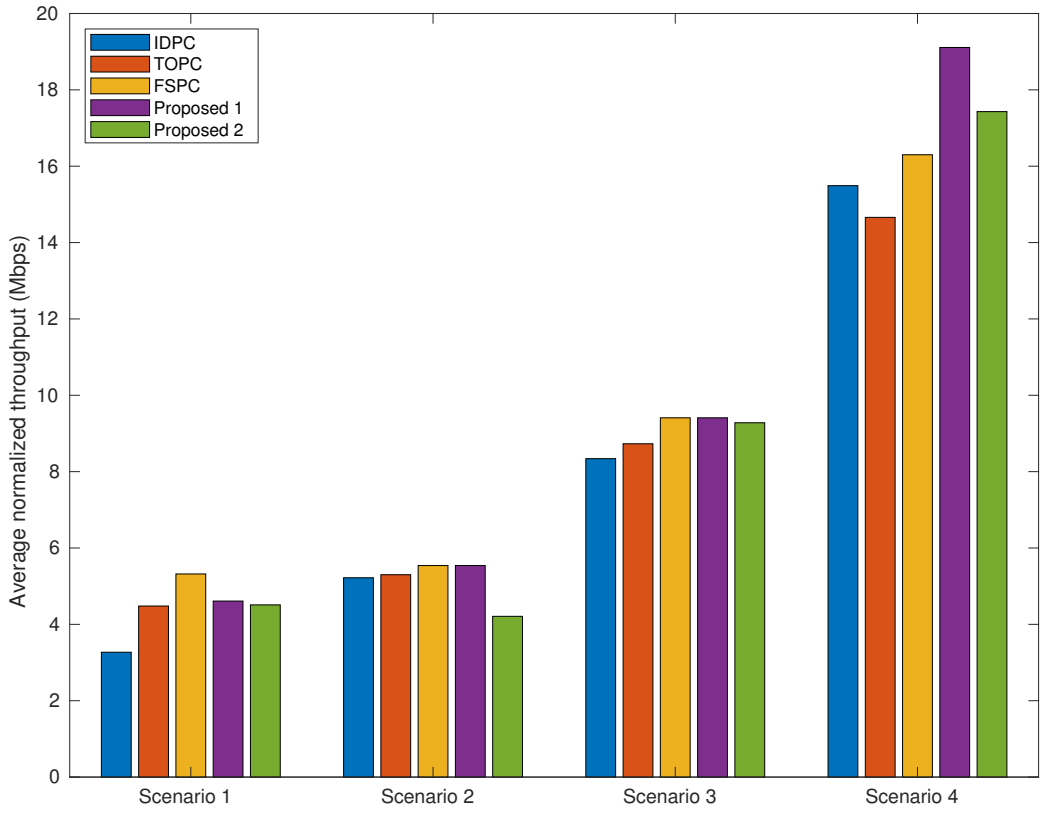

Figure 3.3: The average normalized throughput for four scenarios with five power allocation schemes.

FSPC. IDPC, TOPC, and FSPC provide less than 2.5 Mbps/W average system energy efficiency, while the first proposed scheme has 10.1 Mbps/W, 2.5 Mbps/W, and 2.9 Mbps/W average system energy efficiency for the second, third and fourth scenarios, respectively. The second proposed scheme is the best as it provides 20.5 Mbps/W, 4.6 Mbps/W, and 3.5 Mbps/W average system energy efficiency for the second, third and fourth scenarios, respectively.

3.5 Conclusion

In this chapter, two power allocation schemes for the normalized throughput and energy efficiency in cellular networks were proposed. The goal is to reduce the power consumption and improve the energy efficiency while ensuring user outage probabil-

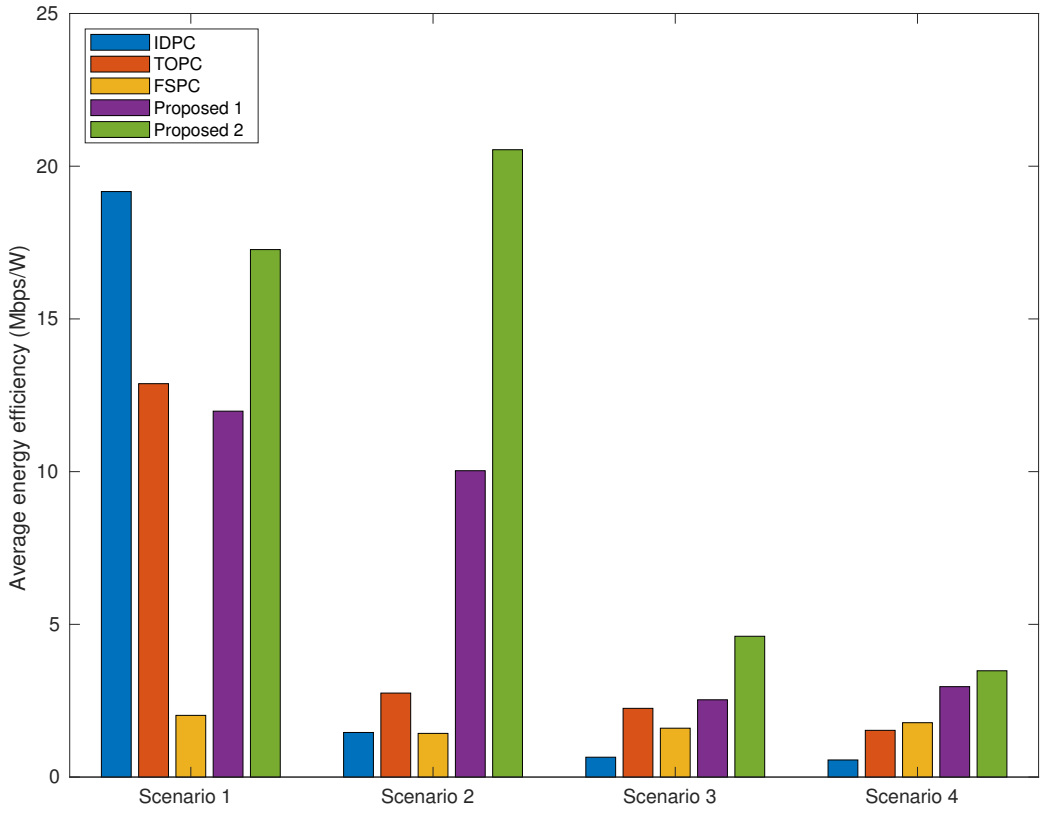

Figure 3.4: The average energy efficiency for four scenarios with five power allocation schemes.

ities are below an outage probability threshold. Performance results were presented which show that the proposed schemes provide a higher energy efficiency than the iterative distributed power control (IDPC), target SINR and opportunistic based power control (TOPC), and fixed step power control (FSPC) schemes. Further, the proposed schemes satisfy the user normalized throughput requirements with the lowest transmit power. Thus, they require less power compared to the IDPC, TOPC and FSPC schemes.

Chapter 4

Power Allocation for Normalized Throughput and Energy Efficiency over Nakagami-m fading Channels in Cellular Networks

Power allocation for normalized throughput and energy efficiency has been studied previously [79–85]. In [79], a distributed target signal to interference plus noise ratio (SINR) tracking power allocation (TTPA) scheme was proposed. The throughput was improved by reducing the interference while ensuring a minimum SINR. A distributed algorithm for opportunistic power allocation (DOPA) in interference channels for delay tolerant services was presented in [80] with a view to maximizing the data rate of each user while satisfying a constraint on the total user transmit power. In [81], gradual removal in wireless networks was considered where the smallest number of users to be removed was determined to satisfy the target SINR requirements of the remaining users. A distributed power allocation algorithm with temporary removal and feasibility check (PARF) was presented. A user whose required transmit power to reach the target SINR exceeds the maximum is temporarily removed, but transmission is resumed if the required power falls below a threshold. In [82], a prioritized power allocation and admission control scheme for cellular networks was proposed. The goal is to satisfy all priority users and as many remaining users as possible. Power allocation in a multi-user wireless system was considered in [83] to maximize the energy efficiency while meeting the power constraints of individual users and the

system. In particular, a water filling algorithm was proposed to solve the corresponding non linear fractional optimization problem as this can provide a solution with low computational complexity. In [84], power allocation for energy efficiency was proposed. The channel state information and circuit power consumption were used to adjust the user transmit power. This was formulated as a non-convex nonlinear programming problem and decomposed into two convex subproblems which are easier to solve. In [85], efficient power allocation algorithms for worst case throughput and energy efficiency scenarios in a multi tier wireless network were investigated.

The relationship between outage probability and normalized SINR over Nakagami-m fading channels is considered. The outage probability is the probability that the user SINR falls below a target SINR. Lower and upper bounds on the outage probability are determined and shown to be tight. The required SINR is satisfied by allocating power so that users with an outage probability greater than a threshold reduce their transmit power and vice versa. A SINR at or above the target SINR is assumed to be required for successful transmission. The proposed method can be interpreted as an efficient approach to adjusting user transmit power levels. Three power allocation problems considering power consumption, throughput and energy efficiency subject to constraints on outage probability and target SINR are presented. These problems are in fractional and logarithmic forms and so are converted into equivalent linear problems and then solved using Lagrangian and parametric transformation methods.

The contributions of this chapter is given below.

1. Expression for the outage probability over Nakagami-m fading is derived. Tight upper and lower bounds on the outage probability are determined.

2. A power allocation problem to minimize the power consumption with an outage probability threshold is proposed. This threshold is determined so that users are satisfied with their target SINRs, and the problem is solved using an iterative approach.

3. A power allocation problem to maximize the normalized throughput an outage probability threshold is proposed and given in Algorithm 7. This is a logarithmic problem, so it is split into two subproblems by introducing an auxiliary variable. These subproblems are solved alternately and iteratively using a differential method.

4. A power allocation problem to improve the energy efficiency with an outage

probability threshold is proposed and given in Algorithm 8. This is a fractional programming problem and so is converted into a linear form using a parametric transformation method.

The remainder of this chapter is organized as follows. The channel model is given in Section II. Expressions for the outage probability, normalized throughput and energy efficiency are presented in Section III. The power allocation problem formulation considering normalized SINR and outage probability is given in Section III. The performance of the proposed approaches is evaluated in Section IV, and finally some concluding remarks are given in Section V.

4.1 System Model

Radio channels have a significant impact on the performance of wireless communication systems and are affected by factors such as path loss, shadowing, and fading. These factors cause variations in the received SINR and can degrade the performance of power allocation schemes. Therefore, channel uncertainties should be considered in the power allocation. Assuming there are k users, indexed $1, 2, \ldots, k$, let the transmit power of user i be p_i.

Considering path loss, the power attenuation is [86]

$$g_i = \bar{g} d_i^{\alpha},$$

where $\bar{g}$ is a constant typically set to 1, d_i is the distance between user i and the corresponding base station (BS), and α is the path loss exponent. A number of values for α have been proposed for different prDOPAgation environments, e.g. for urban environments $\alpha = 4$ is commonly used. The attenuation due to path loss and log normal shadowing can be expressed as [87]

$$h_i = g_i 10^{\frac{\Xi}{10}},$$

where Ξ is assumed to be a Gaussian random variable.

The average received power for user i is given by [88–90]

$$\bar{p_i} = h_i \mathbb{E}\left[x_i\right] p_i = h_i p_i,$$

where x_i denotes the fading component for user i which is assumed to be a Nakagami-m distributed random variable with unit mean. The probability density function (PDF) of x_i is given by

$$f(x) = \begin{cases} \left(\frac{m}{\overline{x}}\right)^m \frac{x^{m-1}}{\Gamma(m)} \exp\left(-\frac{mx}{\overline{x}}\right), \text{if } x \geq 0, \\ 0, \text{if } x < 0, \end{cases}$$

where $\overline{x} = \mathbb{E}[x]$, $\Gamma(\cdot)$ is the gamma function, and m is the fading parameter that ranges from $1/2$ to ∞.

4.1.1 Normalized throughput, energy efficiency and outage probability

The SINR of user i is given by

$$\gamma_i = \frac{h_i x_i p_i}{\sum_{j \neq i} h_j x_j p_j + \sigma_i^2}, \tag{4.1}$$

where σ_i^2 denotes the additive white Gaussian noise (AWGN) at user i, and x_j and h_j are the associated Nakagami-m fading component and channel gain of the interference from user j to user i, respectively.

The average SINR of user i considering the interference from other users and noise is given by

$$\bar{\gamma}_i = \frac{h_i \mathbb{E}\left[x_i\right] p_i}{\sum_{j \neq i} h_j \mathbb{E}\left[x_j\right] p_j + \sigma_i^2} = \frac{h_i p_i}{\sum_{j \neq i} h_j p_j + \sigma_i^2}. \tag{4.2}$$

The normalized SINR of user i is defined as

$$\overline{\Gamma}_i = \frac{\bar{\gamma}_i}{\hat{\gamma}_i} = \frac{h_i p_i}{\hat{\gamma}_i \left\{\sum_{j \neq i} h_j p_j + \sigma_i^2\right\}}, \tag{4.3}$$

where $\hat{\gamma}_i$ is the target SINR, and the normalized throughput is given by

$$R_i = \log\left(1 + \overline{\Gamma}_i\right). \tag{4.4}$$

The power consumption of user i can be expressed as [91, 92]

$$P_i = \xi p_i + p_{ic} \tag{4.5}$$

where ξ is the power amplifier efficiency, $\xi \geq 0$, p_{ic} is the circuit power consumption that is independent of the radiated power and is due to functions such as signal processing. The energy efficiency of user i can be expressed as

$$\eta_i = \frac{R_i}{P_i},$$

so the system energy efficiency is

$$\eta = \sum_{i=1}^{k} \frac{R_i}{P_i}. \tag{4.6}$$

For channel uncertainty, column wise model is used due to its analytical tractability. The normalized SINR can be rewritten as

$$\overline{\Gamma}_i = \frac{\bar{\gamma}_i}{\hat{\gamma}_i} = \frac{h_i p_i}{\hat{\gamma}_i \left(\sum_{j\neq i} h_j p_j + \sigma_i^2\right)} = \frac{p_i}{\hat{\gamma}_i \left(\sum_{j\neq i} \frac{h_j}{h_i} p_j + \frac{\sigma_i^2}{h_i}\right)} = \frac{p_i}{\hat{\gamma}_i \left(\sum_{j\neq i} \bar{h}_j p_j + \bar{\sigma}_i\right)}, \tag{4.7}$$

where $\bar{h}_j = \frac{h_j}{h_i}$ and $\bar{\sigma}_i = \frac{\sigma_i^2}{h_i}$. With the column wise uncertainty model [93–95], the channel gain is given by

$$H_j = \bar{h}_j + \Delta h_j, \quad |\Delta h_j| \leq \epsilon_{ij} \tag{4.8}$$

where Δh_j is the column wise estimation error and $\epsilon_{ij} \geq 0$ is the error bound.

4.1.2 Outage probability

The outage probability is defined as the probability that the target SINR for a user is not achieved. Thus, the outage probability for user i can be expressed as

$$O_i = \mathbb{P}\left(\gamma_i \leq \hat{\gamma}_i\right) = \mathbb{P}\left(h_i x_i p_i \leq \hat{\gamma}_i \left(\sum_{j\neq i} h_j x_j p_j + \sigma_i^2\right)\right).$$

The outage probability when the received power and interference follow the Nakagami-m distribution can be written as [96–98]

$$O_i = 1 - \exp\left(-\frac{\Lambda_i}{\bar{p}_i}\right) \prod_{j=1, j\neq i}^{k} \phi_j \left(\frac{\hat{\gamma}_i}{\bar{p}_i}\right), \tag{4.9}$$

where $\Lambda_i = \sigma_i^2\hat{\gamma}_i$, $\bar{p_i}$ is the mean of the received power and $\phi_j(\cdot)$ is the moment generating function (MGF) of the interference to user i.

In Nakagami-m fading, the MGF of the interference from user j to user i is

$$\begin{aligned}
\phi_j\left(\frac{\hat{\gamma}_i}{\bar{p_i}}\right) &= \int_{-\infty}^{\infty} \exp\left(-\frac{\hat{\gamma}_i}{\bar{p_i}}p_j\right) f\left(p_j\right) dp_j \\
&= \int_{-\infty}^{\infty} \exp\left(-\frac{\hat{\gamma}_i}{\bar{p_i}}p_j\right) f\left(p_j\right) dp_j \\
&= \int_{0}^{\infty} \exp\left(-\frac{\hat{\gamma}_i}{\bar{p_i}}p_j\right) \left(\frac{m_j}{\bar{p_j}}\right)^{m_j} \frac{p_j^{m_j-1}}{\Gamma\left(m_j\right)} \exp\left(-\frac{m_j p_j}{\bar{p_j}}\right) dp_j \\
&= \left(\frac{m_j}{m_j + \bar{p_j}\frac{\hat{\gamma}_i}{\bar{p_i}}}\right)^{m_j} \\
&= \left(1 + \frac{\bar{p_j}\hat{\gamma}_i}{m_j\bar{p_i}}\right)^{-m_j},
\end{aligned} \tag{4.10}$$

where $\bar{p_j}$ is the mean of the interference to user i. From (4.9) and (4.10), the outage probability is

$$O_i = 1 - \exp\left(-\frac{\sigma_i^2\hat{\gamma}_i}{h_i p_i}\right) \prod_{j=1, j\neq i}^{k} \left(1 + \frac{\hat{\gamma}_i h_j p_j}{m_j h_i p_i}\right)^{-m_j}, \tag{4.11}$$

and considering the channel uncertainty is

$$O_i = 1 - \exp\left(-\frac{\bar{\sigma}_i\hat{\gamma}_i}{p_i}\right) \prod_{j=1, j\neq i}^{k} \left(1 + \frac{\hat{\gamma}_i H_j p_j}{m_j p_i}\right)^{-m_j}. \tag{4.12}$$

Upper and lower bounds on outage probability can be determined using the following inequalities [54, 54, 99]

$$1 + a + \sum_{i=1}^{k} r_i x_i \overset{(13a)}{\leq} e^a \prod_{i=1}^{k} \left(1 + r_i x_i\right) \overset{(13b)}{\leq} e^a \prod_{i=1}^{k} \left(1 + x_i\right)^{r_i} \overset{(13c)}{\leq} e^a e^{\sum_{i=1}^{k}(r_i x_i)}, \tag{4.13}$$

where $x_1, x_2, \ldots, x_k \geq 0$, $r_1, r_2, \ldots, r_k \geq 0$ and $a, k \geq 0$. Equation (13a) follows from the Weierstrass product inequality, (13b) from the Bernoulli inequality, and (13c) from the linear and exponential inequalities. The upper bound on the outage

probability from (13c) is

$$\begin{aligned} O_i &\leq 1 - \exp\left(-\frac{\bar{\sigma}_i\hat{\gamma}_i}{p_i}\right)\exp\left(-\sum_{j=1,j\neq i}^{k} m_j\frac{\hat{\gamma}_i H_j p_j}{m_j p_i}\right) \\ &= 1 - \left\{\exp\left[\frac{\hat{\gamma}_i}{p_i}\left(\bar{\sigma}_i + \sum_{j=1,j\neq i}^{k} H_j p_j\right)\right]\right\}^{-1} \\ &= 1 - \left[\exp\left(\frac{1}{\overline{\Gamma}_i}\right)\right]^{-1} \\ &= 1 - \left[\exp\left(-\frac{1}{\overline{\Gamma}_i}\right)\right]. \end{aligned} \tag{4.14}$$

A lower bound on the outage probability is obtained from (13a) as

$$\begin{aligned} O_i &\geq 1 - \left[1 + \frac{\bar{\sigma}_i\hat{\gamma}_i}{p_i} + \sum_{j=1,j\neq i}^{k}\left(m_j\frac{\hat{\gamma}_i H_j p_j}{m_j p_i}\right)\right]^{-1} \\ &= 1 - \left[1 + \frac{\hat{\gamma}_i}{p_i}\left(\bar{\sigma}_i + \sum_{j=1,j\neq i}^{k} H_j p_j\right)\right]^{-1} \\ &= 1 - \left[1 + \frac{1}{\overline{\Gamma}_i}\right]^{-1} \\ &= \frac{1}{\left(1 + \overline{\Gamma}_i\right)}. \end{aligned} \tag{4.15}$$

Using (4.13) and the following inequality [100, 101]

$$1+a+\sum_{i=1}^{k} r_i x_i \leq \left[1 + \frac{\left(a + \sum_{i=1}^{k} r_i x_i\right)}{\frac{k}{q}}\right]^{\frac{k}{q}} < \left[1 + \frac{\left(a + \sum_{i=1}^{k} r_i x_i\right)}{k}\right]^{k} \leq e^a e^{\sum_{i=1}^{k}(r_i x_i)},$$

where $q > 1$. A tighter lower bound is obtained as

$$\begin{aligned} O_i &\geq 1 - \left\{ 1 + \frac{q}{k} \left[\frac{\bar{\sigma}_i \hat{\gamma}_i}{p_i} + \sum_{j=1, j\neq i}^{k} \left(m_j \frac{\hat{\gamma}_i H_j p_j}{m_j p_i} \right) \right] \right\}^{-\frac{k}{q}} \\ &= 1 - \left\{ 1 + \frac{q}{k} \left[\frac{\hat{\gamma}_i}{p_i} \left(\bar{\sigma}_i + \sum_{j=1, j\neq i}^{k} H_j p_j \right) \right] \right\}^{-\frac{k}{q}} \\ &= 1 - \left\{ 1 + \frac{q}{k} \left[\frac{1}{\overline{\Gamma}_i} \right] \right\}^{-\frac{k}{q}}. \end{aligned} \tag{4.16}$$

4.2 Problem Formulation

In this section, the power allocation problem is presented considering the power consumption and system outage probability. A power allocation problem to maximize the throughput is proposed. This problem is in logarithmic form, so a differential method is proposed to simplify the problem. A power allocation problem for energy efficiency is then presented. This problem is in a fractional program form, so Dinkelbach and parametric transformations are used to convert it to a linear form.

4.2.1 Power allocation for the minimum power consumption with an outage probability constraint

The power consumption problem subject to outage probability and transmit power constraints is

$$\begin{aligned} \text{minimize} \quad & \sum_{i=1}^{k} p_i \\ \text{subject to} \quad & p_{\min} \leq p_i \leq p_{\max} \\ & 1 - \exp\left(-\frac{\bar{\sigma}_i \hat{\gamma}_i}{p_i} \right) \prod_{j=1, j\neq i}^{k} \left(1 + \frac{\hat{\gamma}_i H_j p_j}{m_j p_i} \right)^{-m_j} \leq O_{th}, \end{aligned} \tag{4.17}$$

which is equivalent to

$$\begin{aligned} \text{minimize} \quad & \sum_{i=1}^{k} p_i \\ \text{subject to} \quad & \frac{p_{\min}}{p_i} \leq 1 \\ & \frac{p_i}{p_{\max}} \leq 1 \\ & \left[\exp\left(\frac{\bar{\sigma}_i \hat{\gamma}_i}{p_i}\right) \prod_{j=1, j\neq i}^{k} \left(1 + \frac{\hat{\gamma}_i H_j p_j}{m_j p_i}\right)^{m_j}\right] (1 - O_{th}) \leq 1. \end{aligned} \tag{4.18}$$

This is a geometric programming optimization problem with variables $p_1, p_2, \ldots, p_k$.

An iterative power allocation approach for system outage probability can be obtained using the upper bound in (4.14) and the last constraint in (4.17). This is given by

$$1 - \exp\left(-\frac{\bar{\sigma}_i \hat{\gamma}_i}{p_i}\right) \prod_{j=1, j\neq i}^{k} \left(1 + \frac{\hat{\gamma}_i H_j p_j}{m_j p_i}\right)^{-m_j} \leq 1 - \left[\exp\left(-\frac{1}{\overline{\Gamma}_i}\right)\right] \leq O_{th}.$$

The constraint is satisfied as long as the upper bound on outage probability is less than O_{th}, which implies that

$$1 - \left[\exp\left(-\frac{1}{\overline{\Gamma}_i}\right)\right] \leq O_{th},$$

where $\overline{\Gamma}_i = \frac{\bar{\gamma}_i}{\hat{\gamma}_i}$. After some manipulation, the above inequality can be rewritten as

$$\bar{\gamma}_i \geq -\frac{1}{\log(1 - O_{th})} \hat{\gamma}_i.$$

Assuming that the SINR for user i is satisfied, then

$$-\frac{1}{\log(1 - O_{th})} \geq 1,$$

which gives the following upper bound on O_{th}

$$O_{th} \leq 1 - e^{-1}.$$

The power allocation problem can then be rewritten as

$$\begin{aligned} \text{minimize} \quad & \sum_{i=1}^{k} p_i \\ \text{subject to} \quad & \frac{p_{\min}}{p_i} \leq 1 \\ & \frac{p_i}{p_{\max}} \leq 1 \\ & \bar{\gamma}_i \geq -\frac{\hat{\gamma}_i}{\log\left(1 - O_{th}\right)} \\ & O_{th} \leq 1 - e^{-1}. \end{aligned} \tag{4.19}$$

This problem can be solved using the following power update function

$$p_i(t+1) = \max\left\{p_{\min}, \min\left[p_{\max}, -\frac{1}{\log\left(1 - O_{th}\right)}\frac{\hat{\gamma}_i}{\bar{\gamma}_i} p_i\left(t\right)\right]\right\}. \tag{4.20}$$

4.2.2 Power allocation for the normalized throughput maximization with an outage probability constraint

The throughput problem subject to outage probability and transmit power constraints is formulated as

$$\begin{aligned} \text{maximize} \quad & \sum_{i=1}^{k} R_i = \sum_{i=1}^{k} \log\left(1 + \overline{\Gamma}_i\right) \\ \text{subject to} \quad & p_{\min} \leq p_i \leq p_{\max} \\ & 1 - \left[\exp\left(\frac{\bar{\sigma}_i \hat{\gamma}_i}{p_i}\right) \prod_{j=1, j\neq i}^{k} \left(1 + \frac{\hat{\gamma}_i H_j p_j}{p_i}\right)\right]^{-1} \leq O_{th}. \end{aligned} \tag{4.21}$$

where $\overline{\Gamma}_i = \frac{\bar{\gamma}_i}{\hat{\gamma}_i} = \frac{p_i}{\hat{\gamma}_i\left(\sum_{j\neq i} H_j p_j + \bar{\sigma}_i\right)}$. From (4.14) and (4.21), the last constraint is equivalent to

$$\overline{\Gamma}_i \geq -\frac{1}{\log\left(1 - O_{th}\right)}.$$

After some manipulation, (4.21) can be written as

$$\begin{aligned} \text{maximize} \quad & \sum_{i=1}^{k} R_i = \sum_{i=1}^{k} \log \left[1 + \frac{p_i}{\hat{\gamma}_i \left(\sum_{j \neq i} H_j p_j + \bar{\sigma}_i \right)} \right] \\ \text{subject to} \quad & p_{\min} \leq p_i \leq p_{\max} \\ & \frac{p_i}{\hat{\gamma}_i \left(\sum_{j \neq i} H_j p_j + \bar{\sigma}_i \right)} \geq -\frac{1}{\log\left(1 - O_{th}\right)}. \end{aligned} \tag{4.22}$$

Let

$$\Psi_i = \frac{p_i}{\hat{\gamma}_i \left(\sum_{j \neq i} H_j p_j + \bar{\sigma}_i \right)}. \tag{4.23}$$

Introducing two auxiliary function $F(\Psi_i)$ and $F(p_i)$, (4.22) can be expressed as

$$\begin{aligned} \text{maximize} \quad & \sum_{i=1}^{k} R_i = \sum_{i=1}^{k} \left[\log\left(1 + \Psi_i\right) + F(\Psi_i) + G(p_i) \right] \\ \text{subject to} \quad & p_{\min} \leq p_i \leq p_{\max} \\ & \Psi_i \geq -\frac{1}{\log\left(1 - O_{th}\right)}. \end{aligned} \tag{4.24}$$

A differential method is proposed by first taking the derivative of R_i with respect to Ψ_i

$$\frac{\partial R_i}{\partial \Psi_i} = \frac{1}{1 + \Psi_i} + F'(\Psi_i),$$

and setting $\frac{\partial R_i}{\partial \Psi_i}$ to 0 with p_i fixed gives

$$F'(\Psi_i) = -\frac{1}{1 + \Psi_i} = -\frac{\hat{\gamma}_i \left(\sum_{j \neq i} H_j p_j + \bar{\sigma}_i \right)}{\hat{\gamma}_i \left(\sum_{j \neq i} H_j p_j + \bar{\sigma}_i \right) + p_i}.$$

Now taking the integral of $F'(\Psi_i)$ with respect to Ψ_i we obtain

$$\begin{aligned} F(\Psi_i) &= -\frac{\hat{\gamma}_i\left(\sum_{j\neq i} H_j p_j + \bar{\sigma}_i\right)}{\hat{\gamma}_i\left(\sum_{j\neq i} H_j p_j + \bar{\sigma}_i\right) + p_i}\Psi_i \\ &= -\frac{\hat{\gamma}_i\left(\sum_{j\neq i} H_j p_j + \bar{\sigma}_i\right) + p_i - p_i}{\hat{\gamma}_i\left(\sum_{j\neq i} H_j p_j + \bar{\sigma}_i\right) + p_i}\Psi_i \\ &= -\Psi_i + \frac{p_i}{\hat{\gamma}_i\left(\sum_{j\neq i} H_j p_j + \bar{\sigma}_i\right) + p_i}\Psi_i. \end{aligned}$$

The auxiliary function $G(p_i)$ is determined assuming that Ψ_i is fixed and setting $F(\Psi_i) + G(p_i) = 0$ which gives

$$\begin{aligned} G((p_i)) &= \frac{\hat{\gamma}_i\left(\sum_{j\neq i} H_j p_j + \bar{\sigma}_i\right)}{\hat{\gamma}_i\left(\sum_{j\neq i} H_j p_j + \bar{\sigma}_i\right) + p_i}\Psi_i \\ &= \left[\frac{\hat{\gamma}_i\left(\sum_{j\neq i} H_j p_j + \bar{\sigma}_i\right)}{\hat{\gamma}_i\left(\sum_{j\neq i} H_j p_j + \bar{\sigma}_i\right) + p_i}\right]\left[\frac{p_i}{\hat{\gamma}_i\left(\sum_{j\neq i} H_j p_j + \bar{\sigma}_i\right)}\right] \\ &= \frac{p_i}{\hat{\gamma}_i\left(\sum_{j\neq i} H_j p_j + \bar{\sigma}_i\right) + p_i}, \end{aligned}$$

so then

$$\begin{aligned} F(\Psi_i) + G(p_i) &= -\Psi_i + \frac{p_i}{\hat{\gamma}_i\left(\sum_{j\neq i} H_j p_j + \bar{\sigma}_i\right) + p_i}\Psi_i + \frac{p_i}{\hat{\gamma}_i\left(\sum_{j\neq i} H_j p_j + \bar{\sigma}_i\right) + p_i} \\ &= -\Psi_i + \frac{p_i}{\hat{\gamma}_i\left(\sum_{j\neq i} H_j p_j + \bar{\sigma}_i\right) + p_i}(\Psi_i + 1). \end{aligned} \tag{4.25}$$

Finally, the power allocation problem can be rewritten as

$$\begin{aligned}
\text{maximize} \quad & \sum_{i=1}^{k} R_i = \sum_{i=1}^{k} \left[\log\left(1+\Psi_i\right) - \Psi_i + \frac{p_i}{\hat{\gamma_i}\left(\sum_{j\neq i} H_j p_j + \bar{\sigma_i}\right) + p_i}(\Psi_i + 1) \right] \\
\text{subject to} \quad & p_{\min} \leq p_i \leq p_{\max} \\
& \Psi_i \geq -\frac{1}{\log\left(1-O_{th}\right)}.
\end{aligned} \tag{4.26}$$

This can be considered as an outer optimization problem over Ψ_i with fixed p_i and an inner optimization problem over p_i with fixed Ψ_i. A subtractive form of (4.26) can be obtained using a parametric transformation and introducing a variable ψ_i

$$\begin{aligned}
\text{maximize} \sum_{i=1}^{k} R_i \quad = & \sum_{i=1}^{k} \left\{ \log\left(1+\Psi_i\right) - \Psi_i + \frac{1}{2}\sqrt{\psi_i}\left[p_i\left(\Psi_i+1\right)\right]^2 \right. \\
& \left. - \psi_i \left[\hat{\gamma_i}\left(\sum_{j\neq i} H_j p_j + \bar{\sigma_i} \right) + p_i \right] \right\} \\
\text{subject to} \quad & p_{\min} \leq p_i \leq p_{\max} \\
& \Psi_i \geq -\frac{1}{\log\left(1-O_{th}\right)}.
\end{aligned} \tag{4.27}$$

The variable ψ_i is determined by taking the derivative of R_i with respect to ψ_i and setting $\frac{\partial R_i}{\partial \psi_i}$ to 0 which gives

$$\psi_i = \left\{ \frac{\left[p_i\left(\Psi_i+1\right)\right]^2}{4\left[\hat{\gamma_i}\left(\sum_{j\neq i} H_j p_j + \bar{\sigma_i}\right) + p_i\right]} \right\}^2. \tag{4.28}$$

Taking the derivative of R_i with respect to p_i and setting $\frac{\partial R_i}{\partial p_i}$ to zero gives

$$p_i = \frac{\psi_i\left(\hat{\gamma_i}\sum_{j\neq i} H_j + 1\right)}{\sqrt{\psi_i}\left[\left(\Psi_i+1\right)\right]^2}. \tag{4.29}$$

The proposed power control algorithm based on (4.23), (4.28) and (4.29) is given in Algorithm 7.

Algorithm 7 Power Allocation Algorithm for the Normalized Throughput Maximization over Nakagami-m Fading Channels

Step 1: Let the iteration index $t = 1$. User i obtains the outage probability threshold O_{th} from the BS and determines the average SINR $\bar{\gamma}_i$. Set the target SINR $\hat{\gamma}_i$.

Step 2: Users determine $\Psi_i(t)$ using (4.23)

$$\Psi_i(t) = \frac{p_i(t)}{\hat{\gamma}_i \left[\sum_{j \neq i} H_j p_j(t) + \bar{\sigma}_i\right]}, i, j = 1, 2, \ldots, k \text{ and } i \neq j.$$

Step 3: Users determine $\psi_i(t)$ using (4.28)

$$\psi_i(t) = \left\{ \frac{\left[p_i(t)\left(\Psi_i(t)+1\right)\right]^2}{4\left[\hat{\gamma}_i\left(\sum_{j \neq i} H_j p_j(t) + \bar{\sigma}_i\right) + p_i(t)\right]} \right\}^2.$$

Step 4: Users update their transmit power using (4.29)

$$p_i(t+1) = \frac{\psi_i(t)\left(\hat{\gamma}_i \sum_{j \neq i} H_j + 1\right)}{\sqrt{\psi_i(t)}\left[\left(\Psi_i(t)+1\right)\right]^2}.$$

Step 5: Terminate when

$$\max_i |p_i(t+1) - p_i(t)| \leq \epsilon,$$

otherwise go to **Step 2**.

4.2.3 Power allocation for the energy efficiency with an outage probability constraint

The system energy efficiency problem subject to outage probability and transmit power constraints is formulated as

$$\begin{aligned} \text{maximize} \quad & \eta = \sum_{i=1}^{k} \eta_i = \sum_{i=1}^{k} \frac{R_i}{P_i} \\ \text{subject to} \quad & p_{\min} \leq p_i \leq p_{\max} \\ & O_i = 1 - \exp\left(-\frac{\bar{\sigma}_i \hat{\gamma}_i}{p_i}\right) \prod_{j=1, j\neq i}^{k} \left(1 + \frac{\hat{\gamma}_i H_j p_j}{m_j p_i}\right)^{-m_j} \leq O_{th}. \end{aligned} \tag{4.30}$$

Using the upper bound in (4.14), the last constraint can be rewritten as

$$\bar{\gamma}_i \geq -\frac{\hat{\gamma}_i}{\log\left(1 - O_{th}\right)}.$$

A subtractive form of (4.30) can be obtained using a parametric transformation with a variable θ_i

$$\begin{aligned} \text{maximize} \quad & \sum_{i=1}^{k} \eta_i = \sum_{i=1}^{k} \left(2\theta_i R_i - \theta_i^2 P_i\right) \\ \text{subject to} \quad & \frac{p_{\min}}{p_i} \leq 1 \\ & \frac{p_i}{p_{\max}} \leq 1 \\ & \bar{\gamma}_i \geq -\frac{\hat{\gamma}_i}{\log\left(1 - O_{th}\right)}. \end{aligned} \tag{4.31}$$

The variable θ_i is obtained by taking the derivative of η_i with respect to θ_i and setting $\frac{\partial \eta}{\partial \theta_i}$ to 0 which gives

$$\theta_i = \frac{R_i}{P_i}. \tag{4.32}$$

Using P_i from (4.5) and R_i from (4.27), the terms in the objective function of (4.31) can be expressed as

$$\begin{aligned}\eta_i =& 2\theta_i \left\{ \log\left(1+\Psi_i\right) - \Psi_i + \frac{1}{2}\sqrt{\psi_i}\left[p_i\left(\Psi_i+1\right)\right]^2 - \psi_i \left[\hat{\gamma}_i\left(\sum_{j\neq i} H_j p_j + \bar{\sigma}_i\right) + p_i\right]\right\} \\ & - \theta_i^2(\xi p_i + p_{ic}).\end{aligned}$$

Taking the derivative of η_i with respect p_i and setting $\frac{\partial \eta_i}{\partial p_i}$ to 0 gives

$$\begin{aligned} p_i =& \frac{\theta_i \xi}{2\sqrt{\psi_i}\left[\left(\Psi_i+1\right)\right]^2} + \frac{2\psi_i\left(\hat{\gamma}_i \sum_{j\neq i} H_j + 1\right)}{2\sqrt{\psi_i}\left[\left(\Psi_i+1\right)\right]^2} \\ =& \frac{\theta_i \xi + 2\psi_i\left(\hat{\gamma}_i \sum_{j\neq i} H_j + 1\right)}{2\sqrt{\psi_i}\left[\left(\Psi_i+1\right)\right]^2}. \end{aligned} \tag{4.33}$$

Using the Dinkelbach method [102], (4.30) becomes

$$\begin{aligned} \text{maximize} \quad & \eta = \sum_{i=1}^{k} \eta_i = \sum_{i=1}^{k} \left(R_i - \theta_i P_i\right) \\ \text{subject to} \quad & \frac{p_{\min}}{p_i} \leq 1 \\ & \frac{p_i}{p_{\max}} \leq 1 \\ & \bar{\gamma}_i \geq -\frac{\hat{\gamma}_i}{\log\left(1-O_{th}\right)}. \end{aligned} \tag{4.34}$$

This problem can be solved using the iterative Newton method [103]. The user transmit power is then determined by

$$\begin{aligned} p_i(t+1) &= p_i(t) - \frac{\eta_i(t)}{\eta_i'(t)} \\ &= p_i(t) - \frac{R_i(t) - \theta_i P_i(t)}{R_i'(t) - \theta_i P_i'(t)}. \end{aligned} \tag{4.35}$$

where

$$P_i'(t) = \xi,$$

and $R_i'(t)$ is obtained by taking the derivative of R_i in (4.27) with respect to p_i

$$R_i'(t) = \sqrt{\psi_i} p_i(t)(\Psi_i + 1)^2 - \psi_i \left(\hat{\gamma}_i \sum_{j \neq i} H_j + 1 \right).$$

The proposed power control algorithm based on (4.23), (4.32), (4.33) and (4.35) is given in Algorithm 8.

4.3 Numerical Results

In this section, Monte Carlo simulation is used to evaluate the performance of the proposed power allocation schemes. The performance is compared with that of the target signal to interference plus noise ratio (SINR) tracking power allocation (TTPA), power allocation with temporary removal and feasibility check (PARF) and distributed opportunistic power allocation (DOPA) schemes. The channel gain is $h_i = \bar{g} d_i^{\alpha} 10^{\frac{\Xi}{10}}$. As in the related literature [104, 105], the path loss exponent is set to $\alpha = 4$ which corresponds to urban and suburban environments, and $\bar{g} = 0.97$ is a constant. The column wise error bound ϵ_{ij} is randomly chosen in the range $[0, 0.1]$, and the stopping criteria is $\epsilon = 10^{-5}$.

Different values of q in the range $[1, 20]$ were tested, and $q = 3$ gives the best lower bound for the outage probability. Thus, the constant $q = 3$ in (4.16) is used in the remainder of this section. The number of the Nakagami-m fading taps is set to 4 [106]. The real and imaginary parts of the channel coefficients are randomly chosen from a Gaussian distribution. The magnitude is then Nakagami-m distributed and the phase is uniformly distributed between 0 and 2π. The fading parameters considered are $m = 0.5, 1, 2, 4, 8$. The user noise power is $\sigma^2 = 0.01$ W and the initial power level for all users is 1 W. The maximum transmit power is $p_{\max} = 2$ W. The users are uniformly distributed in the geographic area of the BS. The results are obtained for 10000 trials for each number of users with the user locations changed each trial.

In the first scenario, there is one femtocell with 4 users. The BS is located at the center of a square geographic area with dimensions 50 m $\times$ 50 m. Table 4.1 presents the average power, throughput from (4.4), energy efficiency from (4.6), outage probability from (4.12) and number of unsatisfied users for the TTPA, PARF, DOPA, and proposed algorithms. The average power for TTPA is the highest with 0.97 W followed by Algorithm 7 with 0.71 W. The average powers for PARF, DOPA

Algorithm 8 Power Allocation Algorithm for the Energy Efficiency over Nakagami-m Fading Channels

Step 1: Set $t = 1$. User i obtains the outage probability threshold O_{th} from the BS and determines the average SINR $\bar{\gamma}_i$. Set the target SINR $\hat{\gamma}_i$.

Step 2: Users determine $\Psi_i(t)$ using (4.23)

$$\Psi_i(t) = \frac{p_i(t)}{\hat{\gamma}_i \left[\sum_{j \neq i} H_j p_j(t) + \bar{\sigma}_i\right]}, i, j = 1, 2, \ldots, k \text{ and } i \neq j.$$

Step 3: Users determine $\psi_i(t)$ using (4.28)

$$\psi_i = \left\{ \frac{\left[p_i \left(\Psi_i + 1\right)\right]^2}{4\left[\hat{\gamma}_i \left(\sum_{j \neq i} H_j p_j + \bar{\sigma}_i\right) + p_i\right]} \right\}^2.$$

Step 4: Users determine $\theta_i(t)$ using (4.32)

$$\theta_i(t) = \frac{R_i(t)}{P_i(t)}.$$

Step 5: Users update their transmit power
using (4.33)

$$p_i(t+1) = \frac{\theta_i(t)\xi + 2\psi_i(t)\left(\hat{\gamma}_i \sum_{j \neq i} H_j + 1\right)}{2\sqrt{\psi_i(t)}\left[\left(\Psi_i(t) + 1\right)\right]^2},$$

or using (4.35)

$$p_i(t+1) = p_i(t) - \frac{R_i(t) - \theta_i(t)P_i(t)}{R_i'(t) - \theta_i(t)P_i'(t)}.$$

Step 6: Terminate when

$$\max_i |p_i(t+1) - p_i(t)| \leq \epsilon,$$

otherwise go to **Step 2**.

and Algorithm 8 are almost identical at 0.02 W. The highest average throughput is obtained by Algorithm 7 which is 5.44 Mbps. This is followed by TTPA and DOPA. PARF and Algorithm 8 have the lowest average throughput, 2.78 Mbps and 3.28 Mbps, respectively. The highest average energy efficiency is given by Algorithm 8 with 22.4 Mbps/W followed by PARF with 20.9 Mbps/W. TTPA give the lowest average energy efficiency of 0.69 Mbps/W. TTPA and Algorithm 7 provide the lowest average outage probability. The average outage probability with PARF is the highest at 0.63. Note that there is one unsatisfied user with DOPA.

Table 4.1: Performance of the TTPA, PARF, DOPA and Proposed Algorithms with 4 Users

Power Allocation Scheme	Average Power (W)	Average Throughput (Mbps)	Average Energy Efficiency (Mbps/W)	Average Outage Probability (%)	Unsatisfied Users
TTPA	0.97	5.36	0.69	0.38	0
PARF	0.02	2.78	20.9	0.63	0
DOPA	0.19	5.17	3.49	0.43	1
Algorithm 1	0.71	5.44	0.96	0.36	0
Algorithm 2	0.02	3.28	22.4	0.56	0

In the second scenario, there is one femtocell with 8 users. The BS is located at the center of a square geographic area with dimensions 50 m $\times$ 50 m. Table 4.2 presents the average power, throughput, energy efficiency, outage probability and number of unsatisfied users for the TTPA, PARF, DOPA, and proposed algorithms. The average power for TTPA is the highest with 1.99 W followed by Algorithm 7 with 1.6 W. The average powers for PARF, DOPA and Algorithm 8 are similar around 0.05 W. The highest average throughput is obtained by TTPA at 7.64 dB, and Algorithm 7 is slightly less. PARF and Algorithm 8 have the lowest average throughput with 5.58 Mbps and 6.15 Mbps, respectively. The highest average energy efficiency is given by Algorithm 8 with 17.3 Mbps/W, and followed by PARF with 13.2 Mbps/W. TTPA and Algorithm 7 have the lowest average energy efficiency at 0.48 Mbps/W and 0.6 Mbps/W, respectively. Algorithm 7 give the lowest average outage probability with 0.51, and followed closely by TTPA with 0.52. The average outage probability with PARF is the highest at 0.63. There are two unsatisfied users with DOPA and three with TTPA.

In the third scenario, there is one picocell with 16 users. The BS is located at the center of a square geographic area with dimensions 300 m $\times$ 300 m. Table 4.3 presents the average power, throughput, energy efficiency, outage probability and

Table 4.2: Performance of the TTPA, PARF, DOPA and Proposed Algorithms with 8 Users

Power Allocation Scheme	Average Power (W)	Average Throughput (Mbps)	Average Energy Efficiency (Mbps/W)	Average Outage Probability (%)	Unsatisfied Users
TTPA	1.99	7.64	0.48	0.52	3
PARF	0.05	5.58	13.2	0.63	0
DOPA	0.33	7.37	2.79	0.55	2
Algorithm 1	1.60	7.59	0.60	0.51	0
Algorithm 2	0.05	6.15	17.3	0.59	0

number of unsatisfied users for the TTPA, PARF, DOPA, and proposed algorithms. The average power for TTPA is the highest with 1.98 W followed by Algorithm 8 with 0.96 W. The average power for PARF and Algorithm 8 is similar at 0.11 W and 0.10 W, respectively. The highest average throughput is obtained by Algorithm 7 with 11.9 Mbps. This is followed closely by TTPA with 11.8 Mbps and DOPA with 11.7 Mbps. The average throughput for PARF and Algorithm 8 is similar at 11.1 Mbps and 11.2 Mbps, respectively. The highest average energy efficiency is given by Algorithm 8 with 7.31 Mbps/W followed by PARF with 6.27 Mbps/W. TTPA and Algorithm 7 have the lowest average energy efficiency with 0.37 Mbps/W and 0.38 Mbps/W, respectively. TTPA and Algorithm 7 also have the lowest average outage probability. The average outage probability with TTPA, PARF, DOPA and the proposed algorithms is similar at 0.63. There are 9 unsatisfied users with DOPA which is the highest, while TTPA and Algorithm 7 have 5 unsatisfied users.

Table 4.3: Performance of the TTPA, PARF, DOPA and Proposed Algorithms with 16 Users

Power Allocation Scheme	Average Power (W)	Average Throughput (Mbps)	Average energy Efficiency (Mbps/W)	Average Outage Probability (%)	Unsatisfied Users
TTPA	1.98	11.8	0.37	0.63	5
PARF	0.11	11.1	6.27	0.63	0
DOPA	0.32	11.7	2.22	0.63	9
Algorithm 1	1.96	11.9	0.38	0.62	5
Algorithm 2	0.10	11.2	7.31	0.63	0

In the fourth scenario, there is one picocell with 32 users. The BS is located at the center of a square geographic area with dimensions 300 m $\times$ 300 m. Table 4.4 presents the average power, throughput, energy efficiency, outage probability and number of unsatisfied users for the TTPA, PARF, DOPA, and proposed algorithms. The average

powers for TTPA and Algorithm 7 are the highest at 1.98 W followed by Algorithm 7 at 0.71 W. The average power for DOPA is the lowest at 0.33 W. The average power for PARF and Algorithm 8 is almost the same at 0.88 W and 0.92 W, respectively. The highest average throughput is obtained by the Algorithm 7 which is 24.5 Mbps. This is followed by TTPA with 24.4 Mbps and DOPA with 24.3 Mbps. PARF and Algorithm 8 have the lowest average throughput which is 20.6 Mbps. The highest average energy efficiency is for DOPA with 2.33 Mbps/W. This is followed by PARF with 0.73 Mbps/W and Algorithm 8 with 0.70 Mbps/W. TTPA and Algorithm 7 have the lowest average energy efficiency at 0.39 Mbps/W. The average outage probability with TTPA, DOPA, PARF and the proposed algorithms are almost identical ranging from 0.65 to 0.67. Algorithm 8 has the lowest number of unsatisfied users with 6, while PARF is the highest with 21. The number of unsatisfied users for TTPA and Algorithm 7 is 16 and 14, respectively.

Table 4.4: Performance of the TTPA, PARF, DOPA and Proposed Algorithms with 32 Users

Power Allocation Scheme	Average Power (W)	Average Throughput (Mbps)	Average Energy Efficiency (Mbps/W)	Average Outage Probability (%)	Unsatisfied Users
TTPA	1.98	24.4	0.39	0.65	16
PARF	0.88	20.6	0.73	0.67	21
DOPA	0.33	24.3	2.33	0.66	19
Algorithm 1	1.98	24.5	0.39	0.65	14
Algorithm 2	0.92	20.6	0.70	0.67	6

Fig. 4.1 shows the lower bound (4.16), upper bound (4.14), and exact average outage probability versus the target SINR (4.12) with Nakagami-m fading. This shows that the average outage probability is more severe with $m < 1$, and less severe with $m > 1$ compared to Rayleigh fading. Rayleigh fading is an special case of Nakagami-m as $m = 1$. The maximum gap between the exact outage probability and upper bound is 1.39% for $m = 0.5$, 0.47% for $m = 1$, 0.16% for $m = 2$, and 0.08% for $m = 4$. The maximum gap between the exact outage probability and lower bound is 0.05% for $m = 0.5$, 0.23% for $m = 1$, 0.48% for $m = 2$, and 0.41% for $m = 4$. The average gap over 4 scenarios is 0.29% for the lower bound, which is lightly tighter than the upper bound with 0.53%.

Fig. 4.2 shows the average average outage probability versus the target SINR for different numbers of users and $m = 0.5$ averaged over 100 trials. This shows that the upper and lower bounds are almost exact. As the number of users increases, the

average outage probability increases, as expected. The maximum gap between the average outage probability and upper bound is 0.51% for 8 users, 0.63% for 16 users, 0.62% for 32 users, 0.93% for 64 users, and 0.64% for 128 users. The maximum gap between the average outage probability and lower bound is 0.10% for 8 users, 0.07% for 16 users, 0.13% for 32 users, 0.23% for 64 users, and 0.20% for 128 users. The maximum outage probability is 15.6% for 8 users, 23.7% for 16 users, 34.9% for 32 users, 63.4% for 64 users, and 88.3% for 128 users.

Fig. 4.3 shows the average average outage probability versus the target SINR for different numbers of users and $m = 1$ averaged over 100 trials. This shows that the upper and lower bounds are almost exact. The maximum gap between the average outage probability and upper bound is 0.10% for 8 users, 0.26% for 16 users, 0.31% for 32 users, 0.36% for 64 users, and 0.38% for 128 users. The maximum gap between the average outage probability and lower bound is 0.05% for 8 users, 0.03% for 16 users, 0.10% for 32 users, 0.09% for 64 users, and 0.10% for 128 users. The maximum outage probability is 10.3% for 8 users, 19.9% for 16 users, 34.1% for 32 users, 51.4% for 64 users, and 84.5% for 128 users.

Fig. 4.4 shows the average outage probability versus the target SINR for different numbers of users and $m = 2$ averaged over 100 trials. Again the upper and lower

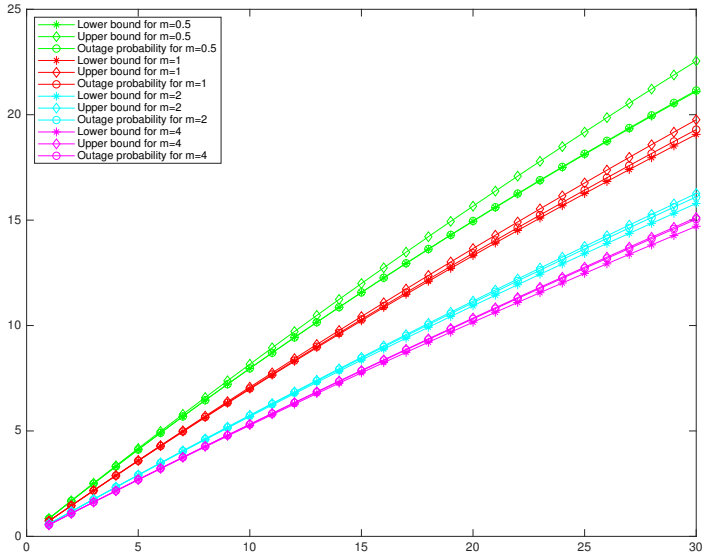

Figure 4.1: Upper bound, lower bound and exact average outage probability in Nakagami-m fading.

bounds are almost exact. The maximum gap between the average outage probability

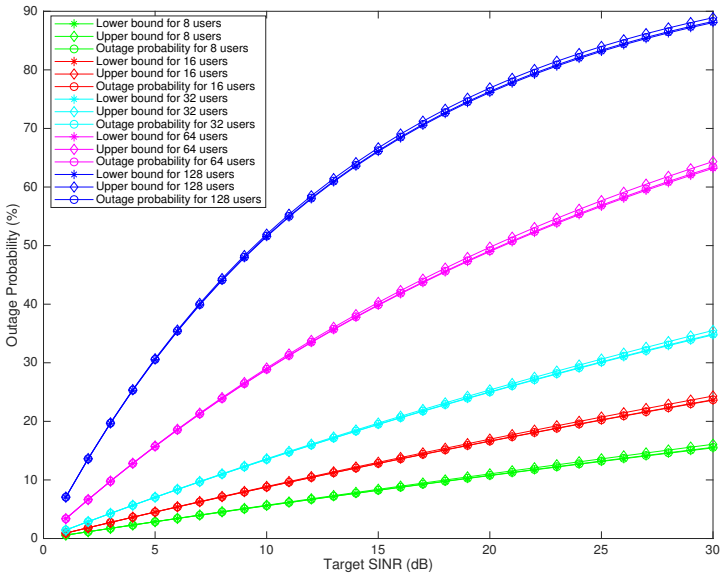

Figure 4.2: Lower and upper bounds and the exact average outage probability in Nakagami-m fading for $m = 0.5$.

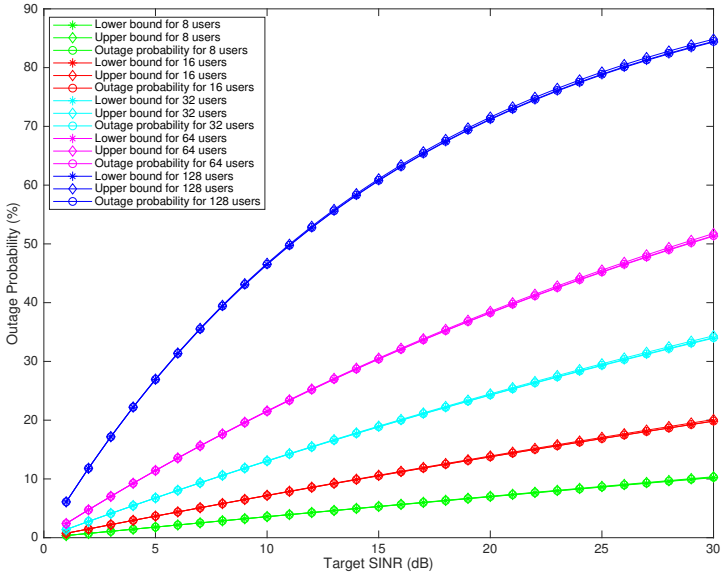

Figure 4.3: Lower and upper bounds and the exact average outage probability in Nakagami-m fading for $m = 1$.

and upper bound is 0.06% for 8 users, 0.12% for 16 users, 0.15% for 32 users, 0.25% for 64 users, and 0.21% for 128 users. The maximum gap between the average outage probability and lower bound is 0.10% for 8 users, 0.13% for 16 users, 0.16% for 32 users, 0.36% for 64 users, and 0.31% for 128 users. The maximum outage probability is 10.0% for 8 users, 17.5% for 16 users, 27.3% for 32 users, 56.2% for 64 users, and 76.9% for 128 users.

Fig. 4.5 gives the average power, outage probability, and SINR with PARF for 8 users. This shows that PARF converges after 3 iterations. The average power is 0.05 W and all users are satisfied with their target SINRs. The average outage probability is 0.61. Fig. 4.6 gives the average power, outage probability, and SINR with Algorithm 7. This shows that the algorithm converges after 3 iterations, similar to PARF, while the average power is 1.60 W, which is higher than with PARF. All users are satisfied with their target SINRs. The average outage probability is 0.51 which is much better than PARF. Fig. 4.7 gives the average power, outage probability, and SINR with Algorithm 8. This algorithm converges after 3 iterations as with PARF, while the average power is 0.02 W, which is lower than with PARF. All users are satisfied with their target SINRs. The average outage probability is 0.56, which is less than PARF but higher than Algorithm 7. Algorithm 8 outperforms

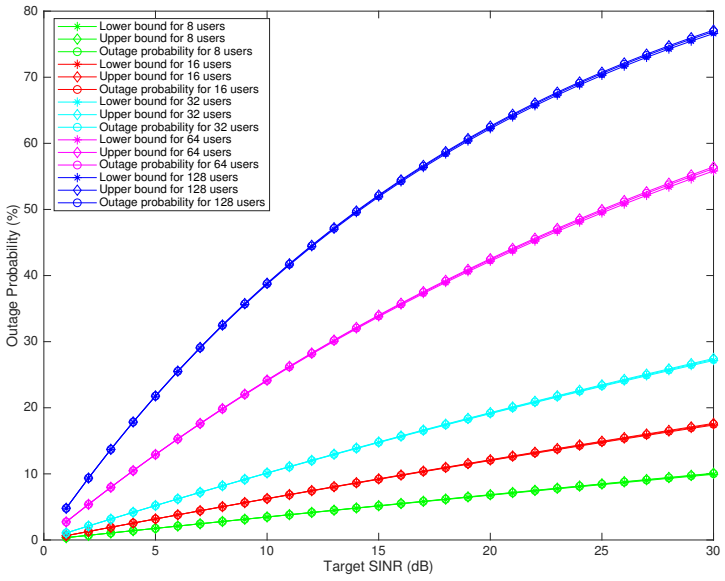

Figure 4.4: Lower and upper bounds and the exact average outage probability in Nakagami-m fading for $m = 2$.

TTPA in terms of power consumption and outage probability, and the average outage probability using Algorithm 7 is the lowest. .

4.4 Conclusion

In this chapter, upper and lower bounds on the outage probability over Nakagami-m fading channels were determined. Power allocation schemes to maximize the throughput and minimize the energy efficiency were proposed. The goal is to improve the power consumption, throughput and energy efficiency. Performance results were presented which show that Algorithm 7 outperforms the power allocation with temporary removal and feasibility check (PARF) and distributed opportunistic power allocation (DOPA) schemes in term of throughput and outage probability for all scenarios. Algorithm 7 is better than the target signal to interference plus noise ratio (SINR) tracking power allocation (TTPA) scheme in term of the average throughput for all scenarios except scenario 2. The performance of TTPA is the best for scenario 2. Considering the number of users unsatisfied with their target SINRs, Algorithm 7

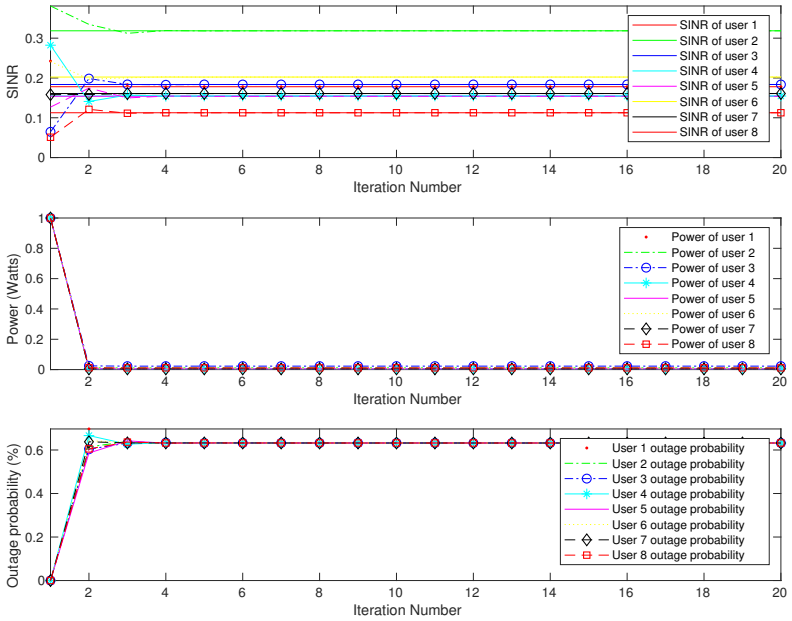

Figure 4.5: The average power, outage probability, and SINR with the PARF algorithm.

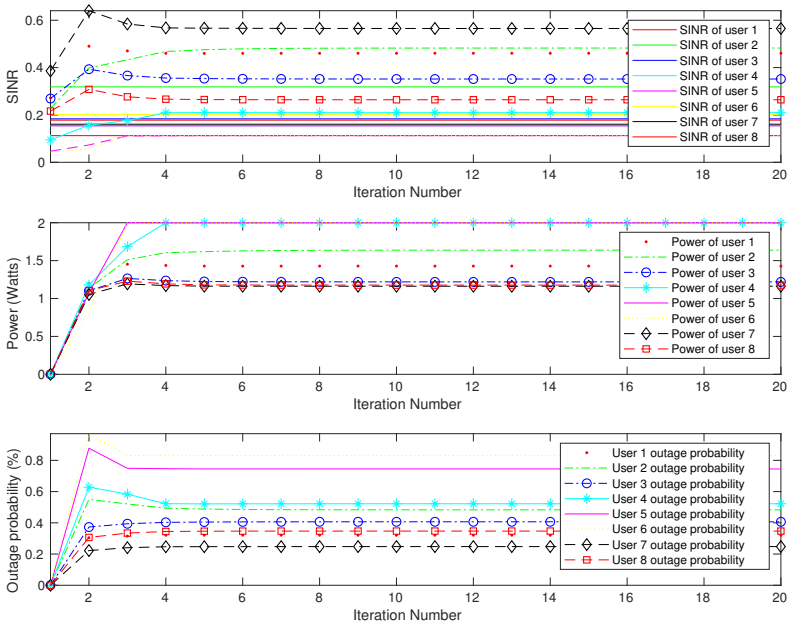

Figure 4.6: The average power, outage probability, and SINR with Algorithm 7.

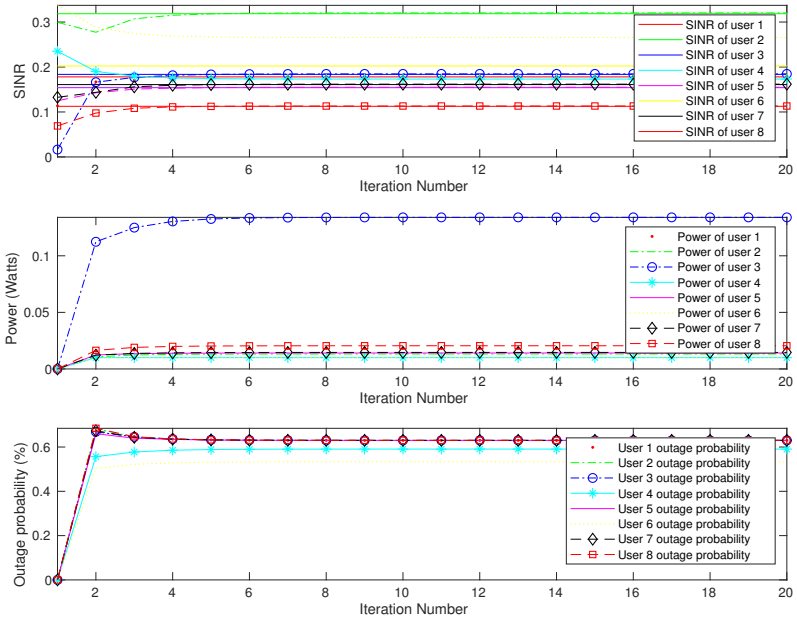

Figure 4.7: The average power, outage probability, and SINR with Algorithm 8.

is better than PARF for all scenarios except scenario 2. Algorithm 8 is better than TTPA and DOPA in terms of power consumption, energy efficiency and the number of satisfied users for all scenarios. The performance of Algorithm 8 and PARF is similar in terms of energy efficiency and power consumption, but the number of unsatisfied users with Algorithm 8 is less than PARF for a large number of users. Algorithm 8 gives the highest average energy efficiency and lowest number of unsatisfied users, while Algorithm 7 gives the best average throughput.

Chapter 5

Prioritized and Selective Power Allocation in Cellular Wireless Networks

In cellular communication systems, power allocation is important to maintain network capacity and user satisfaction. The goal of power allocation is to reduce the aggregate power consumption while satisfying as many users as possible with their target signal to interference plus noise ratio (SINR) by managing the mutual interference between users. There are two types of power allocation, centralized power allocation (CPA) and distributed power allocation (DPA) [107]. With CPA, the core network determines the power levels for all users simultaneously using the channel state information and target SINR levels. This requires frequent channel measurements and communication overhead between the core network and base stations (BSs), which is challenging in a typical system. With DPA, users determine their power levels using only local information and minimum feedback from the BS. Therefore, DPA is simpler than CPA and requires less overhead. However, the resulting power levels may result in degraded performance. In general, DPA is preferred to CPA and so is considered in this chapter.

There are three types of DPA, single target SINR, variable SINR, and multiple target SINR [108]. In [109], [110], single target SINR tracking power allocation (TSPA) was proposed. The objective of TSPA is to minimize the transmit power while satisfying the SINR requirements of all users. With TSPA, users adjust their power levels until their target SINRs are satisfied. If there is no power level that satisfies the

target SINR, they transmit with their maximum power, which is not efficient. This causes significant interference to other users, resulting in many unsatisfied users.

Variable SINR opportunistic power allocation (VOPA) was proposed in [111] to overcome the problems with TSPA. With VOPA, users increase their transmit power if the channel conditions are good, and vice versa. Thus, users who cannot attain their target SINRs reduce their power instead of transmitting at maximum power. This improves the system throughput (sum of all user throughputs) and reduces the interference to other users. However, if many users experience poor channel conditions, a large number will not be satisfied with their target SINRs, which is not acceptable.

In [112], dynamic target SINR tracking power allocation (DTPA) was presented. With DTPA, a BS employs an upper power level. If the power required by a user to reach their target SINR is above this level, they do not adjust their target SINR or power. However, they can increase their power if the required power is below this level. This enables users to reach higher SINRs than the target SINRs. With this approach, the system throughput is significantly improved compared to TSPA and the number of unsatisfied users is reduced compared to VOPA. However, all users with good channel conditions can increase their transmit power levels, which may not be efficient. In [113], variable target SINR tracking power allocation (VTPA) was proposed. With VTPA, a BS assigns lower and upper power levels to all associated users. These levels are determined based on the user channel conditions and the number of associated users. If the power required for a user to attain a target SINR goes above the upper level, the lowest target SINR is assigned. However, if the required power is below the lower level, the highest target SINR is assigned to the user. Otherwise, the power is set between the lowest and highest levels based on the level required to achieve the target SINR. The objective of DTPA and VTPA is to improve the system throughput and allow users to dynamically change their target SINRs. While many power allocation techniques exist in the literature, none solves the uplink power allocation problem considering both user priority and user satisfaction. To provide a solution, in this chapter three types of users are considered, namely priority users (PUs), satisfied normal users (NUs) and unsatisfied NUs.

In a cellular network, users who require high and stable data rates, and active users, should have priority. Thus, these users are considered to be PUs. Users who can tolerate low and variable data rates, and new users, are considered to be NUs. After all PUs are satisfied with their target SINRs, the goal is to satisfy the highest

number of NUs. In the proposed power allocation scheme, NUs who are currently satisfied with their target SINRs are not required to adjust their transmit power levels in order to limit the interference to other users. Conversely, unsatisfied NUs update their transmit power levels in order to attain their target SINRs. The goal is to reduce the aggregate power consumption and improve the power efficiency with different user priorities. Power efficiency is defined as the ratio of network utility to power consumption. Network utility is the difference between the sum of the throughput of all users and the aggregate power consumption.

User data rates over 1 Gb/s have been proposed for 5G networks. Thus, users who require data rates greater than 1 Gb/s can be considered as PUs, and the rest as NUs. In addition, future cellular networks are expected to accommodate flexible requirements, so user target SINRs should be adjusted according to their demands [114]. In enhanced mobile broadband networks there are both BSs and hotspots. The coverage area for a BS is large and a BS is expected to serve many users. Conversely, the coverage area for a hotspot is small and the number of users served is low [115]. In this case, users associated with BSs can be considered as PUs, and users in hotspot areas as NUs. The proposed scheme can also be used for mobile health services. For example, patients and medical staff in urgent situations can be monitored closely as PUs.

Users can be classified as either low or high handoff frequency. Those with high handoff frequency can be designated as PUS and the remainder as NUs [116]. In addition, high mobility users (speeds greater than 50 km/h) can be considered as PUs. Then these users can satisfy their target SINRs as quickly as possible. Low mobility users (speeds less than 50 km/h) have more stable channel conditions and so can be designated as NUs [117].

Ultra dense cellular networks (UDCNs) have been proposed for 5G networks which include macrocells, picocells and femtocells [118]. In addition to cellular traffic, 5G networks will also support device to device (D2D) and internet of things (IoT) communications [119]. However, satisfying users in the presence of a large number of interferers is a challenging task. Hence, coexistence through interference management is essential to achieving the potential of 5G networks, and power allocation is a key technology used in cellular networks for this purpose. A UDCN requires additional BS control and/or cooperation. This can be achieved by allowing the BSs to employ decentralized power allocation so the requirements of the associated users can be satisfied. Centralized control can be implemented by using an upper tier algorithm

which works in conjunction with the algorithms at the BSs. BSs can also cooperate to improve performance. Regardless of the approach, power allocation will be employed at the BSs, and as shown in this chapter, the proposed algorithm outperforms existing techniques. Further, the concept of PUs and NUs can be used to differentiate between users and devices. A number of technologies have been proposed for 5G networks such as UDCNs and non-orthogonal multiple access (NOMA) [120], and power allocation is essential for effective interference management.

The rest of the chapter is organized as follows. The system model and a review of power allocation techniques are given in Section II. Section III presents the proposed prioritized and selective power allocation scheme given in Algorithm 9. The performance of the proposed scheme is evaluated and compared with existing techniques in Section IV. Finally, some concluding remarks are given in Section V.

5.1 System Model and Preliminaries

In this section, the system model and existing power allocation schemes are presented.

5.1.1 System model

A single cell network is considered with one BS at the center. The users are separated into PUs, satisfied NUs and unsatisfied NUs. The PUs and NUs are assumed to be uniformly distributed over the BS coverage area. The number of PUs is k_1 with indices $1, 2, \ldots, k_1$. The number of current satisfied and unsatisfied NUs is k_2 and k_3, respectively, with indices $k_1+1, k_1+2, \ldots, k_1+k_2$ and $k_1+k_2+1, k_1+k_2+2, \ldots, K$. The total number of users is $K = k_1 + k_2 + k_3$.

Define the transmit power of user i as p_i, $i = 1, 2, \ldots, p_K$, with $0 \leq p_i \leq p_{\max}$ where $p_{\max}$ is the maximum transmit power. The channel gain between the ith user and the BS is denoted by g_i. The maximum received power for user i is then $\varphi_{i\max} = p_{\max} g_i$.

The SINR between the BS and user i is defined as

$$\gamma_i = \frac{p_i g_i}{\sum_{j=1, j\neq i}^{K} p_j g_j + \sigma^2} = \frac{p_i}{R_i}, \tag{5.1}$$

where σ^2 is the additive white Gaussian noise (AWGN) power at the BS, and

$$R_i = \frac{\sum_{j=1, j\neq i}^{K} p_j g_j + \sigma^2}{g_i},$$

is the interference plus noise to channel gain ratio. The effective SINR between the BS and user i can then be defined as

$$\begin{aligned}\theta_i &= \frac{p_i g_i}{p_i g_i + \sum_{j=1, j\neq i}^{K} p_j g_j + \sigma^2} \\ &= \frac{\gamma_i}{\gamma_i + 1} = \frac{p_i g_i}{\rho_i},\end{aligned} \tag{5.2}$$

and the received power plus noise and interference is

$$\rho_i = \frac{p_i g_i}{\theta_i} = \frac{\varphi_i}{\theta_i} = p_i g_i + \sum_{j=1, j\neq i}^{K} p_j g_j + \sigma^2. \tag{5.3}$$

From (5.1), (5.2), and (5.3), the user transmit power is

$$p_i = \frac{\theta_i \rho_i}{g_i} = \gamma_i R_i. \tag{5.4}$$

The target SINR and target effective SINR for user i are denoted by $\hat{\gamma}_i$ and $\hat{\theta}_i$, respectively. The achievable throughput of user i is defined as

$$T_i = \log_2(1 + \gamma_i). \tag{5.5}$$

The network utility is defined as [114]

$$U = \sum_{i=1}^{K} (T_i - p_i), \tag{5.6}$$

where T_i is in Mbps and p_i is in Watts. The power efficiency is then

$$E = \frac{U}{\sum_{i=1}^{K} p_i}. \tag{5.7}$$

5.1.2 Power allocation schemes

There are three main types of power allocation schemes, single target SINR, variable SINR and multiple target SINRs. In [110], single target SINR tracking power allocation (TSPA) was considered. The power update function (PUF) to achieve a target SINR with and without an upper power level constraint is

$$\text{unconstrained TSPA} : p_i(t+1) = \hat{\gamma}_i R_i(t) = \frac{\hat{\gamma}_i}{\gamma_i(t)} p_i(t),$$
$$\text{constrained TSPA} : p_i(t+1) = \min\left\{\hat{\gamma}_i R_i(t), p_{th}\right\}$$
$$= \min\left\{\frac{\hat{\gamma}_i}{\gamma_i(t)} p_i(t), p_{th}\right\},$$

where t is the iteration index, $\hat{\gamma}_i$ is the target SINR for user i, and p_{th} is an upper power level with $p_{th} \leq p_{\max}$. The upper level is determined based on the channel conditions and the number of users currently connected to the BS. At iteration t, user i increases its the power level if the current SINR is lower than the target SINR $\hat{\gamma}_i$, and vice versa. With unconstrained TSPA, if there is no power level that satisfies the target SINR, user i transmits at the maximum power, which is inefficient since the mutual interference caused by this user others is maximum. With constrained TSPA, users who cannot attain their target SINRs transmit at the upper power level, which is more efficient than unconstrained TSPA. However, there is still interference to other users which can increase the number of unsatisfied users. In addition, with TSPA there is a single target SINR for all users, which can be far from optimal.

In [111], variable SINR opportunistic power allocation (VOPA) was proposed. The PUF for VOPA is

$$\text{constrained VOPA} : p_i(t+1) = \min\left\{\xi_i\left(\frac{1}{R_i(t)}\right)^{\phi_i}, p_{th}\right\}$$
$$= \min\left\{\xi_i\left(\frac{\gamma_i(t)}{p_i(t)}\right)^{\phi_i}, p_{th}\right\},$$

where ξ_i and ϕ_i are control parameters. With VOPA, users with good channel conditions have higher SINRs. Further, these users are allowed to increase their transmit power levels. In contrast, users with poor channel conditions have lower SINRs, so their transmit power levels are reduced. Similar to constrained TSPA, an upper power level is employed to restrict the transmit power. Therefore, the problem of excessive interference is addressed with VOPA, and the system throughput is enhanced compared to TSPA.

Distributed dynamic target SINR tracking power allocation (DTPA) is a combi-

nation of TSPA and VOPA [112]. The PUF for this scheme is

$$p_i(t+1) = \hat{\gamma}_i(t) R_i(t) = \frac{\hat{\gamma}_i(t)}{\gamma_i(t)} p_i(t),$$

where the dynamic target SIR $\hat{\gamma}_i(t)$ is given by

$$\hat{\gamma}_i(t) = \begin{cases} \hat{\gamma}_i, & \text{if } p_i(t) > p_{th} \\ \xi_i \left(\frac{1}{R_i(t)}\right)^{\phi_i - 1}, & \text{if } p_i(t) \leq p_{th}. \end{cases}$$

With DTPA, users do not adjust their target SINR levels when the channel conditions are poor, i.e. the required power to attain these levels is higher than p_{th}. However, users increase their target SINRs if the channel conditions are good, i.e. the required power to attain their target SINRs is less than p_{th}. Thus, users with good channel conditions can attain higher SINRs than their target SINRs while the remaining users can reach their target SINRs. The system throughput is better than with VOPA and TSPA and a higher number of users are satisfied with their target SINRs, but a higher average power is required.

Variable target SINR power allocation (VTPA) was proposed in [113]. The PUF for VTPA is given by

$$p_i(t+1) = \left(\frac{\hat{\gamma}_i(t)}{\gamma_i(t)}\right)^{\phi_i} p_i(t),$$

where ϕ_i is the control parameter and $\hat{\gamma}_i(t)$ is the variable target SINR for user i. The target SINR is adjusted as follows

$$\hat{\gamma}_i(t) = \begin{cases} \hat{\gamma}_{i\,\max}, & p_i(t) \leq p_{\min}, \\ \hat{\gamma}_{i\,\max} \left(\frac{p_i(t)}{p_{\min}}\right)^u, & p_{\min} \leq p_i(t) \leq p_{th}, \\ \hat{\gamma}_{i\,\min}, & p_i(t) \geq p_{th}, \end{cases}$$

where

$$u = \frac{\log(\frac{\hat{\gamma}_{i\max}}{\hat{\gamma}_{i\min}})}{\log(\frac{p_{th}}{p_{\min}})},$$

$$\hat{\gamma}_{i\max} = \hat{\gamma}_i \sqrt[\phi_i]{\frac{p_i(t)}{p_{\min}}},$$

$$\hat{\gamma}_{i\min} = \hat{\gamma}_i \sqrt[\phi_i]{\frac{p_i(t)}{p_{\max}}},$$

and $p_{\min}$ and p_{th} are the lower and upper power levels, respectively. With VTPA, users adjust their transmit power levels until the SINRs for all users are satisfied. The variable target SINR $\hat{\gamma}_i(t)$ is determined according to the required transmit power. When $p_i(t) \leq p_{\min}$, users attempt to achieve the highest possible data rate by setting their target SINR to $\hat{\gamma}_{i\max}(t)$. Conversely, $p_i(t) \geq p_{th}$ implies that the channel condition is poor, so a low target SINR $\hat{\gamma}_{i\min}(t)$ is assigned to the corresponding users. When $p_{\min} \leq p_i(t) \leq p_{th}$, the target SINR is a function of the required transmit power.

5.2 Problem Formulation

In this section, a prioritized and selective power allocation scheme is presented to reduce the aggregate power consumption and increase the power efficiency. Three type of users are considered, PUs, satisfied NUs and unsatisfied NUs. First, all PU requirements should be satisfied by adjusting their target SINRs. Second, satisfied NUs (those for which the required transmit power to attain their target SINRs is feasible), do not adjust their target SINRs. Feasibility means that there is a transmit power that satisfies the target SINR and does not exceed the upper power level. Third, unsatisfied NUs reduce their target SINRs and hence their transmit power. As a result, the interference to other users and the aggregate power consumption are reduced.

5.2.1 Power consumption problem formulation

The aggregate power consumption problem subject to PUs achieving their target SINRs is

$$\begin{aligned} \min_{p_i} \quad & \sum_{i=1}^{k_1} p_i, \\ \text{subject to} \quad & \gamma_i \geq \hat{\gamma}_i(1+\alpha), \end{aligned} \tag{5.8}$$

where α is a safety margin for PUs against interference from the NUs. Thus, the SINRs for the PUs are always kept at or above their target SINRs. The aggregate power consumption problem subject to the target SINRs for the satisfied NUs is

$$\begin{aligned} \min_{p_i} \quad & \sum_{i=k_1+1}^{k_1+k_2} p_i, \\ \text{subject to} \quad & \gamma_i \geq \hat{\gamma}_i. \end{aligned} \tag{5.9}$$

The problem of aggregate power consumption subject to a target SINR for the unsatisfied NUs is given by

$$\begin{aligned} \min_{p_i} \quad & \sum_{i=k_1+k_2+1}^{K} p_i, \\ \text{subject to} \quad & \gamma_i \geq \hat{\gamma}_i(1-\alpha). \end{aligned} \tag{5.10}$$

The PUF for the PUs is then

$$p_i(t+1) = \begin{cases} \frac{(1+\alpha)\hat{\gamma}_i}{\gamma_i(t)} p_i(t), & \text{if } \gamma_i(t) \geq \hat{\gamma}_i, \\ (1+\alpha)p_i(t), & \text{if } \gamma_i(t) < \hat{\gamma}_i, \end{cases} \tag{5.11}$$

and for the satisfied NUs is

$$p_i(t+1) = \frac{\hat{\gamma}_i}{\gamma_i(t)} p_i(t). \tag{5.12}$$

The PUF for unsatisfied NUs is then given by

$$p_i(t+1) = \begin{cases} (1-\alpha)\frac{\hat{\gamma}_i}{\gamma_i(t)} p_i(t), & \text{if } (\gamma_i(t) < \hat{\gamma}_i \text{ and } \varphi_i(t) \geq \bar{\varphi}_{\max}), \\ \frac{1}{(1-\alpha)}\frac{\hat{\gamma}_i}{\gamma_i(t)} p_i(t), & \text{if } (\gamma_i(t) < \hat{\gamma}_i \text{ and } \varphi_i(t) < \bar{\varphi}_{\max}). \end{cases} \tag{5.13}$$

where

$$\bar{\varphi}_{\max} = \min \left\{ g_i \frac{\gamma_i}{R_i} \right\}, i = 1, 2, \ldots, k_1.$$

5.2.2 Network utility problem formulation

The network utility problem of user i is given by

$$\max_{p_i} \sum_{i=1}^{K} (T_i - p_i).$$

Then, the power allocation problem for the PUs can be formulated as

$$\begin{aligned} \max_{p_i} \quad & \sum_{i=1}^{k_1} (T_i - p_i), \\ \text{subject to} \quad & \gamma_i \geq \hat{\gamma}_i(1+\alpha). \end{aligned} \tag{5.14}$$

The above problem is concave and the constraint is a linear inequality. Thus, Slaters condition is satisfied and strong duality holds. Hence, the Lagrangian method can be used to solve this problem [121, 122]. The Lagrangian function with Lagrange multiplier μ_i is given by

$$\mathscr{L}(p_i, \mu_i) = \sum_{i=1}^{k_1} (T_i - p_i) + \sum_{i=1}^{k_1} \mu_i(\gamma_i - \hat{\gamma}_i(1+\alpha)). \tag{5.15}$$

The corresponding dual Lagrangian function is

$$g(\mu_i) = \max_{p_i} \mathscr{L}(p_i, \mu_i), \tag{5.16}$$

and the dual problem is

$$\min_{\mu_i} g(\mu_i), \quad \mu_i \geq 0. \tag{5.17}$$

The objective functions of problems (5.15) and (5.17) are differentiable with respect to the primal variable p_i and the dual variable μ_i, respectively. Thus, both problems can be iteratively solved using the gradient method

$$\begin{aligned} p_i(t+1) = \quad & p_i(t) + \eta \left(\frac{\partial \mathscr{L}(p_i, \mu_i)}{\partial p_i} \right), \\ \mu_i(t+1) = \quad & \mu_i(t) + \nu \left(\frac{\partial \mathscr{L}(p_i, \mu_i)}{\partial \mu_i} \right), \end{aligned} \tag{5.18}$$

where t is the iteration index, and η and ν are positive step sizes with $0 \leq \eta \leq (|\frac{\partial \mathscr{L}(p_i,\mu_i)}{\partial p_i}|)^{-1}$ and $0 \leq \eta \leq (|\frac{\partial \mathscr{L}(p_i,\mu_i)}{\partial \mu}|)^{-1}$ [121, 122]. Then a solution can be obtained

by setting $\frac{\partial \mathscr{L}(p_i,\mu)}{\partial p_i}$ to zero. The derivative of $\frac{\partial \mathscr{L}(p_i,\mu)}{\partial p_i}$ is

$$\frac{\partial \mathscr{L}(p_i,\mu_i)}{\partial p_i} = \frac{\gamma_i}{p_i \ln 2}\left(\frac{1}{\gamma_i+1}+\mu_i\right)-1, \tag{5.19}$$

and the problem solution is

$$p_i^* = \min\left\{\frac{\gamma_i}{\ln 2}\left(\frac{1}{\gamma_i+1}+\mu_i, p_{\max}\right)\right\}. \tag{5.20}$$

The derivative of $\frac{\partial \mathscr{L}(p_i,\mu)}{\partial \mu}$ is

$$\frac{\partial \mathscr{L}(p_i,\mu_i)}{\partial \mu_i} = \gamma_i - \hat{\gamma}_i(1+\alpha). \tag{5.21}$$

The power allocation problem for the satisfied NUs can be formulated as

$$\begin{aligned} \max_{p_i} \quad & \sum_{i=k_1+1}^{k_1+k_2}(T_i - p_i), \\ \text{subject to} \quad & \gamma_i \geq \hat{\gamma}_i. \end{aligned} \tag{5.22}$$

The corresponding Lagrangian function with Lagrange multiplier μ_i is

$$\mathscr{L}(p_i,\mu_i) = \sum_{i=k_1+1}^{k_1+k_2}(T_i-p_i) + \sum_{i=k_1+1}^{k_1+k_2}\mu_i(\gamma_i-\hat{\gamma}_i). \tag{5.23}$$

Thus, the power and Lagrange multiplier update functions are given by

$$\begin{aligned} p_i(t+1) = \quad & p_i(t) + \eta\left(\frac{\partial \mathscr{L}(p_i,\mu_i)}{\partial p_i}\right), \\ \mu_i(t+1) = \quad & \mu_i(t) + \nu\left(\frac{\partial \mathscr{L}(p_i,\mu_i)}{\partial \mu}\right), \end{aligned} \tag{5.24}$$

where

$$\frac{\partial \mathscr{L}(p_i,\mu_i)}{\partial p_i} = \frac{\gamma_i}{p_i \ln 2}\left(\frac{1}{\gamma_i+1}+\mu_i\right)-1,$$

and

$$\frac{\partial \mathscr{L}(p_i,\mu_i)}{\partial \mu_i} = \gamma_i - \hat{\gamma}_i.$$

The corresponding solution is

$$p_i^* = \min\left\{\frac{\gamma_i}{\ln 2}\left(\frac{1}{\gamma_i+1}+\mu_i\right), p_{\max}\right\}. \tag{5.25}$$

The power allocation problem for the unsatisfied NUs can be formulated as

$$\begin{aligned} \max_{p_i} \quad & \sum_{i=k_1+k_2+1}^{K} (T_i - p_i), \\ \text{subject to} \quad & \gamma_i \geq \hat{\gamma}_i(1-\alpha). \end{aligned} \tag{5.26}$$

The corresponding Lagrangian function with Lagrange multiplier μ_i is

$$\mathscr{L}(p_i,\mu_i) = \sum_{i=k_1+k_2+1}^{K} (T_i - p_i) + \sum_{i=k_1+k_2+1}^{K} \mu_i(\gamma_i - \hat{\gamma}_i(1-\alpha)). \tag{5.27}$$

Thus, the power and Lagrange multiplier update functions are given by

$$\begin{aligned} p_i(t+1) = \quad & p_i(t) + \eta\left(\frac{\partial \mathscr{L}(p_i,\mu_i)}{\partial p_i}\right), \\ \mu_i(t+1) = \quad & \mu_i(t) + \nu\left(\frac{\partial \mathscr{L}(p_i,\mu_i)}{\partial \mu}\right), \end{aligned} \tag{5.28}$$

where

$$\frac{\partial \mathscr{L}(p_i,\mu_i)}{\partial p_i} = \frac{\gamma_i}{p_i \ln 2}\left(\frac{1}{\gamma_i+1}+\mu_i\right) - 1,$$

$$\frac{\partial \mathscr{L}(p_i,\mu_i)}{\partial \mu_i} = \gamma_i - \hat{\gamma}_i(1-\alpha).$$

The corresponding solution is

$$p_i^* = \min\left\{\frac{\gamma_i}{\ln 2}\left(\frac{1}{\gamma_i+1}+\mu_i\right), p_{\max}\right\}. \tag{5.29}$$

5.2.3 Distributed power allocation algorithm

The proposed scheme is distributed as users only require local information to adjust their transmit power in an iteration, and the user target SINRs are used to ensure that the transmit power is in the desired range. The proposed distributed power allocation algorithm based on (5.11)-(5.13), (5.15), (5.23), and (5.27) is given in Algorithm 9.

Algorithm 9 Proposed Distributed Power Allocation Algorithm

Step 1: Obtain the Lagrange multiplier $\mu_i(t)$ and safety margin α broadcast by the BS. User i determines the received SINR γ_i and sets the target SINR $\hat{\gamma}_i$.

Step 2: Power allocation for

Minimum power consumption

PUs update their transmit power using

$$p_i(t+1) = \begin{cases} \frac{(1+\alpha)\hat{\gamma}_i}{\gamma_i(t)} p_i(t), & \text{if } \gamma_i(t) \geq \hat{\gamma}_i, \\ (1+\alpha) p_i(t), & \text{if } \gamma_i(t) < \hat{\gamma}_i. \end{cases}$$

Satisfied NUs update their transmit power using

$$p_i(t+1) = \frac{\hat{\gamma}_i}{\gamma_i(t)} p_i(t).$$

Unsatisfied NUs update their transmit power using

$$p_i(t+1) = \begin{cases} (1-\alpha)\frac{\hat{\gamma}_i}{\gamma_i(t)} p_i(t), \\ \text{if } (\gamma_i(t) < \hat{\gamma}_i \text{ and } \varphi_i(t) \geq \bar{\varphi}_{\max}), \\ \frac{1}{(1-\alpha)}\frac{\hat{\gamma}_i}{\gamma_i(t)} p_i(t), \\ \text{if } (\gamma_i(t) < \hat{\gamma}_i \text{ and } \varphi_i(t) < \bar{\varphi}_{\max}). \end{cases}$$

Maximum network utility

The user transmit powers are updated using

$$p_i(t+1) = \min \left\{ \frac{\gamma_i(t)}{\ln 2} \left(\frac{1}{\gamma_i(t)+1} + \mu_i(t) \right), p_{\max} \right\}.$$

Step 3: Terminate when $|p_i(t+1) - p_i(t)| \leq \epsilon$, otherwise go to **step 4**.

Step 4: Update the Lagrange multiplier $\mu_i(t+1)$ using (5.18) for PUs, (5.24) for satisfied NUs, and (5.28) for unsatisfied NUs.

5.3 Numerical Results

In this section, Monte Carlo simulation is used to evaluate the proposed power allocation scheme using a single BS under five different scenarios. The channel gain is $g_i = hd_i^{-\alpha}$, where $h = 0.97$ is a constant, d_i is the distance between user i and the BS, and $\alpha = 3$ is the path loss exponent which corresponds to urban and suburban environments. The noise power at the BS is set to $\sigma^2 = 0.01$ W, and the initial power level for all users is set to 1 W. The maximum transmit power $p_{\max}$ is 3 W. The upper and lower power levels are set to 2 W and 0.01 W, respectively. The target SINRs were randomly chosen from a uniform distribution between 0.1 dB and 0.8 dB. The performance of the proposed power allocation scheme is compared with that of existing power allocation approaches in terms of power consumption, network utility and power efficiency. The PUs and NUs are uniformly distributed in the geographic area of a femtocell, picocell or macrocell. The results are obtained for 10000 trials for each number of users with the user locations changed each trial and $\epsilon = 0.001$.

In the first scenario, there is one femtocell with 4 PUs and 4 NUs. The femtocell is located at the center of a square geographic area with dimensions 50 m $\times$ 50 m. With TSPA and DTPA, the target SINRs for the users are

$$\hat{\gamma}_k = [0.38 \;\; 0.22 \;\; 0.28 \;\; 0.36 \;\; 0.15 \;\; 0.20 \;\; 0.16 \;\; 0.31] \text{ dB},$$

which were randomly chosen. With the proposed power allocation scheme, the first four values are for PUs and the last four are for NUs. Table 5.1 gives the average power, network utility, power efficiency and SINR for the TSPA, VOPA, DTPA, VTPA and proposed schemes. This shows that the proposed scheme has the highest average power efficiency which is 3.42. The average network utility is 0.23, which is better than with TSPA, DTPA and VTPA. The average power with VOPA is 0.03 W which is slightly lower than the 0.07 W with the proposed scheme, but the average network utility with VOPA is only 0.02. This is because when the channel conditions are poor, the users reduce their power, resulting in a low network utility.

In the second scenario, there is one femtocell with 7 PUs and 9 NUs. The femtocell is located at the center of a square geographic area with dimensions 50 m $\times$ 50 m. With TSPA and DTPA, the target SINRs for the users are

$$\begin{aligned}\hat{\gamma}_k = &[0.37 \;\; 0.22 \;\; 0.28 \;\; 0.24 \;\; 0.15 \;\; 0.20 \;\; 0.16 \;\; 0.31 \\ &0.28 \;\; 0.22 \;\; 0.28 \;\; 0.32 \;\; 0.15 \;\; 0.20 \;\; 0.16 \;\; 0.31] \text{ dB},\end{aligned}$$

Table 5.1: Average Power, Network Utility, Power Efficiency and SINR for Five Power Allocation Schemes with 8 Users

TSPA	0.14	0.23	1.63	0.26
VOPA	0.03	0.02	0.85	4.55
DTPA	1.99	0.27	0.13	0.32
VTPA	0.62	0.25	0.39	0.29
Proposed	0.07	0.23	3.42	0.26

which were randomly chosen. With the proposed power allocation scheme, the first seven correspond to the PUs and the last nine to the NUs. Table 5.2 gives the average power, network utility, power efficiency and SINR for the TSPA, VOPA, DTPA, VTPA and proposed power allocation schemes. This shows that the proposed scheme again has a higher average power efficiency compared to TSPA, DTPA and VTPA. The average required power and network utility of the proposed scheme are 1.03 W and 0.13, respectively, which is better than TSPA, DTPA and VTPA. The average power is higher than that with VOPA, 0.01 W, but the average network utility with VOPA, 0.11, is higher.

Table 5.2: Average Power, Network Utility, Power Efficiency and SINR for Five Power Allocation Schemes with 16 Users

Power Allocation Scheme	Average Power (W)	Average Network Utility	Average Power Efficiency	Average SINR (dB)
TSPA	1.87	0.13	0.07	0.14
VOPA	0.01	0.11	11.3	0.13
DTPA	2.00	0.13	0.07	0.14
VTPA	1.87	0.13	0.07	0.14
Proposed	1.03	0.13	0.13	0.14

In the third scenario, there is one picocell with 8 PUs and 24 NUs. The picocell is located at the center of a square geographic area with dimensions 300 m $\times$ 300 m. With TSPA, DTPA and the proposed scheme, the target SINRs are randomly chosen between 0.3 dB and 0.7 dB. The same values are used with the three schemes for a fair comparison. Table 5.3 gives the average power, network utility, power efficiency and average SINR for the TSPA, VOPA, DTPA, VTPA and proposed power allocation schemes. This shows that the proposed scheme has a higher power efficiency than

DTPA and VTPA. The average power and network utility with the proposed scheme are 1.12 W and 0.43, respectively, which is better than with DTPA and VTPA. The average power with TSPA and VOPA is 0.03 W and 0.01 W, respectively, which is lower than with the proposed scheme, but the average network utility with TSPA and VOPA is only 0.45 and 0.47.

Table 5.3: Average Power, Network Utility, Power Efficiency and SINR for Five Power Allocation Schemes with 32 Users

Power Allocation Scheme	Average Power (W)	Average Network Utility	Average Power Efficiency	Average SINR (dB)
TSPA	0.03	0.45	17.7	0.57
VOPA	0.01	0.47	47.1	0.66
DTPA	1.89	0.48	0.25	0.65
VTPA	1.99	0.48	0.24	0.66
Proposed	1.12	0.43	0.38	0.69

In the fourth scenario, there is one picocell with 20 PUs and 44 NUs. The picocell is located at the center of a square geographic area with dimensions 300 m $\times$ 300 m. With TSPA, DTPA and the proposed scheme, the target SINRs are randomly chosen in the range 0.2 to 0.8 dB. Table 5.4 gives the average power, network utility, power efficiency and average SINR for the TSPA, VOPA, DTPA, VTPA and proposed power allocation schemes. This shows that the proposed scheme has a higher power efficiency compared to TSPA, DTPA and VTPA. The average power and network utility of the proposed scheme are 0.19 W and 0.26, respectively, which is better than with DTPA and VTPA. The average power consumption is higher than VOPA which is 0.01 W. The power efficiency of the proposed scheme, 1.35, is higher than with TSPA, DTPA and VTPA.

In the fifth scenario, there is one macrocell with 52 PUs and 76 NUs. The macrocell is located at the center of a square geographic area with dimensions 500 m $\times$ 500 m. With TSPA, DTPA and the proposed scheme, the target SINRs are randomly chosen in the range 0.1 to 0.9 dB. Table 5.5 shows the average power, network utility, power efficiency and SINR for the TSPA, VOPA, DTPA, VTPA and proposed power allocation schemes for the 128 users. This shows that the proposed scheme has a higher average power efficiency than TSPA, DTPA and VTPA. The average power and network utility are 0.03 W and 0.37, respectively, which is better than with DTPA and VTPA. The average power of the proposed scheme is higher than VOPA with

Table 5.4: Average Power, Network Utility, Power Efficiency and SINR for Five Power Allocation Schemes with 64 Users

Power Allocation Scheme	Average Power (W)	Average Network Utility	Average Power Efficiency	Average SINR (dB)
TSPA	1.16	0.27	0.23	0.32
VOPA	0.01	0.27	26.7	0.32
DTPA	2.00	0.27	0.13	0.32
VTPA	2.00	0.27	0.13	0.32
Proposed	0.19	0.26	1.35	0.32

0.01 W, and the average power efficiency, 13.7, is higher than that of TSPA, DTPA and VTPA.

Table 5.5: Average Power, Network Utility, Power Efficiency and SINR for Five Power Allocation Schemes with 128 Users

Power Allocation Scheme	Average Power (W)	Average Network Utility	Average Power Efficiency	Average SINR (dB)
TSPA	0.04	0.38	10.2	0.46
VOPA	0.01	0.14	14.4	0.16
DTPA	2.00	0.14	0.07	0.16
VTPA	2.00	0.26	0.13	0.32
Proposed	0.03	0.37	13.7	0.46

Fig. 5.1 presents the average power for the TSPA, VOPA, DTPA, VTPA and proposed power allocation schemes for the 5 scenarios. This show that the average power of DTPA and VTPA is the highest. With DTPA and VTPA, the average power is the maximum as the number of users increases. With 16 or more users associated with the BS, the average power is in the range 1.87 W to 2 W. While VOPA has the lowest average power, with 16 or more users associated with the BS, most reduce their transmit power which implies that many are unsatisfied since the average power is only 0.01 W. The average power of the proposed scheme is the lowest and outperforms TSPA in all scenarios but the third.

Fig. 5.2 shows the average network utility for the TSPA, VOPA, DTPA, VTPA and proposed power allocation schemes for the 5 scenarios. The average network utility of the proposed scheme is similar to that of TSPA, DTPA, and VTPA in most

cases, while VOPA is the lowest. The average network utility is the highest in scenario 3 with 32 users because of the large network area given the number of users which allows the network to use the resources efficiently.

Fig. 5.3 shows the average power efficiency for the TSPA, VOPA, DTPA, VTPA and proposed power allocation schemes for the 5 scenarios. The average power efficiency of the proposed scheme is higher than TSPA, DTPA and VTPA in most cases, and is the second highest for scenarios 2 to 5. The average power efficiency of VOPA is the highest.

Fig. 5.4 shows the average SINR for the TSPA, VOPA, DTPA, VTPA and proposed power allocation schemes for 5 scenarios. The average SINR with TSPA, VOPA, DTPA, and VTPA is similar in scenarios 2, 3, and 4. The average SINR for VOPA is the highest for the first scenario, and the worst for the last scenario. The reason is that with VOPA the SINR is determined based on channel conditions so the performance can vary significantly.

Table 5.6 gives the average number of iterations with the TSPA, VOPA, DTPA and proposed power allocation schemes. This is the average of 10000 trials for each

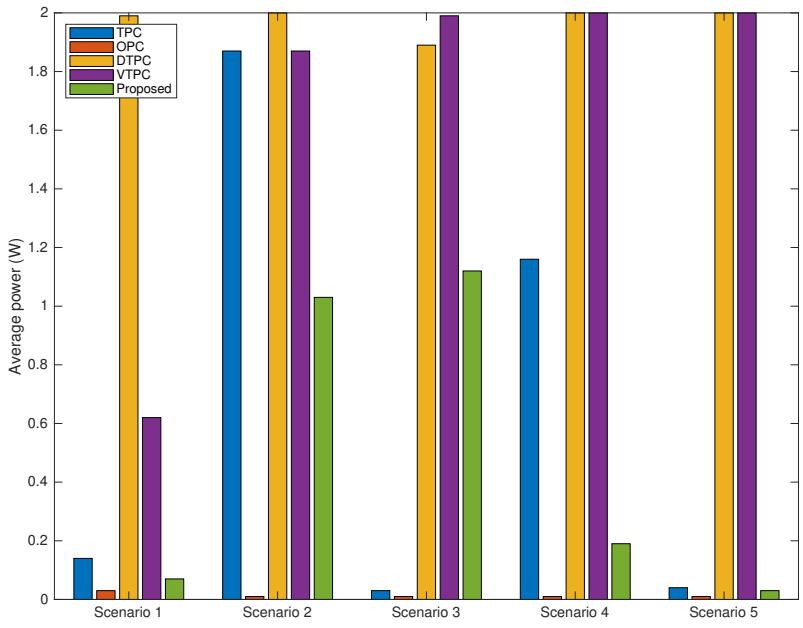

Figure 5.1: The average power for the five scenarios with the five power allocation schemes.

of the five scenarios. This shows that VOPA requires the fewest number of iterations, but it has the worst performance. The average number of iterations with the proposed scheme is highest for four of the scenarios, but it is not significantly greater than with the TSPA, DTPA and VTPA schemes and provides better performance.

Table 5.6: Average Number of Iterations for Five Power Allocation Schemes

Power Allocation Scheme	Scenario 1	Scenario 2	Scenario 3	Scenario 4	Scenario 5
TSPA	25	31	13	21	21
VOPA	4	5	8	10	13
DTPA	23	22	14	22	14
VTPA	11	5	23	25	20
Proposed	30	51	15	37	26

Fig. 5.5 gives the number of unsatisfied users for the five scenarios with the TSPA, VOPA, DTPA and proposed power allocation schemes. with the proposed scheme, all PUs are satisfied with their target SINRs and the number of unsatisfied NUs is

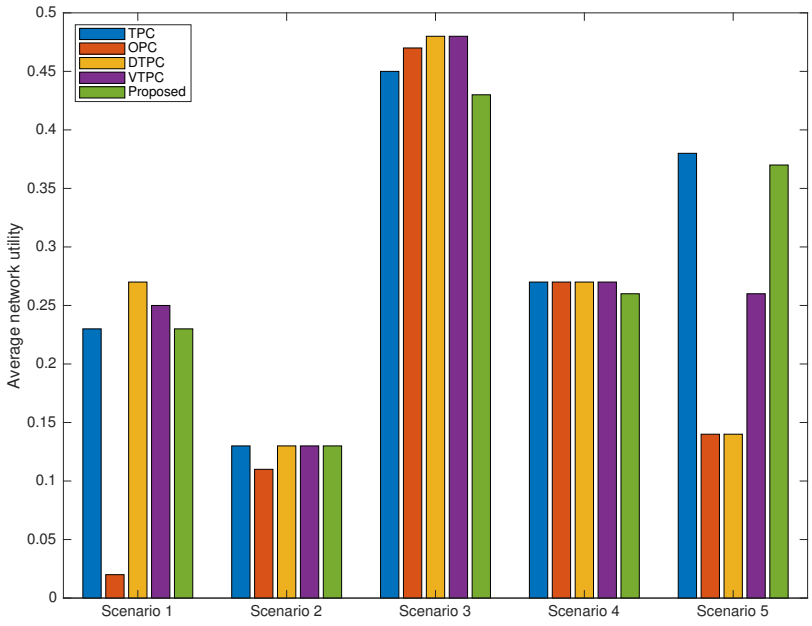

Figure 5.2: The average network utility for the five scenarios with the five power allocation schemes.

low. The total number of unsatisfied users for the five scenarios is 22 for the proposed scheme followed by TSPA with 38, and VTPA with 43. DTPA and VOPA are the worst with 77 and 93 unsatisfied users, respectively.

5.4 Conclusion

In this chapter, a selective and prioritized power allocation scheme was proposed. The goal is to reduce the power consumption and improve the power efficiency while ensuring all priority users (PUs) are satisfied and as many normal users (NUs) are satisfied with their target SINRs as possible. Performance results were presented which show that the proposed power allocation scheme provides a higher power efficiency than target SINR tracking power allocation (TSPA), variable SINR opportunistic power allocation (VOPA), dynamic target SINR tracking power allocation (DTPA), and variable target SINR power allocation (VTPA). The performance of VOPA degrades as the number of users increases, and the proposed scheme has a lower power consumption compared to DTPA and VTPA. Finally, the proposed scheme gives the

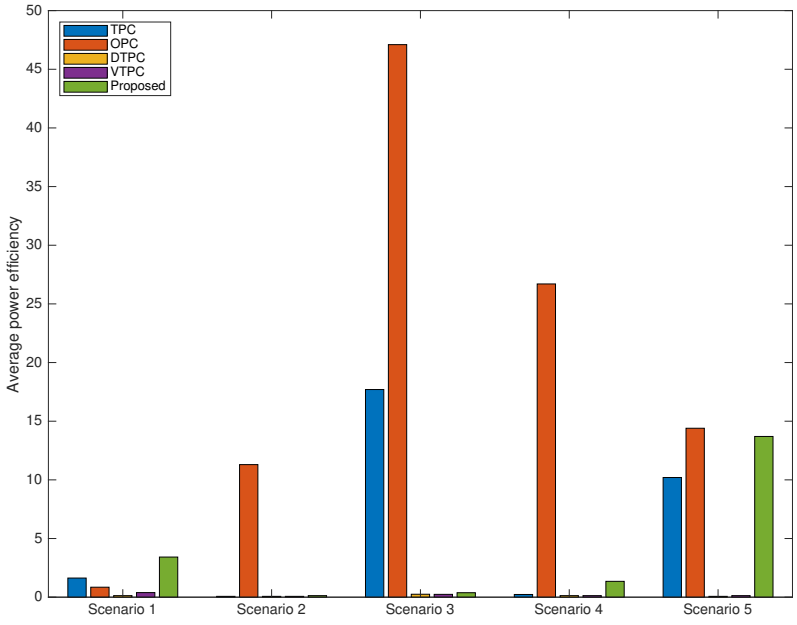

Figure 5.3: The average power efficiency for the five scenarios with the five power allocation schemes.

highest number of satisfied users.

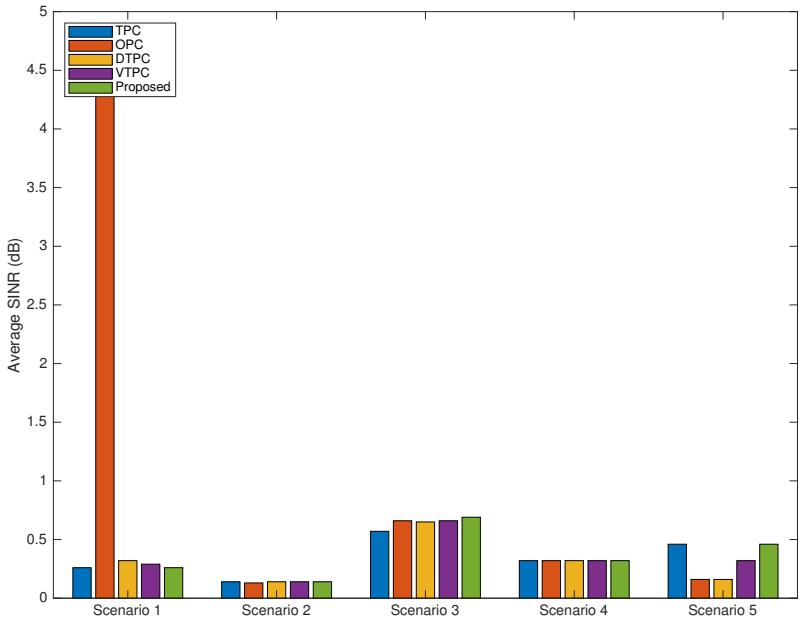

Figure 5.4: The average SINR for the five scenarios with the five power allocation schemes.

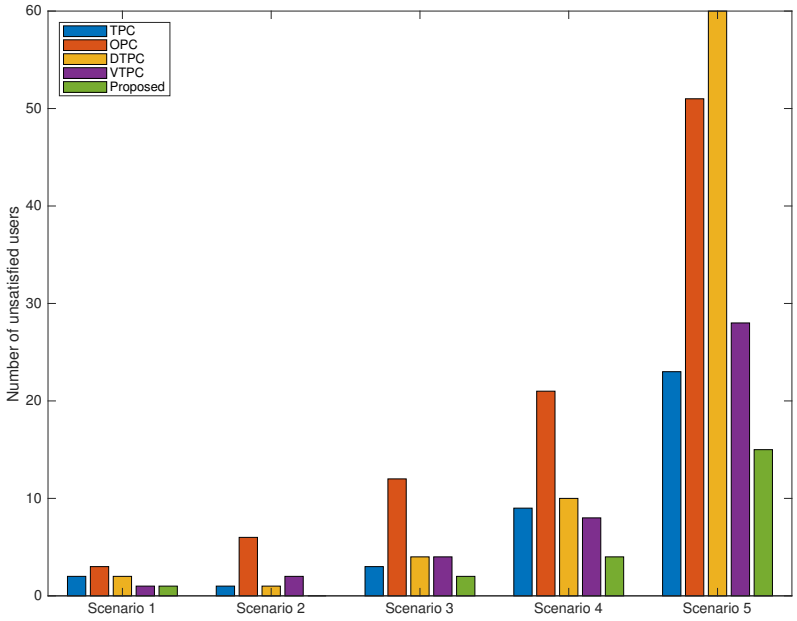

Figure 5.5: The number of unsatisfied users for the five scenarios with the five power allocation schemes.

Chapter 6

Prioritized Cell Association and Power Allocation in the HetNet Uplink

A conventional macrocellular network is designed assuming uniform coverage and traffic distribution, and so cannot adequately deal with variable traffic and data rate requirements [123]. Possible solutions to handle the growth in mobile data traffic are to improve the macrocell base station (MBS) architecture, increase MBS density, or employ heterogeneous networks (HetNets). They consist of MBSs and small base stations (SBSs) with lower transmit power and smaller coverage which can be deployed quickly. While MBSs are used to cover large areas with many users, SBSs are used to enhance capacity and energy efficiency in crowded areas such as large buildings, train stations, shopping malls, city centers and at concerts and festivals. HetNets can be used to efficiently accommodate increased traffic and data rate requirements [124]. They have also been employed to reduce the reuse distance (the distance between two BSs), and the communication distance (the distance between a user and BS) which improve the system capacity and energy efficiency [125]. However, disparate BS transmit powers and random SBS locations can result in higher interference among users compared to conventional MBS networks.

With signal strength cell association, users are associated with the BS that provides the highest signal strength. As a result, most users are connected to MBSs and few are associated with SBSs since the strength of a signal from a MBS is typically higher than from SBSs at the same distance [126]. Thus, the available SBS resources

may not be fully utilized. Further, users associated with SBSs often receive strong interference from MBSs, which degrades HetNet performance. At the MBSs, this cell association criterion can cause overloading and low data rates due to insufficient MBS resources [127]. Therefore, a more efficient cell association scheme with load balancing is needed to improve HetNet performance. In a cellular network, users who require high and stable data rates, and active users should have a high priority, and so are called priority users (PUs). Active users are defined as currently connected users. Users who require low and variable data rates, and new users are called normal users (NUs). To satisfy data rate requirements and reduce power consumption, prioritized cell association and power allocation (CAPA) in the HetNet uplink can be employed.

In HetNets, there is a need to efficiently assign users to BSs and to effectively control user transmit power to maintain effective communication links with minimal interference. Further, users have different signal strengths and channel conditions from MBSs and SBSs. These problems can be addressed with a suitable CAPA scheme. In particular, cell association is used to establish network utility (the sum of the data rates of all users), and connect users with BSs according to the user channel conditions and BS load. power allocation is used to ensure that users transmit with appropriate power levels to maintain link quality without imposing excessive interference on other users.

Recently, CAPA in HetNets has attracted significant research interest. In [128], distributed joint CAPA in the uplink of a two tier HetNet was studied. The objective was to mitigate intra tier and inter tier interference and maximize the network utility. A solution for user cell association and power control was obtained using the dual decomposition method. Further, the signal to interference plus noise ratio (SINR) requirements of all users were satisfied. In [129], a combined CAPA scheme was investigated for the HetNet uplink in which each channel is used by only one MBS. A distributed iterative CAPA algorithm was proposed and shown to converge to a Nash equilibrium of a noncooperative game.

In [130], joint power allocation and load aware user association with load balancing in a two tier HetNet was investigated. Load balancing between MBSs and SBSs was used to mitigate intercell interference in the network. In [131], a joint user association and power allocation for load balancing in HetNets was proposed to maximize the weighted sum of effective (long term) rates. The power update function for users was derived using a two sided scalable function. In [132], joint user association, power allocation and scheduling in multi cell 5G networks was proposed. The user

association employs both network and user center approaches. With the network center approach, user association is performed in a centralized manner while in the user center approach, distributed association is used to reduce the complexity.

In [133], a joint BS association and power allocation optimization problem was proposed using game theory. The objective is to maximize the network utility and minimize the corresponding transmit power. In [134], a combination of multiple BS association, power allocation and dynamic interference cancellation in a HetNet was proposed. To the best of our knowledge, a hybrid prioritized CAPA approach does not exist to improve network utility and reduce power consumption while considering user priority. The goal of the proposed scheme is to satisfy the target SINRs for as many NUs as possible while ensuring the requirements of all PUs are met.

The main contributions of this chapter are as follows.

1. Two stage CAPA optimization is proposed. The first stage is employed by PUs and NUs and the second stage is employed by the BSs. First, the product of the channel access likelihood (CAL) and channel gain to interference plus noise ratio (GINR) is considered for PU cell association while network utility is considered for NU cell association. Here, CAL is defined as the reciprocal of the BS load. In CAL and GINR cell association, PUs are associated with the BSs that provide the maximum product of CAL and GINR. This implies that PUs are connect to BSs with a low number of users and good channel conditions. NUs are connected to BSs so that the network utility is maximized, and this is achieved using an iterative algorithm. Second, prioritized power control is used to reduce power consumption and satisfy as many NUs with their target SINRs as possible while ensuring that PU requirements are satisfied.

2. The proposed optimization problem is nonconvex. Thus, a two loop algorithm is employed which alternately optimizes the user transmit power and cell association. Specifically, the outer loop performs cell association using Lagrange multipliers, and user transmit power is adjusted in the inner loop using a power update function (PUF).

3. A distributed iterative CAPA scheme given in Algorithm 10 is proposed which uses the Nesterov method and an exponential rule to accelerate the outer and inner loop convergence, respectively.

4. The performance of the proposed scheme is compared with several well-known

algorithms in the literature under AWGN and Rayleigh fading channels. The results obtained show that this scheme provides superior performance.

The rest of the chapter is organized as follows. The system model and related work are described in Section II. The prioritized CAPA algorithm is presented in Section III. In Section IV, the performance of the proposed approach is evaluated and compared with other solutions in the literature. Finally, some concluding remarks are given in Section V.

6.1 System Model and Preliminaries

In this chapter, a two tier HetNet consisting of BSs and users is considered using a random spatial model [135]. The number of BSs is N and the number of users is K. They are divided into two classes of BSs (MBSs and SBSs) and two types of users (PUs and NUs). The number of MBSs is N_1 and the number of SBSs is N_2, with $N = N_1 + N_2$. It is assumed that the indices of the MBSs are $1, 2, \ldots, N_1$ and the indices of the SBSs are $N_1 + 1, N_1 + 2, \ldots, N$. The number of PUs is K_1 and the number of NUs is K_2, with $K = K_1 + K_2$. It is assumed that the indices of the PUs are $1, 2, \ldots, K_1$ and the indices of the NUs are $K_1 + 1, K_1 + 2, \ldots, K$.

Define the transmit power of user k as p_k, $0 \leq p_k \leq p_{\max}$, where $p_{\max}$ is the maximum transmit power. Then the received power from user k at BS n is $\varphi_{nk} = p_k g_{nk}$ where g_{nk} is the channel gain. The maximum received power is $\varphi_{nk\max} = p_{\max} g_{nk}$. The SINR between BS n and user k is defined as [136, 137]

$$\gamma_{nk} = \frac{p_k g_{nk}}{\sum_{j=1, j\neq k}^{K} p_j g_{nj} + \sigma_n^2} = p_k \Gamma_{nk}, \tag{6.1}$$

where σ_n^2 is the additive white Gaussian noise (AWGN) power at BS n. $\Gamma_{nk} = \frac{g_{nk}}{\sum_{j=1, j\neq k}^{K} p_j g_{nj} + \sigma_n^2}$ is denoted as the channel gain to interference plus noise ratio (GINR). The achievable rate of user k associated with BS n is defined as $r_{nk} = \log_2(1 + \gamma_{nk})$. The load of BS n is given by $y_n = \sum_{k=1}^{K} x_{nk}$, where $x_{nk} = 1$ if user k is associated with BS n, and $x_{nk} = 0$ otherwise. Thus, the load y_n is the number of users associated with BS n. The reciprocal of y_n is the channel access likelihood (CAL) of BS n. Users are assumed to have the same CAL regardless of the channel conditions [138]. If y_n users are associated with BS n, the effective rate of user k associated with BS n is defined

as $R_{nk} = \frac{r_{nk}}{y_n}$. The effective SINR between BS n and user k can then be defined as

$$\theta_{nk} = \frac{p_k g_{nk}}{p_k g_{nk} + \sum_{j=1, j\neq k}^{K} p_j g_{nj} + \sigma_n^2} = \frac{\gamma_{nk}}{\gamma_{nk} + 1} = \frac{p_k g_{nk}}{\rho_{nk}}, \tag{6.2}$$

and the received interference power plus noise as

$$\rho_{nk} = \frac{p_k g_{nk}}{\theta_{nk}} = \frac{\varphi_{nk}}{\theta_{nk}} = p_k g_{nk} + \sum_{j=1, j\neq k}^{K} p_j g_{nj} + \sigma_n^2. \tag{6.3}$$

From (6.1), (6.2), and (6.3), the user transmit power is

$$p_k = \frac{\theta_{nk}\rho_{nk}}{g_{nk}} = \frac{\gamma_{nk}}{\Gamma_{nk}}. \tag{6.4}$$

The target SINR and target effective SINR for user k are $\hat{\gamma}_k$ and $\hat{\theta}_k$, respectively.

6.1.1 Cell association schemes

Three well-known signal strength cell association schemes are max SINR [139], max reference signal received power (RSRP) [140], and max reference signal received quality (RSRQ) [141]. In these approaches, users are associated with the BS that provides the largest SINR, highest RSRP or maximum RSRQ, respectively. However, due to transmit power differences between MBSs and SBSs, most users will connect to MBSs which can cause overloaded MBSs and underutilized SBSs. Thus, max signal strength with cell range expansion (CRE) [142, 143] was proposed as a solution to this load balancing problem.

In CRE, the cell association condition for users can be formulated as $n^* = \arg\max_n(\gamma_{nk} + \tau_n)$, where τ_n is a positive bias value for BS n. τ_n is in the range [0 18] dB for SBSs and $\tau_n = 0$ for MBSs. The SBS coverage areas are increased by adding a positive bias to their signal strengths. As a result, more MBS users are transferred to SBSs and thus the load balance is improved compared to other max signal strength schemes. However, users in the CRE region can have a poor quality SBS channel and strong inter tier interference from MBSs.

CRE with almost blank subframe (ABS) [144] uses time domain orthogonalization at the MBSs which leaves some subframes almost blank. This provides a window for SBSs to serve users in the CRE region with reduced inter tier interference. How-

ever, this solution wastes MBS subframes and thus throughput, and the blank to number of subframes ratio (ABS ratio) needs to be determined carefully. CRE with BS load awareness [141] takes the cell load distribution into consideration. In fact, without incorporating cell load information, the cell association scheme may not be efficient since new users should be associated with an underloaded BS rather than an overloaded BS.

The channel access cell association in [145] considers channel quality indicators and traffic load information from the BSs to improve spectral efficiency and achieve load balancing in HetNets. In [146], load and interference aware cell association was proposed which considers the load and interference for user rate maximization in the uplink of a cellular network. The cell association condition in [145] and [146] can be formulated as $n^* = \arg\max_n(\frac{\gamma_{nk}}{y_n})$.

6.1.2 Power allocation schemes

There are three main types of power allocation schemes, single target SINR, variable target SINR and multiple target SINRs. Single target SINR implies that each user has one target SINR. With a variable target SINR, the user target SINRs are determined based on channel conditions, while with multiple target SINRs there are multiple values for each user. The PUF to achieve a target SINR in the single target SINR tracking power allocation (TPA) is

$$\text{Unconstrained TPA (UTPA)} : p_k(t+1) = \frac{\hat{\gamma}_k}{\Gamma_{nk}(t)}$$
$$\text{Constrained TPA (CTPA)} : p_k(t+1) = \min\left\{\frac{\hat{\gamma}_k}{\Gamma_{nk}(t)}, p_{th}\right\},$$

where t is the iteration index, $\hat{\gamma}_k$ is the target SINR for user k, and p_{th} is the power threshold with $p_{th} \leq p_{\max}$. The goal of user k is to maintain a transmit power which satisfies the target SINR $\hat{\gamma}_k$ so that $\gamma_{nk} \geq \hat{\gamma}_k$. When this target is not satisfied with UTPA, users transmit at their maximum power levels which can result in strong interference to other users and is power inefficient. With CTPA, users who cannot attain their target SINRs transmit at the power threshold which is more power efficient than UTPA. However, there can still be significant interference to other users which can increase the number of users who are not satisfied with their target SINRs. Another issue is the single target SINR for all users with UTPA and CTPA, which is

not optimum.

The PUF for constrained opportunistic power allocation (COPA) is

$$\text{COPA} : p_k(t+1) = \min\{\xi_k \Gamma_{nk}(t), p_{th}\},$$

where ξ_k is a predefined constant. With this scheme, users with better channel conditions have a higher SINR than other users, and vice versa. Similar to constrained CTPA, a power threshold is employed to limit the user transmit power so the interference to others is restricted.

Distributed temporary removal and feasibility check power allocation (DTPA) is a mixture of CTPA and COPA. DTPA outperforms COPA and CTPA in terms of convergence, number of satisfied users, and power consumption. The PUF for this scheme is

$$p_k(t+1) = \begin{cases} \frac{\hat{\gamma}_k}{\Gamma_{nk}(t)}, & \text{if } \frac{\hat{\gamma}_k}{\Gamma_{nk}(t)} \leq p_k^{th1} \text{ and } p_k(t) \neq 0 \\ 0, & \text{if } \frac{\hat{\gamma}_k}{\Gamma_{nk}(t)} > p_k^{th1} \text{ and } p_k(t) \neq 0 \\ \frac{\hat{\gamma}_k}{\Gamma_{nk}(t)}, & \text{if } \frac{\hat{\gamma}_k}{\Gamma_{nk}(t)} \leq p_k^{th2} \text{ and } p_k(t) = 0 \\ 0, & \text{if } \frac{\hat{\gamma}_k}{\Gamma_{nk}(t)} > p_k^{th2} \text{ and } p_k(t) = 0, \end{cases}$$

where p_k^{th1} and p_k^{th2} are the upper and lower power thresholds for user k which are given by

$$p_k^{th1} = p_{\max} \text{ and } p_k^{th2} = \frac{\sigma_n^2(\widehat{\gamma}_k + 1)}{p_{\max} g_{nk} + \sigma_n^2} p_{\max}.$$

With DTPA, users decrease their transmit power level to less than p_k^{th2} when the transmit power required to obtain their target SINR is above p_k^{th1}. Further, they increase their power level if the required transmit power to obtain their target SINR is below p_k^{th2}. There are several advantages to DTPA. First, the interference to other users is reduced compared to CTPA and COPA. Second, the power consumption is reduced, and a higher number of users are satisfied with their target SINRs compared to CTPA. Third, compared to COPA, users have a lower power threshold which allows them to reach their target SINRs faster while the interference to other users is limited.

With this approach, the target SINR for user k in the multiple target SINR tracking power allocation (MTPA) is adjusted according to

$$\hat{\gamma}_k(t) = \begin{cases} \sqrt{\xi_k \Gamma_{nk}(t)} & \text{if } p_k(t) \leq p_k^{th3} \\ \hat{\gamma}_k & \text{if } p_k(t) > p_k^{th3}, \end{cases}$$

where $p_k^{th3} = \frac{p_k^{th1}}{\hat{\gamma}_k}$ and $p_k^{th2} \leq p_k^{th3} \leq p_k^{th1}$. The corresponding PUF is

$$p_k(t+1) = \frac{1}{\Gamma_{nk}(t)} \begin{cases} \sqrt{\xi_k \Gamma_{nk}(t)} & \text{if } p_k(t) \leq p_k^{th3} \\ \hat{\gamma_k} & \text{if } p_k(t) > p_k^{th3}. \end{cases}$$

With MTPA, user k updates p_k^{th3} and the PUF is separated into two zones. If $p_k(t) \leq p_k^{th3}$, the target SINR for user k is increased. If $p_k(t) > p_k^{th3}$, the target SINR is not changed, which is similar to DTPA and CTPA. The goal of MTPA is to maximize the sum rate and increase the number of satisfied users that attain their target SINRs.

6.2 Prioritized CAPA in the HetNet Uplink

In this section, the CAPA optimization problem is formulated and solved with an iterative algorithm using Lagrangian dual decomposition. Further, the convergence rate of the algorithm is accelerated using the Nesterov approach and an exponential rule [147].

6.2.1 Prioritized CAL and GINR cell association

Cell association is employed to maximize the network utility while all PUs are associated to BSs. PUs are associated with BSs that provide the maximum CAL and GINR, and NUs are associated with BSs to maximize the network sum rate. The following constraints are considered for the rate maximization problem.

1. The cell association variables are binary, $x_{nk} \in \{0, 1\}$.
2. Each user is associated with at most one BS, $\sum_{n=1}^{N} x_{nk} = 1\ ,\ k = 1, 2, \ldots, K$.
3. No more than $y_{\max}$ users are associated with BS n, $y_n \leq y_{\max},\ \ n = 1, 2, \ldots, N$.
4. The total number of users associated with BS n is $y_n = \sum_{k=1}^{K} x_{nk},\quad n = 1, 2, \ldots, N$.

The cell association problem for PU k is

$$\begin{aligned} \max_{n} \quad & \frac{\Gamma_{nk}}{y_n} \\ \text{subject to} \quad & x_{nk} \in \{0,1\} \\ & \sum_{n=1}^{N} x_{nk} = 1 \ , \ k = 1,2,\ldots,K_1 \\ & \sum_{k=1}^{K} x_{nk} = K_1, \quad n = 1,2,\ldots,N. \end{aligned} \tag{6.5}$$

and the corresponding cell association problem for NU k is

$$\begin{aligned} \max_{x_{nk},y_n} \quad & \sum_{n=1}^{N}\sum_{k=1}^{K} x_{nk}\log(R_{nk}) \\ \text{subject to} \quad & x_{nk} \in \{0,1\} \\ & \sum_{n=1}^{N} x_{nk} = 1 \ , \ k = K_1+1, K_1+2,\ldots,K \\ & y_n \leq y_{\max} \\ & \sum_{k=1}^{K} x_{nk} = y_n, \quad n = 1,2,\ldots,N. \end{aligned} \tag{6.6}$$

Comparing (6.5) and (6.6) indicates that the cell association criterion for NUs is more complex than that for PUs. The main difference between problems (6.5) and (6.6) is that the cell association criterion for PUs is based on user requirements while NU cell association is based on network requirements. First, each PU connects to a BS that has good channel conditions and sufficient capacity. Thus, the PU SINR requirements are satisfied first. Then, as many NUs as possible are served by the BSs providing that all PUs are associated.

For convenience, let Φ denote the feasible region corresponding to the constraints in (6.6). Cell association for PU k is based on satisfying the following criterion

$$n^* = \arg\max_{n} \frac{\Gamma_{nk}}{y_n}, k = 1,2,\ldots,K_1 \text{ and } n = 1,2,\ldots,N.$$

The cell association optimization problem for NU k is

$$\max_{x_{nk},y_n\in\Phi} F(x_{nk},y_n)=\sum_{n=1}^{N}\sum_{k=1}^{K}x_{nk}\log(R_{nk}), \tag{6.7}$$

which can be written as

$$\begin{aligned}\max_{x_{nk},y_n\in\Phi} F(x_{nk},y_n)&=\sum_{n=1}^{N}\sum_{k=1}^{K}x_{nk}\log(r_{nk})-\sum_{n=1}^{N}\sum_{k=1}^{K}x_{nk}\log\left(y_n\right)\\&=\sum_{n=1}^{N}\sum_{k=1}^{K}x_{nk}\log(r_{nk})-\sum_{n=1}^{N}y_n\log\left(y_n\right).\end{aligned} \tag{6.8}$$

The coupling constraint in (6.6) is $\sum_{k=1}^{K}x_{nk}=y_n,\ n=1,2,\ldots,N$. The Lagrangian dual decomposition approach in [147] is employed to relax this constraint using the Lagrange multiplier λ_n. The dual problem is then

$$\begin{aligned}\max_{\lambda_n} F(\lambda_n)&=\sum_{n=1}^{N}\sum_{k=1}^{K}x_{nk}\log(r_{nk})-\sum_{n=1}^{N}y_n\log\left(y_n\right)-\sum_{n=1}^{N}\lambda_n(\sum_{k=1}^{K}x_{nk}-y_n)\\&=\sum_{n=1}^{N}\sum_{k=1}^{K}x_{nk}\log(r_{nk})-\sum_{n=1}^{N}\sum_{k=1}^{K}x_{nk}\lambda_n+\sum_{n=1}^{N}y_n\lambda_n-\sum_{n=1}^{N}y_n\log\left(y_n\right)\\&=F_{x_{nk}}(\lambda_n)+F_{y_n}(\lambda_n),\end{aligned} \tag{6.9}$$

where $F_{x_{nk}}(\lambda_n)$ is the first subproblem and $F_{y_n}(\lambda_n)$ is the second subproblem. The solution of these problems is given below.

Subproblem 1

$$\begin{aligned}F_{x_{nk}}(\lambda_n)\quad&=\sum_{n=1}^{N}\sum_{k=1}^{K}x_{nk}\log(r_{nk})-\sum_{n=1}^{N}\sum_{k=1}^{K}x_{nk}\lambda_n\\\text{subject to}\quad&x_{nk}\in\{0,1\}\\&\sum_{n=1}^{N}x_{nk}=1\ ,\ k=K_1+1,K_1+2,\ldots,K.\end{aligned} \tag{6.10}$$

This is implemented at the user side using the following two steps.

Step 1: Obtain the load information $y_n(t)$ and Lagrange multiplier $\lambda_n(t)$ broadcast by BS n, and compute the GINR $\Gamma_{nk}(t)$.

Step 2: PU k selects the BS n^* which satisfies

$$n^* = \arg\max_n \frac{\Gamma_{nk}(t)}{y_n(t)}, k = 1, 2, \ldots, K_1 \text{ and } n = 1, 2, \ldots, N,$$

and NU k selects the BS n^* which satisfies

$$n^* = \arg\max_n \left(\log(r_{nk}(t)) - \lambda_n(t)\right),\ k = K_1 + 1, K_1 + 2, \ldots, K \text{ and } n = 1, 2, \ldots, N. \tag{6.11}$$

Subproblem 2

$$F_{y_n}(\lambda_n) = \sum_{n=1}^{N} y_n \lambda_n - \sum_{n=1}^{N} y_n \log(y_n). \tag{6.12}$$

This is implemented at the BS side. After all users have been associated, BS n updates y_n and its Lagrange multiplier λ_n using the following steps and then λ_n is broadcast to the users.

Step 1: The maximum of (6.12) is found by taking the derivative with respect to y_n and setting it to 0. The optimal value is

$$y_n(t+1) = e^{(\lambda_n(t)-1)}, \tag{6.13}$$

and adding the constraint $y_n \leq y_{\max}$ gives

$$y_n(t+1) = \min\{y_{\max}, e^{(\lambda_n(t)-1)}\}. \tag{6.14}$$

Step 2: The Lagrange multiplier is updated using the Nesterov accelerated subgradient method with step size $\mu_n(t)$ where $0 \leq \mu_n(t) \leq (|\frac{\partial F(\lambda_n(t))}{\partial \lambda_n(t)}|)^{-1}$ [122] which gives

$$\begin{aligned}
\bar{\lambda}_n(t) &= \lambda_n(t) - \mu_n(t) \left(\frac{\partial F(\lambda_n(t))}{\partial \lambda_n(t)} \right) \\
\frac{\partial F(\lambda_n(t))}{\partial \lambda_n(t)} &= -\sum_{k=1}^{K} x_{nk}(t) + y_n(t) \\
\beta_n(t+1) &= \frac{1 + \sqrt{1 + 4\beta_n^2(t)}}{2} \\
\lambda_n(t+1) &= \bar{\lambda}_n(t) + \frac{\beta_n(t) - 1}{\beta_n(t+1)} \big(\bar{\lambda}_n(t) - \bar{\lambda}_n(t-1)\big),
\end{aligned} \tag{6.15}$$

where $\beta_n(t)$ is the momentum parameter. The multiplier $\lambda_n(t)$ represents the traffic load at BS n and can be interpreted as the price of the BS determined by the load.

It can be positive or negative. The higher the value of $\lambda_n(t)$, the more traffic the BS has. Thus, when BS n has a high load, $\lambda_n(t)$ will increase and fewer users will associate with this BS. Conversely, if BS n has a small load, the price will be reduced to attract additional users.

6.2.2 Prioritized power allocation

In cellular networks, users require a variety of data rates for real time and non real time services. Some users are licensed while others can be unlicensed. Further, active and new users may exist in the network. Active and licensed users should be given a higher level of service than new and unlicensed users. Therefore, different priorities should be assigned to users when determining the power allocation. In this section, three priority based power allocation approaches are proposed. First, we have the following assumptions.

Assumption 1: $\rho_{nk\,\max}$ is the maximum received interference power plus noise for NU k so that the target SINRs for all PUs are satisfied. The upper limit on the received interference power plus noise for NU k is then given by

$$\begin{aligned}\rho_{nk\,\max} &= \{\rho_{nk} \mid 0 \le p_k \le p_{\max}\}, \quad k = K_1+1, K_1+2, \ldots, K \\ &= \left\{\rho_{nk} \mid 0 \le \frac{\theta_{nk}}{g_{nk}}\rho_{nk} \le p_{\max}\right\} = \min\left\{\frac{\varphi_{nk\,\max}}{\hat{\theta}_k}\right\},\end{aligned} \tag{6.16}$$

where $\varphi_{nk\,\max} = p_{\max} g_{nk}$. From (6.2), $\hat{\theta}_k = \frac{\hat{\gamma}_{nk}}{\hat{\gamma}_{nk}+1}$ when the target SINR for NU k is satisfied. Combining (6.2), (6.3) and (6.16), the maximum target SINR for NU k is

$$\hat{\gamma}_{k\,\max} = \frac{\varphi_{nk}}{\left|\left(\min\left(\frac{\varphi_{nk\,\max}}{\hat{\theta}_k}\right) - \varphi_{nk}\right)\right|}, \tag{6.17}$$

and the corresponding maximum transmit power is

$$p_{k\,\max}^{th1} = \frac{\hat{\gamma}_{k\,\max}}{\Gamma_{nk}}. \tag{6.18}$$

Assumption 2: To keep the NU SINR below the maximum allowable SINR, a

power tuning parameter is used which is given by

$$\Upsilon_k(\gamma_{nk}) = \begin{cases} \frac{\hat{\gamma}_{k\max}}{\gamma_{nk}}, \text{if } \gamma_{nk} > \hat{\gamma}_{k\max} \\ 1, \text{if } \gamma_{nk} \leq \hat{\gamma}_{k\max}. \end{cases} \tag{6.19}$$

When the required SINR of NU k is higher than its maximum allowable SINR, the PUF of this user is reduced by a factor $\frac{\hat{\gamma}_{k\max}}{\gamma_{nk}}$. Otherwise, the PUF of user k is left unchanged.

To improve the convergence of the CTPA, DTPA and proposed schemes, an exponential rule is employed with the weighted average of the current and previous transmit powers. Since an exponential function decays faster than a linear function, power allocation with an exponential rule will converge faster than with the linear functions in CTPA and DTPA. The exponential rule is

$$p_k(t+1) = \psi e^{\kappa(\hat{\gamma}_k - \gamma_{nk})} p_k(t) + (1-\psi) p_k(t-1), \tag{6.20}$$

where ψ is in the range $(0; 1]$, and $p_k(t)$ is the transmit power at iteration t. The convergence control parameter κ is given by

$$\kappa = \frac{\log(p_k^*) - \log(p_k)}{\hat{\gamma}_k - \gamma_{nk}}, \tag{6.21}$$

where $p_k^* = \frac{\hat{\gamma}_k}{\Gamma_{nk}}$. With user priority, the goal of the algorithm is to satisfy all PU requirements while satisfying as many NUs as possible. The following approaches are proposed to achieve this goal.

Approach 1: The PUs and NUs adjust their target SINRs using CTPA and DTPA, respectively. CTPA is employed by the PUs so they transmit at power levels which satisfy their target SINRs. DTPA is employed by the NUs which implies that some NUs may have to reduce their transmit power level to reduce the interference to other users. However, employing CTPA for PUs and DTPA for NUs separately may result in some NUs transmitting at the maximum power level even though their target SINRs are not attained, which will cause significant interference to the PUs. To ensure this does not occur, the target SINRs of the NUs should be reduced. Thus, their transmit power is adjusted to restrict the interference to PUs. The PUF for PU

k is then

$$p_k(t+1) = \max\left\{p_k^{th2}, \min\left\{\psi e^{\kappa(\hat{\gamma}_k - \gamma_{nk})} p_k(t) + (1-\psi)p_k(t-1), p_k^{th1}\right\}\right\},\ k = 1, 2, \ldots, K_1, \tag{6.22}$$

and the PUF for NU k, $k = K_1 + 1, K_1 + 2, \ldots, K$, is

$$p_k(t+1) = \begin{cases} \max\left\{p_k^{th2}, \min\left\{\psi e^{\kappa(\hat{\gamma}_k - \gamma_{nk})} p_k(t) + (1-\psi)p_k(t-1), p_k^{th1}\right\}\right\}, \text{if } p_k(t) \leq p_k^{th1} \\ 0, \text{if } p_k(t) > p_k^{th1}. \end{cases} \tag{6.23}$$

Equations (6.22) and (6.23) indicate that PUs and NUs increase their transmit powers until the target SINRs are reached if $\gamma_{nk} < \hat{\gamma}_k$. Conversely, the transmit powers are reduced until the target SINRs are reached if $\gamma_{nk} > \hat{\gamma}_k$. Thus, convergence occurs when $\gamma_{nk} = \hat{\gamma}_k$. The power threshold p_k^{th1} is used to manage the NU interference to PUs. NUs with a transmit power that exceeds this threshold must reduce their transmit power to 0.

Approach 2: The PUs employ CTPA so that PU SINR requirements are satisfied as quickly as possible. The NUs employ either CTPA or DTPA depending on the channel conditions and PU interference. The PUF for the PUs is

$$p_k(t+1) = \max\left\{p_k^{th2}, \min\left\{\psi e^{\kappa(\hat{\gamma}_k - \gamma_{nk})} p_k(t) + (1-\psi)p_k(t-1), p_k^{th1}\right\}\right\},\ k = 1, 2, \ldots, K_1,$$

and the PUF for NU k, $k = K_1 + 1, K_1 + 2, \ldots, K$, is

$$p_k(t+1) = \max\left\{p_k^{th2}, \min\left\{\frac{e^{\kappa(\xi_k + \gamma_{nk})}}{p_k(t)} + (1-\psi)p_k(t-1), \psi e^{\kappa(\hat{\gamma}_k - \gamma_{nk})} p_k(t) + (1-\psi)p_k(t-1), p_k^{th1}\right\}\right. \tag{6.24}$$

where ξ_k is in the range (0,1).

Approach 3: The PUs and NUs both employ CTPA. However, a tuning parameter is used in the NU PUF which depends on the channel conditions and interference to PUs. The PUF for the PUs is

$$p_k(t+1) = \max\left\{p_k^{th2}, \min\left\{\psi e^{\kappa(\hat{\gamma}_k - \gamma_{nk})} p_k(t) + (1-\psi)p_k(t-1), p_k^{th1}\right\}\right\},\ k = 1, 2, \ldots, K_1,$$

and the PUF for NU k, $k = K_1 + 1, K_1 + 2, \ldots, K$, is

$$p_k(t+1) = \max\left\{p_k^{th2}, \min\left\{\Upsilon_k(\Gamma_{nk})e^{\kappa(\hat{\gamma}_k - \gamma_{nk})}p_k(t) + (1-\psi)p_k(t-1), p_k^{th1}\right\}\right\}. \tag{6.25}$$

Computation of $p_k(t+1)$ requires knowledge of $p_k(t)$, $p_k(t-1)$, $\hat{\gamma}_k$, Γ_{nk}, κ, and Υ_k. However, $p_k(t)$, $p_k(t-1)$ and $\hat{\gamma}_k$ are available locally at the PUs and NUs. Further, κ and Υ_k are determined by the BS based on the channel conditions and traffic load. These parameters are used to maintain the PU and NU target SINRs according to the corresponding criteria. Finally, Γ_{nk} can easily be estimated at the BS and sent to the corresponding use via the return downlink channel. Therefore, the proposed approaches to power allocation can be implemented in a fully decentralized manner.

The proposed CAPA algorithm is summarized in Algorithm 10. As before, the PUs are considered first, and then the NUs.

Algorithm 10 Proposed CAPA algorithm

Stage 1: User side

Obtain the load information $y_n(t)$, Lagrange multiplier $\lambda_n(t)$, and $p_{k\max}^{th1}$ broadcast by the BS n.

Measure the GINR $\Gamma_{nk}(t)$.

Loop 1: Cell association

PU k select the BS n^* that satisfies

$$n^* = \arg\max_n \frac{\Gamma_{nk}(t)}{y_n(t)}, k = 1, 2, \ldots, K_1 \text{ and } n = 1, 2, \ldots, N.$$

NU k selects the BS n^* that satisfies

$$n^* = \arg\max_n \left(\log(r_{nk}(t)) - \lambda_n(t)\right), k = K_1 + 1, K_1 + 2, \ldots, K \text{ and } n = 1, 2, \ldots, N.$$

Loop 2: power allocation

PU k updates its transmit power using

$$p_k(t+1) = \max\left\{p_k^{th2}, \min\left\{\psi e^{\kappa(\hat{\gamma}_k - \gamma_{nk})}p_k(t) + (1-\psi)p_k(t-1), p_{k\max}^{th1}\right\}\right\}.$$

NU k updates its transmit power using one of the proposed power allocation approaches.

Stage 2: BS side

Find the maximum $y_n(t+1)$ at BS n by taking the derivative of (6.12).

Update the Lagrange multiplier $\lambda_n(t)$ associated with BS n using the Nesterov subgradient method.

6.3 Performance Results

In this section, Monte Carlo simulation is used to evaluate the proposed algorithms. The channel gain is $g_{nk} = hd_{nk}^{-\alpha}$, where $h = 0.97$ is a constant, d_{nk} is the distance between user k and BS n, and $\alpha = 3$ is the path loss exponent which corresponds to urban and suburban environments. The noise power at BS n is $\sigma_n^2 = 0.01$ W, and all initial transmit powers are set to 1 W which is the maximum transmit power for each user. The simulation results are given in the following sections.

6.3.1 Cell association

The proposed cell association scheme is evaluated using a two tier system model and four different scenarios. The performance is compared using Jain's fairness index [148] which is given by

$$J = \frac{(\sum_{n=1}^{N} y_n)^2}{N \sum_{n=1}^{N} y_n^2},$$

where $\frac{1}{N} \leq J \leq 1$. The closer J is to 1, the better the traffic load distribution, and the more fairly users are associated with MBSs and SBSs. When $J = \frac{1}{N}$, the traffic load is the most imbalanced and all users are associated with one BS.

In the first scenario, there is one MBS (BS9), 8 SBSs (BS1 to BS8), 10 PUs, and 40 NUs. The MBS is located in the center of a square geographic area with dimensions 40 km $\times$ 40 km and origin $(0, 0)$. The MBS is denoted by (x_{MBS}, y_{MBS}) which here is $(20, 20)$ km. The SBSs, PUs and NUs are uniformly distributed in the geographic area. Table 6.1 gives the load distribution and Jain's fairness index for the max signal strength, CRE and proposed cell association schemes averaged over 10000 trials.

With max signal strength cell association, the largest average loads are 34.8% at BS9 and 15.6% at BS8. The average load is the percentage of users associates with a BS averaged over the trials. Thus, BS9 (MBS) and BS8 are highly loaded compared to BS1 to BS7. The average loads at BS1 to BS7 range from 6.87% to 7.84%, which means these BSs are underloaded. There is a difference of 27.9% between the largest and smallest loads, which is a large imbalance between the MBS and SBSs giving $J = 0.44$. Most users are associated with BS9 (MBS) because it provides the largest signal strength.

With CRE cell association, the loads are more balanced than with the max signal strength scheme. The average load at BS9 is 4.33%, which is the smallest, and the

average loads at BS1 to BS8 range from 11.9% to 12.1%. The difference between the largest and smallest loads is only 7.77%, and $J = 0.84$. Fewer users are associated with BS9 because a positive bias was added to the SBS signal strengths to make them more attractive to users.

With the proposed cell association scheme, the load distribution is the fairest as $J = 0.87$ which is the highest. The average load at BS9 is 11.6%, and the average loads at the SBSs (BS1 to BS8) range from 10.9% to 11.1%, so the difference is just 0.71%, which is the smallest.

Table 6.1: Average Loads and Jain's Fairness Index with One MBS and Eight SBSs

Cell Association Scheme	Jain's Fairness Index	BS	Average Load (%)
Max signal strength	0.44	BS1	6.95
		BS2	6.99
		BS3	6.98
		BS4	6.87
		BS5	7.00
		BS6	6.93
		BS7	7.84
		BS8	15.6
		BS9	34.8
CRE	0.84	BS1	12.0
		BS2	12.0
		BS3	11.9
		BS4	12.0
		BS5	12.0
		BS6	11.9
		BS7	12.1
		BS8	11.9
		BS9	4.33
Prioritized CAL and GINR	0.87	BS1	11.1
		BS2	11.1
		BS3	10.9
		BS4	11.1
		BS5	11.0
		BS6	11.1
		BS7	11.0
		BS8	11.0
		BS9	11.6

In the second scenario, there are 4 MBSs, 20 SBSs, 40 PUs, and 160 NUs. The geographic area of 40 km $\times$ 40 km is split into four zones of size 20 km $\times$ 20 km. An MBS is located in the center of each zone. The SBSs, PUs and NUs are uniformly distributed in the four zones but with 25% in each zone. Table 6.2 gives Jain's fairness index for the max signal strength, CRE and proposed cell association scheme averaged over 10000 trials. For a fair comparison, the same channel conditions were used for each scheme in a given trial. These results show that the prioritized CAL and GINR scheme gives the highest fairness index of $J = 0.91$. CRE is next with $J = 0.81$ which is much better than the max signal strength scheme with $J = 0.54$.

Table 6.2: Jain's Fairness Index with Uniform SBS and User Distributions

Cell Association Scheme	Jain's Fairness Index
Max signal strength	0.54
CRE	0.81
Prioritized CAL and GINR	0.91

In the third scenario, the PUs and NUs are again uniformly distributed in the four zones, but the percentage of SBSs in the zones is [24.7 24.3 24.8 26.2] (%). Table 6.3 gives Jain's fairness index for the max signal strength, CRE and proposed cell association schemes averaged over 10000 trials. For a fair comparison, the same channel conditions were used for each scheme in a given trial. Again the prioritized CAL and GINR scheme gives the highest fairness index of $J = 0.91$. CRE is next with $J = 0.82$, which is much better than the max signal strength scheme with $J = 0.54$.

Table 6.3: Jain's Fairness Index with Nonuniform SBS and Uniform User Distributions

Cell Association Scheme	Jain's Fairness Index
Max signal strength	0.54
CRE	0.82
Prioritized CAL and GINR	0.91

In the fourth scenario, the percentage of SBSs in the four zones is [26.1 24.4 24.6 24.9] (%) and the percentage of PUs and NUs in the four zones is [26.3 23.8 25.4 24.5] (%). Table 6.4 gives Jain's fairness index for the max signal strength, CRE and proposed cell association scheme averaged over 10000 trials. For a fair comparison, the

same channel conditions were used for each scheme in a given trial. These results shows that the prioritized CAL and GINR scheme gives the highest fairness index of $J = 0.91$, followed by CRE with $J = 0.83$ and the max signal strength scheme with $J = 0.53$.

Table 6.4: Jain's Fairness Index with Nonuniform SBS and User Distributions

Cell Association Scheme	Jain's Fairness Index
Max signal strength	0.53
CRE	0.83
Prioritized CAL and GINR	0.91

The results in Tables 6.1 to 6.4 show that the proposed scheme provides a fairer traffic load distribution and higher fairness index than the max signal strength and CRE schemes.

6.3.2 Power allocation in additive white Gaussian noise (AWGN) channels

To evaluate the performance of the proposed power allocation approaches, simulation results are presented with 2 PUs (users 1 and 2) and 6 NUs (users 3 to 8) associated with a BS in an AWGN channel. The target SINRs for the users are $\hat{\gamma}_k = [0.27, 0.31, 0.48, 0.35, 0.15, 0.20, 0.16, 0.11]$ dB with an average SINR of 0.26 dB. The performance of the proposed power allocation approaches is compared with that of power allocation based on power consumption, average SINR and number of iterations. Results were obtained for 100 trials with different distances between the users and BS in each trial.

Figs. 6.1 and 6.2 present the SINR, transmit power and GINR for the COPA and MTPA schemes, respectively, for one trial. These results show that when the channel conditions are good, higher SINRs are attained, as expected. In Fig. 6.1, the power and GINR with COPA oscillate. The reason is that COPA is a variable SINR scheme, while MTPA is a variable target SINR scheme. Convergence with COPA requires 40 iterations. The resulting user SINRs are $\gamma_k = [0.72, 0.47, 1.35, 0.21, 0.17, 0.39, 0.03, 0.01]$ dB. The average SINR is 0.42 dB and average user power is 0.75 W. However, the average power for users 1 and 3 is greater than 0.7 W, which is high. In addition, users 4, 5, 7 and 8 are not satisfied with their target SINRs, and one PU (user 2) does

not reach the target SINR. Fig. 6.2 shows that convergence with the MTPA scheme requires 30 iterations, which is less than with COPA. The resulting user SINRs are $\gamma_k = [0.59, 0.48, 0.92, 0.29, 0.23, 0.43, 0.06, 0.01]$ dB. The average SINR is 0.37 dB and the average user power is 0.7 W, so MTPA is more power efficient than COPA. In addition, all PUs are satisfied with their target SINRs, but two NUs (users 7 and 8) are not satisfied.

Fig. 6.3 give the SINR, transmit power and GINR for one trial with proposed approach 1. This shows that this power allocation technique converges faster than MTPA. The corresponding user SINRs are $\gamma_k = [0.28, 0.32, 0.48, 0.36, 0.16, 0.20, 0.16, 0.11]$ dB. The average SINR is 0.26 dB and the average user power is 0.35 W. In addition, all PUs and NUs are satisfied with their target SINRs. These results indicate that this approach is much better than COPA and MTPA. The results obtained with proposed approaches 2 and 3 are similar and so are omitted.

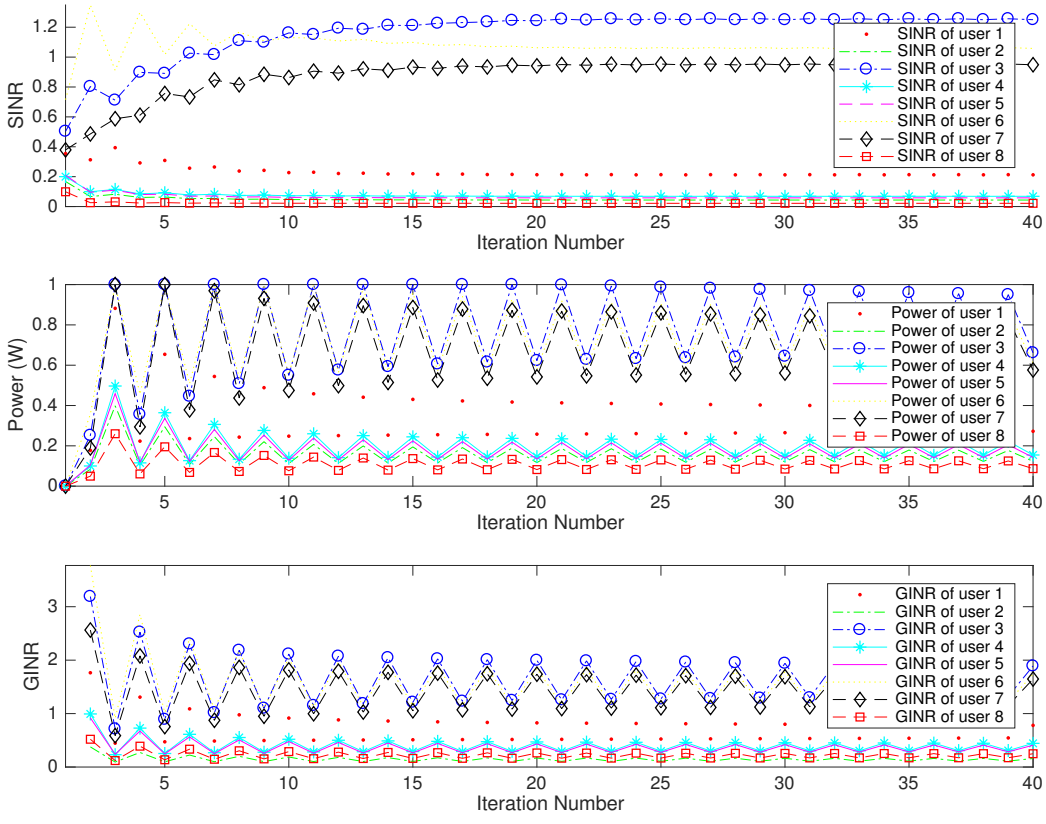

Figure 6.1: Transmit power, SINR and GINR for one trial with the COPA scheme.

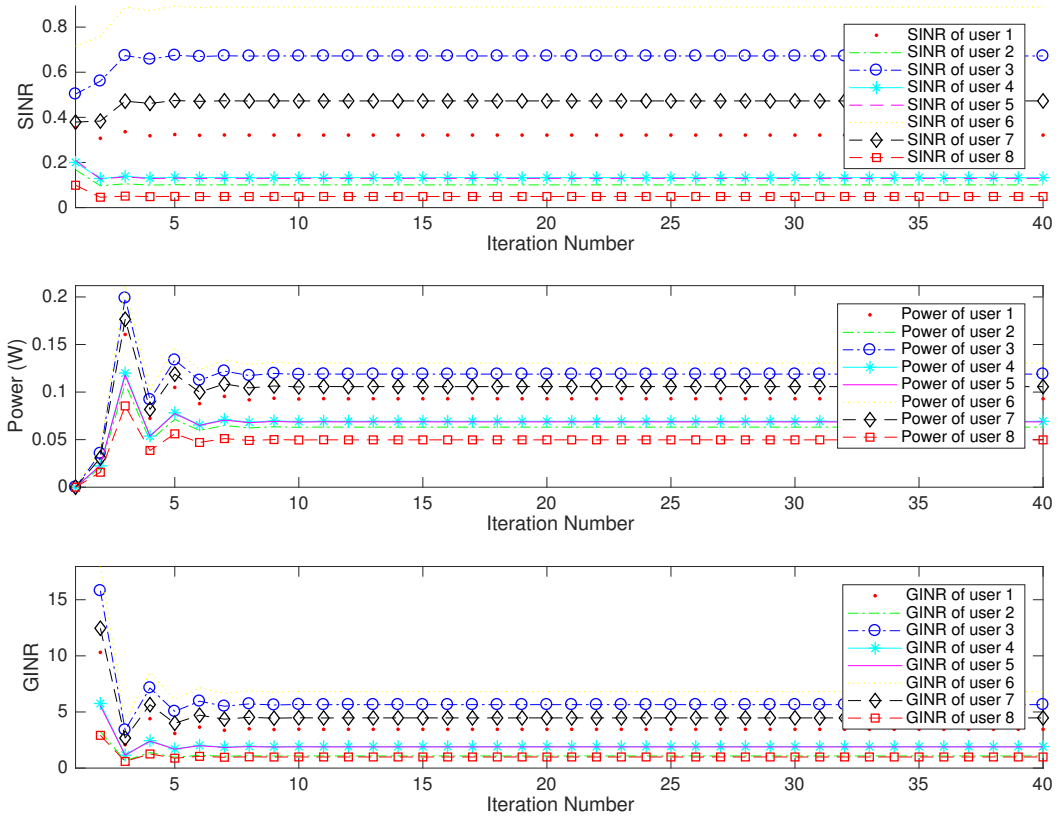

Figure 6.2: Transmit power, SINR and GINR for one trial with the MTPA scheme.

Table 6.5 shows the average number of iterations, user power and SINR for the CTPA, COPA, DTPA, MTPA and proposed approaches averaged over 100 trials. With CTPA, an average of 51 iterations is required for convergence with an average user power of 0.45 W. With DTPA, the target SINRs for the users were attained after an average of 33 iterations with an average user power of 0.35 W, which is better than CTPA. In addition, the number of users who are not satisfied with their target SINRs is less than with CTPA. With proposed approach 1, all users attain their target SINRs and an average of 29 iterations is required. The average user power is 0.35 W. Proposed approach 2 requires an average of 22 iterations and the average user power is 0.67 W, while proposed approach 3 requires an average of 20 iterations and the average user power is 0.7 W. Thus, proposed approach 1 outperforms CTPA, COPA, DTPA and MTPA in terms of user power and number of iterations. Proposed approaches 2 and 3 have faster convergence, but require more power.

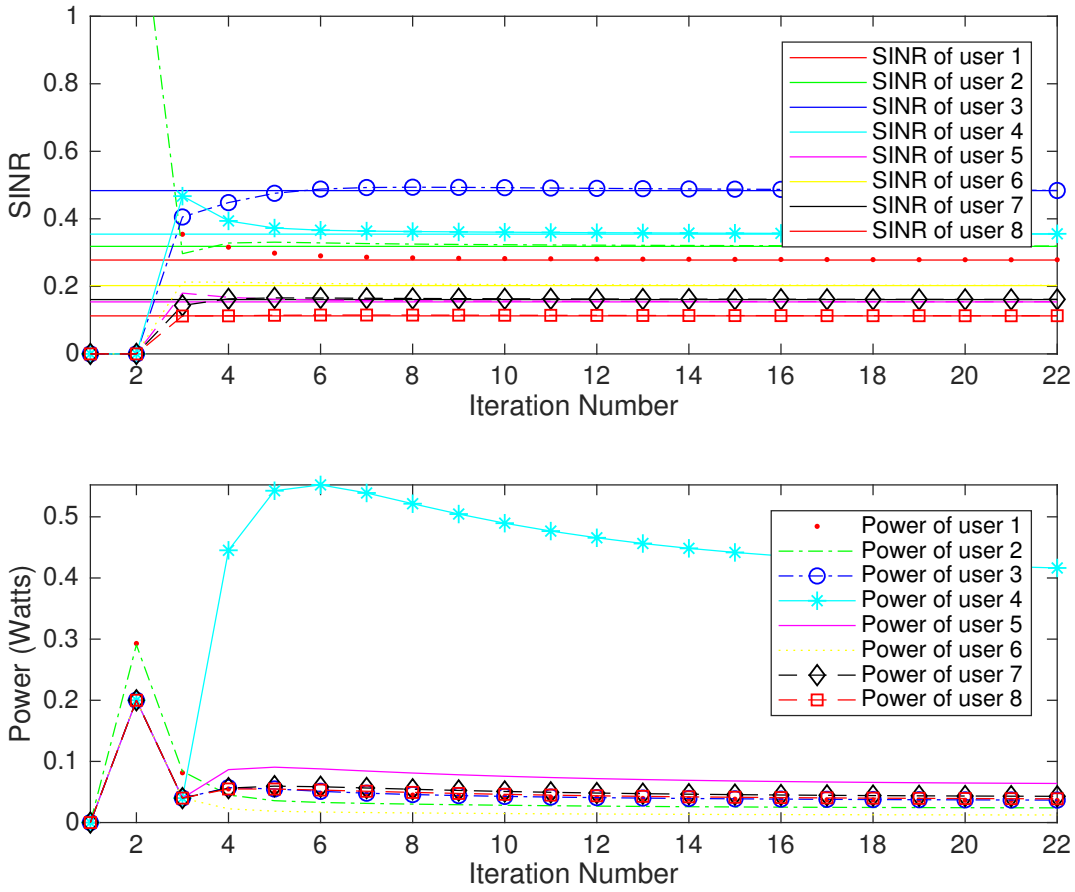

Figure 6.3: Transmit power, SINR and GINR for one trial with proposed approach 1.

6.3.3 Power allocation in Rayleigh fading channels

To evaluate the performance of the proposed approach in Rayleigh fading, results are obtained with different numbers of users associated to a BS. The target SINRs were randomly chosen from a uniform distribution between 0.1 dB and 0.9 dB. The performance of the proposed power allocation scheme is compared with that of the DTPA, CTPA, COPA and MTPA approaches in terms of power consumption, number of iterations for convergence and SINR. The PUs and NUs are uniformly distributed in the geographic area of a cell. The Rayleigh fading channel has T taps where $T = [4, 8, 16, 32, 64]$ [149]. The real and imaginary parts of the channel coefficients are randomly chosen from a Gaussian distribution. The magnitude is then Rayleigh

Table 6.5: Average Number of Iterations, User Power and SINR for the CTPA, COPA, DTPA, MTPA and Proposed Power Allocation Approaches Averaged over 100 Trials

Power Allocation Scheme	Average Number of Iterations	Average User Power (W)	Average SINR (dB)
CTPA	51	0.45	0.26
DTPA	33	0.38	0.26
DTPA	40	0.75	0.42
MTPA	30	0.70	0.37
Proposed 1	29	0.35	0.26
Proposed 2	22	0.67	0.26
Proposed 3	20	0.70	0.26

distributed and the phase is uniformly distributed between 0 and 2π. Results are obtained for 100 trials for each number of users with the user locations changed each trial and $\epsilon = 0.001$.

In the first scenario, there is one femtocell with 1 PU and 3 NUs. This cell is located at the center of a square geographic area with dimensions 50 m $\times$ 50 m. With CTPA and DTPA, the target SINRs for the users are $\hat{\gamma}_k = [0.29 \;\; 0.16 \;\; 0.31 \;\; 0.41]$ dB, which were randomly chosen. With the proposed power allocation scheme, the first value is for the PU and the others are for the NUs. Table 6.6 gives the average number of iterations, user power and SINR for the COPA, MTPA and proposed power allocation approach with 4 users. The CTPA and DTPA algorithms did not converge so no results are given. This shows that the proposed scheme has the lowest average user power which is 0.29 W. The average number of iterations is 5 which is also the lowest. The average user power for COPA is 2.64 W which is lower than MTPA, but the average number of iterations with COPA is 7 which is higher than MTPA. The average SINR for COPA is 1.60 dB, which is the highest followed by MTPA with 0.82 dB. This is because when the channel conditions are good, the user target SINR values are higher resulting in high transmit powers. These results show that the proposed scheme provides a better balance between the required transmit power and user target SINRs compared to COPA and MTPA.

In the second scenario, there is one femtocell with 2 PUs and 6 NUs. The femtocell is located at the center of a square geographic area with dimensions 50 m $\times$ 50 m.

Table 6.6: Average Number of Iterations, User Power and SINR for the COPA, MTPA and Proposed Power Allocation Approaches with 4 Users

Power Allocation Scheme	Average Number of Iterations	Average User Power (W)	Average SINR (dB)
COPA	7	2.64	1.60
MTPA	6	2.80	0.82
Proposed	5	0.29	0.29

With CTPA and DTPA, the user target SINRs are

$$\hat{\gamma}_k = [0.28 \;\; 0.32 \;\; 0.48 \;\; 0.36 \;\; 0.15 \;\; 0.20 \;\; 0.16 \;\; 0.11] \;\; \text{dB},$$

which were randomly chosen. With the proposed power allocation scheme, the first two values are for the PUs and the others are for the NUs. Table 6.7 gives the average number of iterations, user power and SINR for the COPA, MTPA and proposed power allocation approaches with 8 users. The CTPA and DTPA algorithms did not converge so no results are given. This shows that the proposed scheme again has the lowest average user power and number of iterations. The average required power and number of iterations with the proposed scheme are 0.13 W and 6, respectively. The average SINR of the proposed approach is 0.26 dB, while for COPA and MTPA it is 1.53 and 1.54, respectively.

Table 6.7: Average Number of Iterations, User Power and SINR for the COPA, MTPA and Proposed Power Allocation Approaches with 8 Users

Power Allocation Scheme	Average Number of Iterations	Average User Power (W)	Average SINR (dB)
COPA	8	7.07	1.53
MTPA	8	6.90	1.54
Proposed	6	0.13	0.26

In the third scenario, there is one picocell with 6 PUs and 10 NUs. The picocell is located at the center of a square geographic area with dimensions 300 m $\times$ 300 m.

With CTPA and DTPA, the user target SINRs are

$$\begin{aligned}\hat{\gamma}_k &= [0.31 \;\; 0.51 \;\; 0.28 \;\; 0.39 \;\; 0.53 \;\; 0.37 \;\; 0.28 \;\; 0.17 \\ &\quad\; 0.19 \;\; 0.44 \;\; 0.45 \;\; 0.24 \;\; 0.58 \;\; 0.22 \;\; 0.51 \;\; 0.17] \text{ dB},\end{aligned}$$

which were randomly chosen. With the proposed power allocation scheme, the first six correspond to the PUs and the last ten to the NUs. Table 6.8 gives the average number of iterations, user power and SINR for the COPA, MTPA and proposed power allocation approaches with 16 users. As before, the CTPA and DTPA algorithms did not converge so no results are given. The proposed scheme again has the lowest average user power and number of iterations which are 0.83 W and 26, respectively. The performance with COPA and MTPA is almost the same. The average number of iterations is 30 for COPA and 34 for MTPA, and the corresponding average user power is 9.33 W and 10.31 W. The average SINR for COPA and MTPA is 2.68 dB and 2.60 dB, respectively.

Table 6.8: Average Number of Iterations, User Power and SINR for the COPA, MTPA and Proposed Power Allocation Approaches with 16 Users

Power Allocation Scheme	Average Number of Iterations	Average User Power (W)	Average SINR (dB)
COPA	34	9.33	2.68
MTPA	30	10.31	2.60
Proposed	26	0.83	0.30

In the fourth scenario, there is one picocell with 12 PUs and 20 NUs. The picocell is located at the center of a square geographic area with dimensions 300 m $\times$ 300 m. With CTPA, DTPA and the proposed scheme, the target SINRs are randomly chosen between 0.1 dB and 0.6 dB, and the average target SINR is 0.36 dB. The same values are used with the three schemes for a fair comparison. Table 6.9 gives the average number of iterations, user power and SINR for the COPA, MTPA and proposed power allocation approaches with 32 users. Again, CTPA and DTPA did not converge so no results are given. This shows that the proposed scheme has a lower power consumption and number of iterations than COPA and MTPA, which are 2.56 W and 36, respectively. The average user power with COPA and MTPA is 15.02 W and 16.81 W, respectively, which is approximately five times higher than with the proposed scheme, and the corresponding average number of iterations is 40

and 45. The average SINR of the proposed scheme is 0.52 dB which is reasonable as the target SINR is 0.36 dB. These results show that the proposed scheme provides a better balance between the required transmit power and target SINRs compared to COPA and MTPA. The performance of COPA is slightly better than MTPA.

Table 6.9: Average Number of Iterations, User Power and SINR for the COPA, MTPA and Proposed Power Allocation Approaches with 32 Users

Power Allocation Scheme	Average Number of Iterations	Average User Power (W)	Average SINR (dB)
COPA	40	15.02	4.39
MTPA	45	16.81	4.35
Proposed	36	2.56	0.52

In the fifth scenario, there is one macrocell with 24 PUs and 40 NUs. The macrocell is located at the center of a square geographic area with dimensions 500 m $\times$ 500 m. With CTPA, DTPA and the proposed scheme, the target SINRs are randomly chosen in the range 0.1 to 0.9 dB. Table 6.10 shows the average number of iterations, user power and SINR for the DTPA, MTPA and proposed power allocation approaches with 64 users. The CTPA and DTPA algorithms did not converge so no results are given. The proposed scheme again has a lower average user power than COPA and MTPA. The average user power and number of iterations for this scheme are 6.32 W and 38, respectively. The average user power with COPA is 26.39 W which is lower than MTPA, but the average SINR of 5.44 dB is higher than that of MTPA.

Table 6.10: Average Number of Iterations, User Power and SINR for the COPA, MTPA and Proposed Power Allocation Approaches with 64 Users

Power Allocation Scheme	Average Number of Iterations	Average User Power (W)	Average SINR (dB)
COPA	56	26.39	5.44
MTPA	56	30.32	5.37
Proposed	38	6.32	0.39

6.4 Conclusion

In this chapter, an efficient cell association and power allocation (CAPA) scheme was proposed. With cell association, the product of the channel access likelihood (CAL) and channel gain to interference plus noise ratio (GINR) was considered for priority user (PU) cell association while network utility was considered for normal user (NU) cell association. Results were obtained which show that this provides a fairer load distribution between MBSs and SBSs, and a higher fairness index, than the max SINR and cell range expansion (CRE) schemes. In AWGN channels, distributed temporary removal and feasibility check power allocation (DTPA) outperforms constrained target SINR tracking power allocation (CTPA) and multiple target SINR power allocation (MTPA) and is much better than constrained opportunistic power allocation (COPA). Further, the PU target SINRs are not all satisfied with COPA. Many NUs are not satisfied with their target SINRs with MTPA and CTPA, and the target SINRs for the NUs are not always satisfied with DTPA. Three new power allocation approaches were proposed. The results for these methods show that the target SINRs for all PUs are satisfied while a large number of NUs are satisfied. In addition, the proposed approaches require fewer iterations to converge than the CTPA, DTPA, COPA and MTPA schemes. Approach 1 requires the lowest average user power, while approaches 2 and 3 require a higher average user power than CTPA and COPA. In Rayleigh fading channels, the CTPA and DTPA schemes did not converge to a solution while COPA and MTPA provided similar performance. The proposed approach had the best performance for all scenarios in these channels.

Chapter 7

Conclusion and Future Work

7.1 Conclusion

Power allocation schemes for outage probability and normalized SINR were proposed in Chapter 2. The goal is to reduce the outage probability and power consumption and satisfy user signal to interference plus noise ratio (SINR) requirements. A power allocation scheme was also proposed using the outage probability criterion. Results were presented which show that Algorithm 1, Algorithm 2 and geometric programming (GP) produce similar results, but the computation time with Algorithms 1 and 2 is much lower. Further, Algorithms 1 and 2 provide a higher normalized SINR than the distributed uplink power control (DUPC) and rate adaptive opportunistic power control (RAPC) schemes, while iterative SINR tracking power control (ISPC) is the worst. Power allocation schemes were also given to reduce the power consumption (Algorithm 3) and satisfy user SINR requirements (Algorithm 4). Algorithm 3 provides the best average outage probability, followed by Algorithm 4, RAPC and then ISPC, while DUPC is the worst. Algorithm 4 requires the lowest average power, followed by Algorithm 3, RAPC, ISPC, and finally DUPC.

Two power allocation schemes for throughput and energy efficiency in cellular networks were proposed and solved using parametric transformation in Chapter 3. The goal is to reduce the power consumption and improve the energy efficiency while ensuring all user outage probabilities are under an outage probability threshold. Performance results were presented which show that the proposed schemes given in Algorithms 5 and 6 provide a higher energy efficiency than the iterative distributed power allocation (IDPC), target SINR and opportunistic based power control (TOPC), and

fixed step power control (FSPC) schemes. Further, the proposed schemes satisfy the user throughput requirements with the lowest transmit power. Thus, they require less power compared to the IDPC, TOPC and FSPC schemes.

Power allocation problems for throughput and energy efficiency were proposed and solved using Lagrangian and differential methods in Chapter 4. The outage probability in Nakagami-m fading channels was also derived. The goal is to improve the throughput and energy efficiency while ensuring all user normalized SINRs. Performance results were presented which show that Algorithm 7 outperforms the distributed opportunistic power allocation (DOPA) and power allocation with temporary removal and feasibility (PARF) schemes in term of throughput and outage probability for all scenarios. Algorithm 7 is better than the target SINR tracking power allocation (TTPA) scheme in terms of the average throughput. Considering the number of users unsatisfied with their target SINRs, Algorithm 7 is better than PARF. Algorithm 8 is better than TTPA and DOPA in terms of power consumption, energy efficiency and the number of satisfied users. The performance of Algorithm 8 and PARF is similar in terms of energy efficiency and power consumption, but the number of unsatisfied users with Algorithm 8 is less than PARF for a large number of users. Algorithm 8 gives the highest average energy efficiency and lowest number of unsatisfied users, while Algorithm 7 gives the best average throughput.

A selective and prioritized power allocation scheme was proposed in Chapter 5. The goal is to reduce the power consumption and improve the power efficiency while ensuring all priority users (PUs) are satisfied and as many normal users (NUs) are satisfied with their target SINRs as possible. Performance results were presented which show that the proposed power allocation scheme given in Algorithm 9 provides a higher power efficiency than target SINR tracking power allocation (TSPA), variable SINR opportunistic power allocation (VOPA), dynamic target SINR tracking power allocation (DTPA), and variable target SINR power allocation (VTPA). The proposed scheme has a lower power consumption compared to DTPA and VTPA, but higher than VOPA. Finally, the proposed scheme gives the highest number of satisfied users.

Cell association and power allocation (CAPA) in heterogeneous networks (HetNets) was considered in Chapter 6. The product of the channel access likelihood (CAL) and channel gain to interference plus noise ratio (GINR) was considered for priority user (PU) cell association while network utility was considered for normal user (NU) cell association. Results were obtained which show that this provides a fairer load distribution between macro base stations (MBSs) and small cell base

stations (SBSs), and a higher fairness index, than the max SINR and cell range expansion (CRE) schemes. Three new power allocation approaches were proposed. The results for these methods show that the target SINRs for all PUs are satisfied while a large number of NUs are satisfied. In addition, the proposed approaches require fewer iterations to converge than the constrained target SINR tracking power allocation (CTPA), distributed temporary removal and feasibility check power allocation (DTPA), constrained opportunistic power allocation (COPA) and multiple target SINR power allocation (MTPA) schemes. Approach 1 requires the lowest average user power, while approaches 2 and 3 require a higher average user power than CTPA and COPA. In Rayleigh fading channels, the CTPA and DTPA schemes did not converge to a solution while COPA and MTPA provided similar performance. The proposed approach given in 10 had the best performance for all scenarios in these channels.

7.2 Future Work

Power control strategies in device to device (D2D) communications with different user priorities can be considered assuming imperfect channel state information (CSI). The goal is to maximize the network sum rate assuming the interference among device to device users (DUs) and cellular users (CUs) so that the SINR requirements of all CUs are satisfied. Prioritized and adaptive power allocation with channel uncertainty in D2D communications underlaying HetNets can be examined using the target SINR, power and SINR estimation error variance.

Mode selection, resource allocation, and power allocation considering spectrum and energy efficiency can be examined. Mode selection refers to either DU reuse of resources used by CUs or use of dedicated resources. The goal of mode selection and resource allocation is to improve spectrum efficiency while power allocation is used to improve energy efficiency. A two layer approach can be employed. The first layer determines transmission modes so that the spectrum efficiency is maximized. The second layer determines the number of allocated resources and power levels for CUs and DUs so that the energy and resource allocation efficiency are improved.

Cooperative mode selection, resource allocation, and power allocation scheme for interference management can be examined. CU requirements should be satisfied first so CUs should be associated with the lowest load BSs. DU mode selection is determined based on the DU communication distance, CU interference level and the availability of resources at the BS. If DUs operate in reuse or dedicated mode,

variable contrained target SINR power allocation can be used providing that all CUs are satisfied. If DUs operate in reuse mode, single contrained target SINR power allocation can be employed. This is due to the fact that CU resources shared by the DUs cause more interference to CUs than in dedicated mode.

Bibliography

[1] K. Davaslioglu and E. Ayanoglu, "Quantifying potential energy efficiency gain in green cellular wireless networks," *IEEE Commun. Surveys Tuts.*, vol. 16, no. 4, pp. 2065–2091, May 2014.

[2] P. Gandotra, R. Jha, and S. Jain, "Green communication in next generation cellular networks: A survey," *IEEE Access*, vol. 5, pp. 11727–11758, Jun. 2017.

[3] H. Zhou, H. Wang, X. Li, and V. Leung, "A survey on mobile data offloading technologies," *IEEE Access*, vol. 6, pp. 5101–5111, Jan. 2018.

[4] A. Brighente and S. Tomasin, "Power allocation for non-orthogonal millimeter wave systems with mixed traffic," *IEEE Trans. Wireless Commun.*, vol. 18, no. 1, pp. 432–443, Jan. 2019.

[5] T. Pham, R. Farrell, and L. Tran, "Revisiting the MIMO capacity with per-antenna power constraint: Fixed point iteration and alternating optimization," *IEEE Trans. Wireless Commun.*, vol. 18, no. 1, pp. 388–401, Jan. 2019.

[6] N. Miridakis, M. Xia, and T. Tsiftsis, "Optimal power allocation and active interference mitigation for spatial multiplexed MIMO cognitive systems," *IEEE Trans. Veh. Technol.*, vol. 67, no. 4, pp. 3349–3360, Apr. 2018.

[7] L. Dai et al., "Non-orthogonal multiple access for 5G: Solutions, challenges, opportunities, and future research trends," *IEEE Commun. Mag.*, vol. 53, no. 9, pp. 74–81, Sep. 2015.

[8] S. Brueck, "Heterogeneous networks in LTE advanced," in *Proc. IEEE Int. Wireless Commun. Systems Symp.*, Aachen, Germany, pp. 171–175, Jan. 2011.

[9] J. Khoriaty and H. Artail, "Coordinated multipoint in heterogeneous networks with overlapping microcell expanded regions," in *Proc. IEEE Int. Wireless and*

Mobile Comput., Netw. and Commun. Conf., Abu Dhabi, United Arab Emirates, pp. 289–295, Oct. 2015.

[10] S. Yunas, M. Valkama, and J. Niemela, "Spectral and energy efficiency of ultra dense networks under different deployment strategies," *IEEE Commun. Mag.*, vol. 53, no. 1, pp. 90–100, Jan. 2015.

[11] M. Ding, D. Perez, R. Xue, A. Vasilakos, and W. Chen, "On dynamic time division duplex transmissions for small cell networks," *IEEE Trans. Veh. Technol.*, vol. 65, no. 11, pp. 8933–8951, Nov. 2016.

[12] J. Zhou, J. Chen, H. Kikuchi, S. Sasaki, and S. Muramatsu, "Convergence rate evaluation of a DS-CDMA cellular system with centralized power control by genetic algorithms," in *Proc. Int. Conf. on Wireless Commun. and Networking*, Orlando, FL, pp. 177–182, Aug. 2002.

[13] N. Moallemi, M. Biguesh, and S. Gazor, "On the convergence of iterative non-cooperative centralized power controllers for multiple adjacent asynchronous cellular networks," in *Proc. Int. Conf. on Commun*, Kingston, Ontario, pp. 327–330, May 2010.

[14] Y. Yuan, T. Yang, Y. Xu, H. Feng, and B. Hu, "A cascaded channel power allocation for D2D underlaid cellular networks using matching theory," in *Proc. Int. Conf. on Wireless Commun. and Networking*, Barcelona, Spain, pp. 1–6, Jun. 2018.

[15] F. Foukalas, R. Shakeri, and T. Khattab, "Distributed power allocation for multi flow carrier aggregation in heterogeneous cognitive cellular networks," *IEEE Trans. Wireless Commun.*, vol. 17, no. 4, pp. 2486–2498, Apr. 2018.

[16] P. Bithas and A. Rontogiannis, "Mobile communication systems in the presence of fading, shadowing, noise, and interference," *IEEE Trans. Commun.*, vol. 63, no. 3, pp. 724–737, Mar. 2015.

[17] E. Vinogradov, W. Joseph, and C. Oestges, "Measurement based modeling of time variant fading statistics in indoor peer to peer scenarios," *IEEE Trans. Antennas Propag.*, vol. 63, no. 5, pp. 2252–2263, May 2015.

[18] K. Yip and T. Ng, "A simulation model for Nakagami-m fading channels, $m < 1$," *IEEE Trans. Commun.*, vol. 48, no. 2, pp. 214–221, Feb. 2000.

[19] J. Reig and L. Rubio, "Estimation of the composite fast fading and shadowing distribution using the log moments in wireless communications," *IEEE Trans. Wireless Commun.*, vol. 12, no. 8, pp. 3672–3681, Aug. 2013.

[20] A. Zappone, L. Sanguinetti, and M. Debbah, "Energy delay efficient power control in wireless networks," *IEEE Trans. Commun.*, vol. 66, no. 1, pp. 418–431, Jan. 2018.

[21] A. Memmi, Z. Rezki, and M. Alouini, "Power control for D2D underlay cellular networks with imperfect CSI," in *Proc. IEEE Globecom Workshops*, Washington, DC, pp. 1–6, Dec. 2016.

[22] A. Guo, H. Yin, L. Chen, and W. Wang, "Distributed power control with soft removal for uplink energy harvesting wireless network," *IET Commun.*, vol. 10, no. 12, pp. 1456–1463, Nov. 2016.

[23] Y. Xiao, G. Bi, and D. Niyato, "A simple distributed power control algorithm for cognitive radio networks," *IEEE Trans. Wireless Commun.*, vol. 10, no. 11, pp. 3594–3600, Nov. 2011.

[24] M. Dehghani, S. Banizamani, and K. Prabhu, "Modified distributed power control with dynamic target SIR tracking in wireless networks," in *Proc. IEEE Int. Electrical, Electronics, and Optimization Tech. Conf.*, Chennai, India, pp. 1980–1984, 2016.

[25] D. Feng et al., "QoS aware resource allocation for device to device communications with channel uncertainty", *IEEE Trans. Veh. Technol.*, vol. 65, no. 8, pp. 6051–6062, Aug. 2015.

[26] Y. Zou, J. Zhu, and B. Zheng, "Energy efficiency of network cooperation for cellular uplink transmissions", in *Proc. IEEE Int. Commun. Conf.*, Budapest, Hungary, pp. 4394–4398, Jun. 2013.

[27] K. Zheng, B. Fan, J. Liu, Y. Lin, W. Wang, "Interference coordination for OFDM-based multihop LTE-advanced networks", *IEEE Wireless Commun.*, vol. 18, no. 1, pp. 54–63, Feb. 2011.

[28] Yu Xi, Yuyan Zhang, and Hang Long, "An uplink energy-saving cooperation and power control scheme in heterogeneous cellular networks," in *Proc. IEEE Int.*

Microwave, Antenna, Propagation, and EMC Technol. Symp., Shanghai, China, pp. 261–266, Oct. 2015.

[29] J. Li et al., "A novel frequency reuse scheme for coordinated multi-point transmission", in *Proc. IEEE Int. Veh. Technol. Conf.*, May 2010.

[30] C. Botella, T. Svensson, X. Xu, H. Zhang, "On the performance of joint processing schemes over the cluster area", in *Proc. IEEE Int. Veh. Technol. Conf.*, May 2010.

[31] Q. Ye, Beiyu Rong, Y. Chen, C. Caramanis and J. Andrews, "Towards an optimal user association in heterogeneous cellular networks," in *Proc. IEEE Int. Global Commun. Conf.*, Anaheim, CA, pp. 4143–4147, Dec. 2012.

[32] A. Sang, X. Wang, M. Madihian, and R. Gitlin, "A load aware handoff and cell site selection scheme in multi cell packet data systems", in *Proc. IEEE Int. Globecom Telecommun. Conf.*, vol. 6, pp. 3931–3936, Nov. 2004.

[33] Y. Dhungana and C. Tellambura, "Multichannel analysis of cell range expansion and resource partitioning in two tier heterogeneous cellular networks," *IEEE Trans. Wireless Commun.*, vol. 15, no. 3, pp. 2394–2406, Mar. 2016.

[34] D. Perez et al., "Enhanced intercell interference coordination challenges in heterogeneous networks," *IEEE Wireless Commun.*, vol. 18, no. 3, pp. 22–30, Jun. 2011.

[35] H. Hu, J. Weng, and J. Zhang, "Coverage performance analysis of FeICIC low power subframes," *IEEE Trans. Wireless Commun.*, vol. 15, no. 8, pp. 5603–5614, Aug. 2016.

[36] S. Cui, H. Yousefi'zadeh, and X. Gu, "An optimal power control algorithm for STDMA MAC protocols in multihop wireless networks," *IEEE Trans. Wireless Commun.*, vol. 15, no. 5, pp. 3131–3142, May 2016.

[37] Y. Han, X. Tao, and X. Zhang, "Power allocation for device to device underlay communication with femtocell using Stackelberg game," in *Proc. IEEE Int. Wireless Commun. and Netw. Conf.*, Barcelona, Spain, pp. 1–6, Apr. 2018.

[38] H. Wang and Z. Ding, "Power control and resource allocation for outage balancing in femtocell networks," *IEEE Trans. Wireless Commun.*, vol. 14, no. 4, pp. 2043–2057, Apr. 2015.

[39] W. Li, T. Chang, and C. Chi, "On the complexity of SINR outage constrained maxmin fairness multicell coordinated beamforming problem," in *Proc. IEEE Int. Acoustics, Speech and Signal Process. Conf.*, Florence, Italy, pp. 3484–3488, Jul. 2014.

[40] S. Huang, K. Lin, and J. Deng, "Interference alignment with efficient dynamic information selection for LTE-A uplink coordinated multipoint systems," in *Proc. IEEE Int. Wireless and Mobile Conf.*, Bali, Indonesia, pp. 72–77, Oct. 2014.

[41] M. Chiang, C. Tan, D. Palomar, D. O'Neill, and D. Julian, "Power control by geometric programming," *IEEE Trans. Wireless Commun.*, vol. 6, no. 7, pp. 2640–2651, Jul. 2007.

[42] A. Agrawal, J. Andrews, J. Cioffi, and T. Meng, "Power control for successive interference cancellation with imperfect cancellation," in *Proc. IEEE Int. Commun. Conf.*, New York, NY, pp. 356–360, May 2002.

[43] M. Rasti, M. Hasan, L. B. Le, and E. Hossain, "Distributed uplink power control for multicell cognitive radio networks," *IEEE Trans. Commun.*, vol. 63, no. 3, pp. 628–642, Mar. 2015.

[44] H. Kwan, C. Sung, K. Leung, and K. Shum, "Opportunistic power control with rate adaptation for video conferencing services," in *Proc. IEEE Int. Commun. Conf.*, Istanbul, Turkey, pp. 5331–5335, Aug. 2002.

[45] X. Zhang and J. Andrews, "Downlink cellular network analysis with a dual slope path loss model," in *Proc. IEEE Int. Commun. Conf.*, London, UK, pp. 3975–3980, Mar. 2015.

[46] R. Canchi and Y. Akaiwa, "Performance of adaptive transmit power control in $\frac{\pi}{4}$ DQPSK mobile radio systems in flat Rayleigh fading channels," in *Proc. IEEE Int. Veh. Technol. Conf.*, Houston, TX, pp. 1261–1265, May 1999.

[47] R. Amorim et al., "Radio channel modeling for UAV communication over cellular networks," *IEEE Wireless Commun. Letts.*, vol. 6, no. 4, pp. 514–517, Aug. 2017.

[48] A. Altieri, L. Vega, P. Piantanida, and C. Galarza, "On the outage probability of the full duplex interference-limited relay channel," *IEEE J. Select. Areas Commun.*, vol. 32, no. 9, pp. 1765–1777, Sep. 2014.

[49] J. Goldsmith and P. Varaiya, "Capacity of fading channels with channel side information," *IEEE Trans. Infor. Theory*, vol. 43, no. 6, pp. 1986–1992, Nov. 1997.

[50] H. Nam, Y. Ko and B. F. Womack, "Performance analysis of OT-MRC over I.I.D. Nakagami and non-I.I.D. Rayleigh fading channels," *IEEE Trans. Veh. Technol.*, vol. 55, no. 6, pp. 1941–1946, Nov. 2006.

[51] Y. Ko, A. Abdi, M. S. Alouini, and M. Kaveh, "A general framework for the calculation of the average outage duration of diversity systems over generalized fading channels," *IEEE Trans. Veh. Technol.*, vol. 51, no. 6, pp. 1672–1680, Nov. 2002.

[52] S. Alouini and M. Simon, "An MGF based performance analysis of generalized selection combining over Rayleigh fading channels," *IEEE Trans. Commun.*, vol. 48, no. 3, pp. 401–415, Mar. 2000.

[53] L. Lan, L. Xie and H. Chen, "On outage probability analysis of uplink in land mobile satellite cooperative system," in *Proc. IEEE Int. Wireless Commun. and Signal Process. Conf.*, Hefei, China, pp. 1–6, Oct. 2014.

[54] G. Roussas, "Exponential probability inequalities with some applications," *IMS Lecture Notes, Statistics, Probability and Game Theory*, vol. 30, pp. 303–319, 1996.

[55] D. S. Mitrinovic, J. E. Pecaric, and A. M. Fink, *Classical and New Inequalities in Analysis*, Springer, Kluwer Academic, Dordrecht, pp. 69–72, 1993.

[56] L. Zheng, D. Cai, and C. Tan, "Maxmin fairness rate control in wireless networks: Optimality and algorithms by Perron-Frobenius theory," *IEEE Trans. Mobile Comput.*, vol. 17, no. 1, pp. 127–140, Jan. 2018.

[57] X. Zhai, C. Tan, Y. Huang, and B. Rao, "Transmit beamforming and power control for optimizing the outage probability fairness in MISO networks," *IEEE Trans. Commun.*, vol. 65, no. 2, pp. 839–850, Feb. 2017.

[58] S. Ghosh, B. Rao, and J. Zeidler, "Outage efficient strategies for multiuser MIMO networks with channel distribution information," *IEEE Trans. Signal Process.*, vol. 58, no. 12, pp. 6312–6324, Dec. 2010.

[59] S. Pillai, T. Suel, and S. Cha, "The Perron-Frobenius theorem: Some of its applications," *IEEE Signal Process. Mag.*, vol. 22, no. 2, pp. 62–75, Mar. 2005.

[60] S. Kandukuri and S. Boyd, "Optimal power control in interference limited fading wireless channels with outage probability specifications," *IEEE Trans. Wireless Commun.*, vol. 1, no. 1, pp. 46–55, Jan. 2002.

[61] X. Wang and Q. Zhu, "Power control for cognitive radio base on game theory," in *Proc. IEEE Int. Wireless Commun., Netw., and Mobile Comput. Conf.*, Shanghai, China, pp. 1256–1259, Oct. 2007.

[62] T. Alpcan, X. Fan, T. Basar, M. Arcak, and J. Wen, "Power control for multicell CDMA wireless networks: A team optimization approach," in *Proc. IEEE Int. Modeling and Optimization in Mobile, Ad Hoc, and Wireless Netw. Conf.*, Trentino, Italy, pp. 379–388, Apr. 2005.

[63] R. Alhumaima, R. Ahmed, and H. Raweshidy, "Maximizing the energy efficiency of virtualized C-RAN via optimizing the number of virtual machines," *IEEE Trans. Green Commun. Netw.*, vol. 2, no. 4, pp. 992–1001, Dec. 2018.

[64] Z. Du, J. Cheng, and N. Beaulieu, "Accurate error rate performance analysis of OFDM on frequency selective Nakagami-m fading channels," *IEEE Trans. Commun.*, vol. 54, no. 2, pp. 319–328, Feb. 2006.

[65] M. Ahmed and H. Yanikomeroglu, "A novel scheme for aggregate throughput maximization with fairness constraints in cellular networks," in *Proc. IEEE Int. Veh. Technol. Conf.*, Montreal, QC, pp. 1–5, Feb. 2006.

[66] S. Grandhi, R. Vijaya, D. Goodman, "Distributed power control in cellular radio systems", *IEEE Trans. Commun.*, vol. 42, pp. 226-228, 1994.

[67] V. N. Ha and L. B. Le, "Distributed base station association and power control for heterogeneous cellular networks, *IEEE Trans. Veh. Technol.*, vol. 63, no. 1, pp. 282–296, Jan. 2014.

[68] C. Sung and W. S. Wong, "A distributed fixed step power control algorithm with quantization and active link quality protection," *IEEE Trans. Veh. Technol.*, vol. 48, no. 2, pp. 553–562, March 1999.

[69] Y. Jiang et al., "Energy efficient non-cooperative power control in small cell networks," *IEEE Trans. Veh. Technol.*, vol. 66, no. 8, pp. 7540–7547, Aug. 2017.

[70] J. Wang, B. Xia, K. Xiao, Y. Gao, and S. Ma, "Outage performance analysis for wireless non-orthogonal multiple access systems," *IEEE Access*, vol. 6, pp. 3611–3618, Jan. 2018.

[71] H. Keeler, B. Błaszczyszyn, and M. Karray, "SINR based k-coverage probability in cellular networks with arbitrary shadowing," in *Proc. IEEE Int. Inf. Theory Conf.*, Istanbul, Turkey, pp. 1167–1171, Oct. 2013.

[72] X. Gao, K. Yang, J. Wu, Y. Zhang, and J. An, "Energy efficient resource allocation and power control for downlink multi cell OFDMA networks," in *Proc. IEEE Int. Global Commun. Conf.*, Singapore, pp. 1–6, Jan. 2017.

[73] N. Bhargav et al., "On the product of two κ–μ random variables and its application to double and composite fading channels," *IEEE Trans. Wireless Commun.*, vol. 17, no. 4, pp. 2457–2470, Apr. 2018.

[74] A. Annamalai, C. Tellambura, and V. Bhargava, "Simple and accurate methods for outage analysis in cellular mobile radio systems: A unified approach," *IEEE Trans. Commun.*, vol. 49, no. 2, pp. 303–316, Feb. 2001.

[75] A. Magableh and M. Matalgah, "Moment generating function of the generalized α–μ distribution with applications," *IEEE Commun. Letts.*, vol. 13, no. 6, pp. 411–413, Jun. 2009.

[76] X. Li and Q. Zeng, "Capture effect in the IEEE 802.11 WLANs with Rayleigh fading, shadowing, and path loss," in *Proc. IEEE Int. Wireless and Mobile Comput., Netw. and Commun. Conf.*, Montreal, QC, pp. 110–115, Sep. 2006.

[77] S. Han, N. Abu-Ghazaleh, and D. Lee, "Efficient and consistent path loss model for mobile network simulation," *IEEE /ACM Trans. Netw.*, vol. 24, no. 3, pp. 1774–1786, Jun. 2016.

[78] S. Jagannathan, M. Zawodniok, and Q. Shang, "Distributed power control for cellular networks in the presence of channel uncertainties," *IEEE Trans. Wireless Commun.*, vol. 5, no. 3, pp. 540–549, Mar. 2006.

[79] R. Yates, "A framework for uplink power control in cellular radio systems," *IEEE J. Sel. Areas Commun.*, vol. 13, no. 7, pp. 1341–1347, Sep. 1995.

[80] M. Javan and A. Sharafat, "Interference dependent opportunistic power control for multicarrier interference channels," *IEEE Trans. Veh. Technol.*, vol. 63, no. 2, pp. 953–958, Feb. 2014.

[81] M. Monemi et al., "Distributed multiple target SINRs tracking power control in wireless multirate data networks," *IEEE Trans. Wireless Commun.*, vol. 12, no. 4, pp. 1850–1859, Apr. 2013.

[82] M. Rasti and E. Hossain, "Distributed priority based power and admission control in cellular wireless networks," *IEEE Trans. Wireless Commun.*, vol. 12, no. 9, pp. 4483–4495, Sep. 2013.

[83] P. He, S. Zhang, L. Zhao, and X. Shen, "Energy efficient power allocation with individual and sum power constraints," *IEEE Trans. Wireless Commun.*, vol. 17, no. 8, pp. 5353–5366, Aug. 2018.

[84] H. Zhang, H. Liu, J. Cheng, and V. Leung, "Downlink energy efficiency of power allocation and wireless backhaul bandwidth allocation in heterogeneous small cell networks," *IEEE Trans. Commun.*, vol. 66, no. 4, pp. 1705–1716, Apr. 2018.

[85] Z. Sheng, H. D. Tuan, A. Nasir, T. Q. Duong, and H. Poor, "Power allocation for energy efficiency and secrecy of wireless interference networks," *IEEE Trans. Wireless Commun.*, vol. 17, no. 6, pp. 3737–3751, Jun. 2018.

[86] N. Oyie and T. Afullo, "Measurements and analysis of large scale path loss model at 14 and 22 GHz in indoor corridor," *IEEE Access*, vol. 6, pp. 17205–17214, Feb. 2018.

[87] M. Shchekotov, "Automatic calibration for log-normal path loss model based on Bluetooth low energy beacons," in *Proc. IEEE Int. Open Innovations Association Conf.*, Jyvaskyla, Finland, pp. 212–218, Nov. 2016.

[88] S. Hussain and X. Fernando, "Closed form analysis of relay based cognitive radio networks over Nakagami-m fading channels," *IEEE Trans. Veh. Technol.*, vol. 63, no. 3, pp. 1193–1203, Mar. 2014.

[89] P. Dighe, R. Mallik, and S. Jamuar, "Analysis of transmit receive diversity in Rayleigh fading," *IEEE Trans. Commun.*, vol. 51, no. 4, pp. 694–703, Apr. 2003.

[90] S. Yoo et al., "The Fisher-Snedecor $\mathcal{F}$ distribution: A simple and accurate composite fading model," *IEEE Commun. Letts.*, vol. 21, no. 7, pp. 1661–1664, Jul. 2017.

[91] K. Yang, S. Martin, C. Xing, J. Wu, and R. Fan, "Energy efficient power control for device to device communications," *IEEE J. Sel. Areas Commun.*, vol. 34, no. 12, pp. 3208–3220, Dec. 2016.

[92] C. Isheden and G. Fettweis, "Energy efficient multi carrier link adaptation with sum rate dependent circuit power," in *Proc. IEEE Int. Global Telecommun. Conf.*, Miami, FL, pp. 1–6, Dec. 2010.

[93] K. Yang, Y. Wu, J. Huang, X. Wang, and S. Verdu, "Distributed robust optimization for communication networks," in *Proc. IEEE Int. Comput. Commun. Conf.*, Phoenix, AZ, pp. 1157–1165, Apr. 2008.

[94] K. Zhu, E. Hossain, and A. Anpalagan, "Downlink power control in two tier cellular OFDMA networks under uncertainties: A robust Stackelberg game," *IEEE Trans. Commun.*, vol. 63, no. 2, pp. 520–535, Feb. 2015.

[95] J. Ding, L. Jiang, and C. He, "Energy efficient power control for underlaying D2D communication with channel uncertainty: User centric versus network centric," *IEEE J. Commun. Netw.*, vol. 18, no. 4, pp. 589–599, Aug. 2016.

[96] A. Yilmaz, "Calculating outage probability of block fading channels based on moment generating functions," *IEEE Trans. Commun.*, vol. 59, no. 11, pp. 2945–2950, Nov. 2011.

[97] M. Simon and M. Alouini, *Digital Communications over Fading Channels: A Unified Approach to Performance Analysis*, Wiley, New York, NY, 2004.

[98] G. Karagiannidis, N. Sagias, and T. Mathiopoulos, "The $N \times$ Nakagami fading channel model," in *Proc. IEEE Int. Wireless Commun. Systems Symp.*, Siena, Italy, pp. 185–189, Sep. 2005.

[99] J. Steele, *The Cauchy-Schwarz Master Class: An Introduction to the Art of Mathematical Inequalities*, Cambridge University Press, Cambridge, UK, pp. 30–33, 2004.

[100] T. Bromwich, *An Introduction to the Theory of Infinite Series*, Macmillan, London, UK, pp. 450–451, 1959.

[101] N. Lord, "On inequalities equivalent to the inequality of the means," *The Mathematical Gazette*, pp. 529–533, Nov. 2008.

[102] W. Dinkelbach, "On nonlinear fractional programming," *Management Science*, vol. 13, no. 7, ser. A, pp. 492–498, 1967.

[103] F. Hildebrand, *Introduction to Numerical Analysis*, McGraw-Hill, New York, NY, 1956.

[104] J. Chen, L. Wang, and C. Liu, "Coverage probability of small cell networks with composite fading and shadowing," in *Proc. IEEE Int. Symp. on Personal, Indoor, and Mobile Radio Commun.*, Washington, DC, pp. 1965–1969, Sep. 2014.

[105] B. Dulek, N. Vanli, S. Gezici, and P. Varshney, "Optimum power randomization for the minimization of outage probability," *IEEE Trans. Wireless Commun.*, vol. 12, no. 9, pp. 4627–4637, Sep. 2013.

[106] A. Al-Dweik, B. Sharif, and C. Tsimenidis, "Accurate BER analysis of OFDM systems over static frequency selective multipath fading channels," *IEEE Trans. Broadcast.*, vol. 57, no. 4, pp. 895–901, Dec. 2011.

[107] A. Isnawati, R. Hidayat, S. Sulistyo, and I. Mustika, "A comparative study on centralized and distributed power control in cognitive femtocell network," in *Proc. IEEE Int. Inf. Technol. and Electr. Eng. Conf.*, Yogyakarta, Indonesia, pp. 1–6, Feb. 2017.

[108] A. Abdelkader, E. Jorswieck, and M. Zimmerling, "Centralized and distributed optimum power control and beam forming in network flooding," in *Proc. IEEE Int. European Wireless Conf.*, Dresden, Germany, pp. 1–6, Aug. 2017.

[109] G. Foschini and Z. Miljanic, "A simple distributed autonomous power control algorithm and its convergence," *IEEE Trans. Veh. Technol.*, pp. 641–646, Nov. 1993.

[110] S. Grandhi and J. Zander, "Constrained power control in cellular radio systems," in *Proc. IEEE Int. Veh. Technol. Conf.*, Stockholm, Sweden, pp. 824–828, Jun. 1994.

[111] K. Leung and C. Sung, "An opportunistic power control algorithm for cellular network," *IEEE/ACM Trans. on Netw.*, vol. 14, no. 3, pp. 470–478, Jun. 2006.

[112] M. Rasti, A. Sharafat, and J. Zander, "Pareto and energy efficient distributed power control with feasibility check in wireless networks," *IEEE Trans. Inf. Theory*, vol. 57, no. 1, pp. 245–255, Jan. 2011.

[113] Y. De Melo et al., "Power control with variable target SINR for D2D communications underlying cellular networks," in *Proc. IEEE Int. European Wireless Conf.*, Barcelona, Spain, pp. 1–6, May 2014.

[114] E. Dahlman et al., "5G wireless access: Requirements and realization," *IEEE Commun. Mag.*, vol. 52, no. 12, pp. 42–47, Dec. 2014.

[115] S. Gangakhedkar et al., "Use cases, requirements and challenges of 5G communication for industrial automation," in *Proc. IEEE Commun. Workshops*, Kansas City, MO, pp. 1–6, May 2018.

[116] J. Zhang, "Mobility enhancement and performance evaluation for 5G ultra dense networks," in *Proc. IEEE Int. Wireless Commun. and Netw. Conf.*, New Orleans, LA, pp. 1793–1798, Mar. 2015.

[117] V. Yazici, U. Kozat, and M. Sunay, "A new control plane for 5G network architecture with a case study on unified handoff, mobility, and routing management," *IEEE Commun. Mag.*, vol. 52, no. 11, pp. 76–85, Nov. 2014.

[118] J. Zhu, M. Zhao, and S. Zhou, "An optimization design of ultra dense networks balancing mobility and densification," *IEEE Access*, vol. 6, pp. 32339–32348, Jun. 2018.

[119] Y. Teng et al., "Resource allocation for ultra dense networks: A survey, some research issues and challenges," *IEEE Commun. Surveys Tuts.*, vol. 21, no. 3, Q3, 2018.

[120] A. Yadav and O. Dobre, "All technologies work together for good: A glance at future mobile networks," *IEEE Wireless Commun.*, vol. 25, no. 4, pp. 10–16, Aug. 2018.

[121] D. Bertsekas, *Convex Optimization Theory*, Athena Scientific, 2009.

[122] Y. Nesterov, *Introductory Lectures on Convex Optimization: A Basic Course*, Springer, New York, NY, 2004.

[123] H. Beyranvand, W. Lim, M. Maier, C. Verikoukis, and J. Salehi, "Backhaul aware user association in FiWi enhanced LTE a heterogeneous networks," *IEEE Trans. Wireless Commun.*, vol. 14, no. 6, pp. 2992–3003, Jun. 2015.

[124] A. Gupta and R. Jha, "A survey of 5G network: Architecture and emerging technologies," *IEEE Access*, vol. 3, pp. 1206–1232, Jul. 2015.

[125] A. Adejo, S. Boussakta, and J. Neasham, "Interference modelling for soft frequency reuse in irregular heterogeneous cellular networks," in *Proc. IEEE Int. Ubiquitous and Future Netw. Conf.*, Milan, Italy, pp. 381–386, Jul. 2017.

[126] A. Taufique, M. Jaber, A. Imran, Z. Dawy, and E. Yacoub, "Planning wireless cellular networks of future: Outlook, challenges and opportunities," *IEEE Access*, vol. 5, pp. 4821–4845, Mar. 2017.

[127] H. Elsawy, E. Hossain, and D. Kim, "HetNets with cognitive small cells: User offloading and distributed channel access techniques," *IEEE Commun. Mag.*, vol. 51, no. 6, pp. 28–36, Jun. 2013.

[128] T. Anh, S. Kim, and C. Hong, "Joint base station association and power control for uplink cognitive small cell network," in *Proc. IEEE Int. Asia Pacific Network Operations and Management Symp.*, Kanazawa, Japan, pp. 1–6, Nov. 2016.

[129] C. Singh, A. Kumar, and R. Sundaresan, "Combined base station association and power control in multichannel cellular networks," *IEEE/ACM Trans. Netw.*, vol. 24, no. 2, pp. 1065–1080, Apr. 2016.

[130] P. Chiang, P. Huang, S. Sun, W. Liao, and W. Chen, "Joint power control and user association for traffic offloading in heterogeneous networks," in *Proc. IEEE Int. Global Commun. Conf.*, Austin, TX, pp. 4424–4429, Feb. 2014.

[131] T. Zhou, Z. Liu, J. Zhao, C. Li, and L. Yang, "Joint user association and power control for load balancing in downlink heterogeneous cellular networks," *IEEE Trans. Veh. Technol.*, vol. 67, no. 3, pp. 2582–2593, Mar. 2018.

[132] B. Maaz, K. Khawam, S. Tohme, S. Lahoud, and J. Nasreddine, "Joint user association, power control and scheduling in multi cell 5G networks," in *Proc. IEEE Int. Wireless Commun. and Netw. Conf.*, San Francisco, CA, pp. 1–6, May 2017.

[133] L. P. Qian, Y. Wu, H. Zhou, and X. Shen, "Joint uplink base station association and power control for small-cell networks with non-orthogonal multiple access," *IEEE Trans. Wireless Commun.*, vol. 16, no. 9, pp. 5567–5582, Sep. 2017.

[134] A. Liu and V. Lau, "Joint BS user association, power allocation, and user side interference cancellation in cell free heterogeneous networks," *IEEE Trans. Signal Process.*, vol. 65, no. 2, pp. 335–345, Jan. 2017.

[135] D. Liu et al., "User association in 5G networks: A survey and an outlook," *IEEE Commun. Surveys Tut.*, vol. 18, no. 2, pp. 1018–1044, Q2 2016.

[136] A. Shojaeifard, K. Hamdi, E. Alsusa, D. So, and J. Tang, "Exact SINR statistics in the presence of heterogeneous interferers," *IEEE Trans. Infor. Theory*, vol. 61, no. 12, pp. 6759–6773, Dec. 2015.

[137] Y. Chen and C. Sung, "Characterization of SINR region for multiple interfering multicast in power-controlled systems," *IEEE Trans. Commun.*, vol. 67, no. 1, pp. 165–175, Jan. 2019.

[138] H. Tabassum, U. Siddique, E. Hossain, and M. Hossain, "Downlink performance of cellular systems with base station sleeping, user association, and scheduling," *IEEE Trans. Wireless Commun.*, vol. 13, no. 10, pp. 5752–5767, Oct. 2014.

[139] J. Sangiamwong et al., "Investigation on cell selection methods associated with intercell interference coordination in heterogeneous networks for LTE advanced downlink," in *Proc. European Wireless Sustainable Wireless Technol. Conf.*, Vienna, Austria, pp. 1–6, Jul. 2011.

[140] R. Thakur, S. Mishra, and C. Murthy, "A load conscious cell selection scheme for femto assisted cellular networks," in *Proc. IEEE Int. Symp. on Personal, Indoor, and Mobile Radio Commun.*, London, UK, pp. 2378–2382, Nov. 2013.

[141] G. Chou, K. Liu, and S. Su, "Load based cell association for load balancing in HetNets," in *Proc. IEEE Int. Personal, Indoor, and Mobile Radio Commun. Symp.*, Hong Kong, China, pp. 1681–1686, Dec. 2015.

[142] I. Guvenc, "Capacity and fairness analysis of heterogeneous networks with range expansion and interference coordination," *IEEE Wireless Commun. Lett.*, vol. 15, no. 10, pp. 1084–1087, Sep. 2011.

[143] S. Deb, P. Monogioudis, J. Miernik, and J. Seymour, "Algorithms for enhanced inter-cell interference coordination (eICIC) in LTE HetNets," *IEEE/ACM Trans. Netw.*, vol. 22, no. 1, pp. 137–150, Feb. 2014.

[144] Y. Wang and Y. Hu, "Distributed CoMP transmission for cell range expansion with almost blank subframe in downlink heterogeneous networks," in *Proc. IEEE Int. Intelligent Computing and IoT Conf.*, Harbin, China, pp. 127–130, May 2015.

[145] U. Siddique, H. Tabassum, E. Hossain, and D. Kim, "Channel access aware user association with interference coordination in two tier downlink cellular networks," *IEEE Trans. Veh. Technol.*, vol. 65, no. 7, pp. 5579–5594, Jul. 2016.

[146] K. Shen and W. Yu, "Load and interference aware joint cell association and user scheduling in uplink cellular networks," in *Proc. IEEE Int. Signal Process. Advances in Wireless Commun. Workshop*, Edinburgh, UK, pp. 1–5, Aug. 2016.

[147] H. Boostanimehr and V. Bhargava, "Unified and distributed QoS driven cell association algorithms in heterogeneous networks," *IEEE Trans. Wireless Commun.*, vol. 14, no. 3, pp. 1650–1662, Mar. 2015.

[148] A. Sediq et al., "Optimal tradeoff between sum rate efficiency and Jain fairness index in resource allocation," *IEEE Trans. Wireless Commun.*, vol. 12, no. 7, pp. 3496–3509, Jul. 2013.

[149] S. Sagari, W. Trappe, and L. Greenstein, "Equivalent tapped delay line channel responses with reduced taps," in *Proc. IEEE Int. Veh. Technol. Conf.*, Las Vegas, NV, pp. 1–5, Jan. 2014.